UNIVERSITÉ POLYTECHNIQUE HAUTS-DE-FRANCE

INSTITUT DES SCIENCES ET TECHNIQUES

VALENCIENNES

Mémoire du Projet de Fin d'études

Présenté pour l'obtention du diplôme du

Master 2, Mention : Transport, Réseau, Mobilité

Spécialité : Ingénierie en Automatique, Homme et Mobilité

Sous le thème :

Modeling and observer design for two wheeled vehicules : Application to road-tire adherence estimation and stability analysis in curves

Réalisé par

Anass TAOUFIK

Soutenu le 11 Septembre 2018 devant le jury composé de :

Président	:	Mr. Mohamed DJEMAI	Pr. à l'UPHF
Examinateur	:	Mr. Abdelghani BEKRAR	Pr. à l'UPHF
Examinateur	:	Mr. Jimmy LAUBER	Pr. à l'UPHF
Examinateur	:	Mr. Patrick MILLOT	Pr. à l'UPHF

Centre d'études et d'expertise sur les risques, l'environnement, la mobilité et l'aménagement.
Direction Centre-Est. Département Laboratoire de Lyon. Bron.

Année Universitaire : 2017-2018

Résumé/Abstract

Accidents involving motorbikes constitute an important part of the overall road accidents in France, and death rates reach 20%, efforts to reduce them led to an increase in research in stability analysis of these vehicles. Corners and curves are the situations that lead the most to instability, as they make the driver make control decisions that might turn out to be counter intuitive. And as the study and analysis of these motorcycle's critical driving situations, falls and accidents, are difficult to be described analytically because of the simultaneity of different and complex phenomena which make the dynamics quite elaborate. In this work, a model able to describe the strong non-linearities conveyed by the complex dynamic of a two-wheeled vehicle in curves, is presented. The model takes into account the necessary components needed to accurately calculate the adherence, and thus use a state observer for difference situations, to estimate it in curves, along with the forces involving the tire-road contact dynamics. A stability analysis in these situations has been done for different critical variables along with the forward speed. The ultimate objective being the synthesis of an alert system in case of instability.

Les accidents impliquants des motos constituent une partie importante des accidents routières en France et présente un taux de mortalité de 20%, des prorammes de recherches sur ce types de vehicules ont était renforcé afin de réduire le risque des accidents pour type de véhicules. Les virages sont les situations qui mènent le plus à l'instabilité de ces deux roues motorisés, puisqu'ils déclenche un changement parfois brusque et incontrolable chez le conducteur. Ces scénarios sont importants et ils sont difficiles à analyser analytiquement en raison de la simultanéité des différentes situations. Dans ce travail, un modèle capable de décrire les fortes non-linéarités véhiculées par la dynamique complexe d'un véhicule à deux roues dans les virages est présenté. Le modèle prend en compte les composants nécessaires pour calculer avec précision l'adhérence, et utilise donc un observateur d'états pour des différentes situations, pour l'estimation de ceux-ci dans les virages, ainsi que les forces impliquant la dynamique du contact pneumatique-chaussée. Une analyse de stabilité dans ces situations a été effectuée pour différentes variables critiques, ainsi que la vitesse. L'objectif ultime étant la synthèse d'un système d'alerte en cas d'instabilité.

List of Figures

List of Tables

List of abbreviations and Symbols

- **Cerema** ..... Center for studies and expertise, on risks, environmental, mobility, urban country planning
- **DLL** ..... Lyon Labratory Departement
- **2RM/DRM** ..... 2 Roues Motorisés / Deux Roues Motorisés
- **OLG** ..... Generalized Luenberger Observers
- **SMO** ..... Sliding Mode Observer
- **DoF** ..... Degree of Freedom
- a_i ..... Crown radius of rear wheel, or front wheel
- b_i ..... Centreline radius of rear or front wheel
- m_i ..... Mass of body i
- i_i ..... Inertia around body i
- j_i ..... Inertia around other axes for front and rear wheels
- x_i ..... Mass local x position
- z_i ..... Mass local z position
- k_i ..... Stiffness term for body i
- f_i ..... Friction coefficient of body i
- t_i ..... Tangential stiffness of body i
- d_i,e_i,p_i ..... Damping, rebound and pre-load damping of body i
- O_i ..... Joint position of body i
- q_i ..... Generalized coordinate i
- R_i ..... Rotation matrix of generalized coordinate q_i
- M ..... Mass Matrix
- C ..... Cristoffel Matrix
- P ..... Gravity Vector
- W ..... Work Vector
- μ ..... Grip/Friction/Adhesion/Adherence
- $F_{v/t/l}$ ..... Vertical/lateral/longitudinal force
- $F_{r/f}$ ..... Rear wheel or front wheel force

Contents

CHAPTER 1

INTRODUCTION

1.1 Background

Currently, motorized two-wheelers (M2W or 2RM / Deux roues motorisés in French, for the sake of this work being done in a french company, this term will be used) is an increasingly popular means of transport, especially for the possibilities it offers to avoid traffic congestion. This is justified by the number of 2RMs circulating daily and involving more and more traffic. This increase in the fleet of motorized two-wheelers is followed by the explosion of the number of accidents related to their use.

For several decades, the French society, like all industrialized societies, has recorded on its roads several thousands of deaths and several tens of thousands of wounded per year. These worrying figures have prompted successive French and European governments to make a strong commitment to the fight against road insecurity by adopting severe measures (withdrawal of points from the driver's license, the installation of speed limitation radars, the control of alcoholemia ...). These measures have lead to good results, as the number of deaths has dropped significantly in recent years.

However, while the number of killed has generally decreased on the roads, the 2RM still remains a mode of transport particularly dangerous and its users very vulnerable. The number of drivers of 2RM victims of accidents in France represents more than 23% of all deaths (15% for Europe as a whole) and 40% of total injuries [1].

The development of safety systems for cars, unlike the motorcycle, has experienced tremendous growth. Active and passive (non-mandatory) safety systems have strengthened the safety of motorized cars, the main ones being the conductive Airbags and passengers, brake booster, traction control, seat belt pretensioners. During the same period, the delay by the bike has increased considerably. The most prominent example is that of ABS, which has been in existence for more than 20 years and is still not required, while the braking resistor is relatively light in the market. still remaining marginal. The latest technological innovation in this area is the Airbag, which has only required 15 years of Honda's development, which should be critically reviewed for its effectiveness, because of the lack of cockpit.

Indeed, manufacturers' policy in terms of safety systems, following the 2RMs, has been geared towards adapting existing technologies to four-wheeled vehicles. to the world of two-wheelers. However, the particularly complex dynamics of two-wheeled vehicles makes any trans-

position of the safety system, developed for the auto-mobile world, difficult or even ineffective. It must then be taken into account that 2RMs have a specific dynamic behaviour that will sometimes lead to greater control difficulties. Their size and performance can create particular difficulties.

1.2 Motivation and Objectives

It is well known that the most dangerous situation where a two-wheeler is at a high risk of falling (instability) is in a cornering situation (turn situation), especially that a motorcycle is inherently unstable and its stability is usually hard to evaluate, and depends on numerous and multiple factors such as forward speed and steering force.

It is thus very important to consider a model that takes into account this situation, and predicts the 2RM's dynamics with most fidelity in such a scenario, that would of course include the road profile, the adherence, and the different angles and positions to fully describe it.

Not surprisingly, this work focuses and tries to help fill the gap of an effective safety offer for 2RMs to reduce the number of deaths, its objective being to develop a precautionary adherence estimator in corners, we would do this using model based / state based observers. For this, the choice of a realistic model with a realistic tyre model with all the important degrees of freedom that a real motorcycle has, is crucial.

1.3 Host Company

This work is part of an internship realised within the french state company Cerema, a french acronym that stands for : The center of studies and expertise on risks, the environment, mobility and development, and specifically within the Lyon Laboratory Department, this section presents these two entities in general as well as their activities and research interests.

1.3.1 Presentation of Cerema

The center of studies and expertise on risks, the environment, mobility and development or Cerema (Le centre d'études et d'expertise sur les risques, l'environnement, la mobilité et l'aménagement, in french) is a public administrative institution under the joint supervision of the French Minister of Ecology, Sustainable Development and energy, and the Minister of Transport, Equality of Territories and Rurality. Cerema develops close relationships with the local authorities that are present in its governing bodies. It was created on January 1, 2014. Its head office is located in Bron, on the site of the former CETE Lyon

1.3.2 Cerema's activities and objectives

Cerema's missions concern all aspects of planning and sustainable development (town planning, environment, transport infrastructure, risk management, etc.). It provides support, in particular, to local authorities and decentralized State services.

Thanks to its multidisciplinary research potential, its technical expertise and its transversal know-how, Cerema intervenes in particular in the fields of planning, housing, the city and sustainable buildings, transport and their infrastructure, mobility, road safety, the environment, risk prevention, the sea, energy and the climate. Cerema's mission is to provide enhanced scientific and technical support for Develop, implement and evaluate public policies for sustainable development and development, involving all the stakeholders involved (State, local authorities,

economic or associative actors, scientific partners).

For this, the Cerema :

- Develop methodologies and tools to respond to new modes of territorial management.
- Works closely and in complementarity with all actors (partnerships, co-construction, animation and participation in networks, implementation of projects)
- Ensures the link between research developed in research organizations and application in the field, through continuous innovation and experimentation
- Develops a multidisciplinary and transversal approach that integrates all environmental, economic and social factors
- Provides state and territorial support in terms of engineering and technical expertise on sustainable development and development projects
- Assists public clients in managing their transport infrastructure assets and real estate assets
- Contributes to the standardization activity and the development of regulations and technical methodology on priority issues at national, European and international levels
- Promotes the rules of art and know-how developed in the framework of its missions, diffuses them and capitalizes them

For the accomplishment of its missions, the establishment implements activities of advice, assistance, studies, control, innovation and experimentation, expertise, tests, research and capitalization. dissemination of knowledge as is show in Figure 1.1.

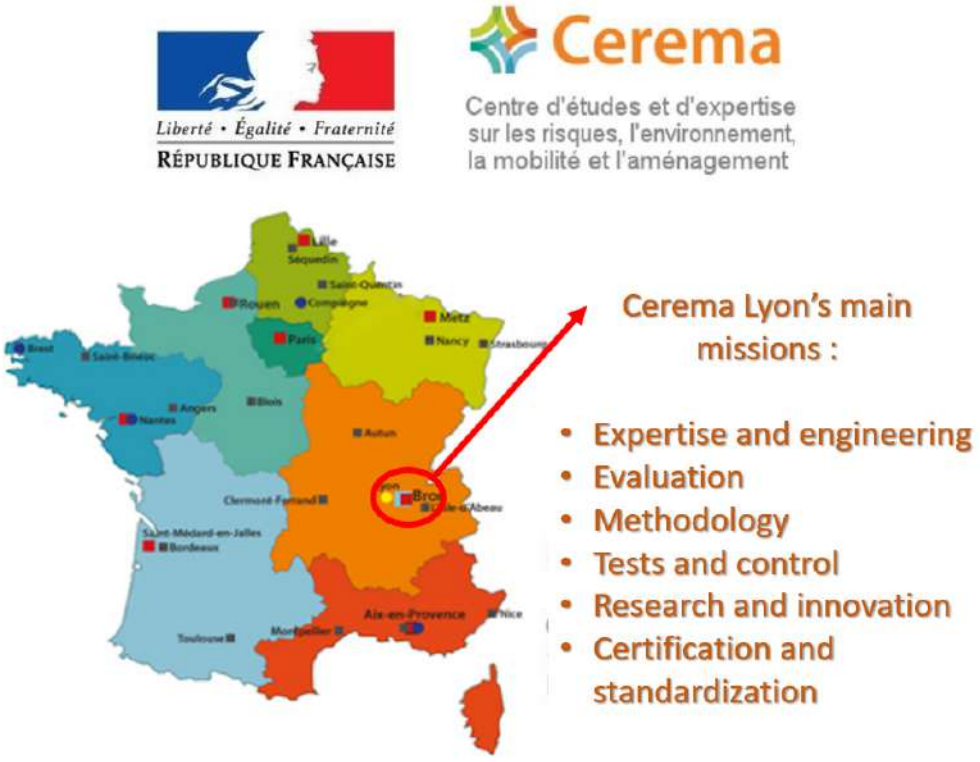

Figure 1.1: Cerema Lyon's main activities.

1.3.3 DLL : Lyon Laboratory Department

The site of Bron in which the internship was done, includes three entities :

- The management and support functions of Cerema Center-Est.
- The laboratory department of Lyon.
- The mobility department.

The laboratory department of Lyon is specialized in the following themes (Fig. 1.2) :

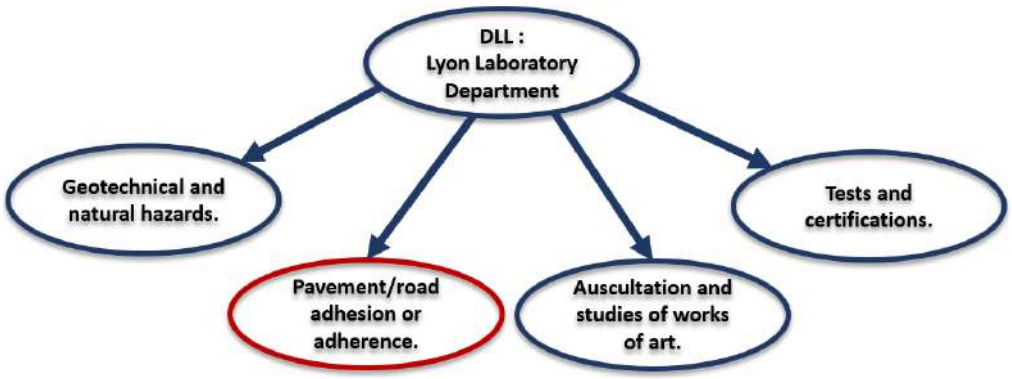

Figure 1.2: DLL's missions and research fields.

the French government decided to make the fight against the road accidents one of the large programs of its actual period. In spite of encouraging results obtained since the installation of speed control systems, the motorcycle remains a particularly dangerous mean of transport: the number of death is still very high, and if one takes account of the number of travelled kilometres, the risk of death for a motorcycle rider is 21 times higher than that of other transportation modes.

Even if motorcycles are now experimenting several electronic equipments such as front-rear coupled braking, ABS systems on the top range models, accident still occur because of inadequacy between the dynamics, the inputs of the driver (or various other inputs) and infrastructure characteristics, accidents occur because of a loss in stability, and a loss in stability is due to an interrupted or a too weak of an adherence. In fact, the driver could always be surprised by sudden change in road curvature or profile which affect adherence, his inputs could lead to overreactions as a consequence. This is why one of the most important roles of the Lyon Laboratory Department is studying road adherence.

1.4 Contribution

This report describes a motorcycle model that unifies all motorcycle dynamics in one model. The model is robust since it is valid for all driving conditions of a motorcycle, including turning or cornering situations.

This motorcycle model available in literature has its roots in robot modelling and will be coupled with a tyre-road model. This model will be used to elaborate a state observer that will be used to estimate the forces applied to the motorcycle, and consequently the adherence in cornering situations, in order to asses and analyse stability in these situations used to eventually consider a security system as is shown in figure 1.3.

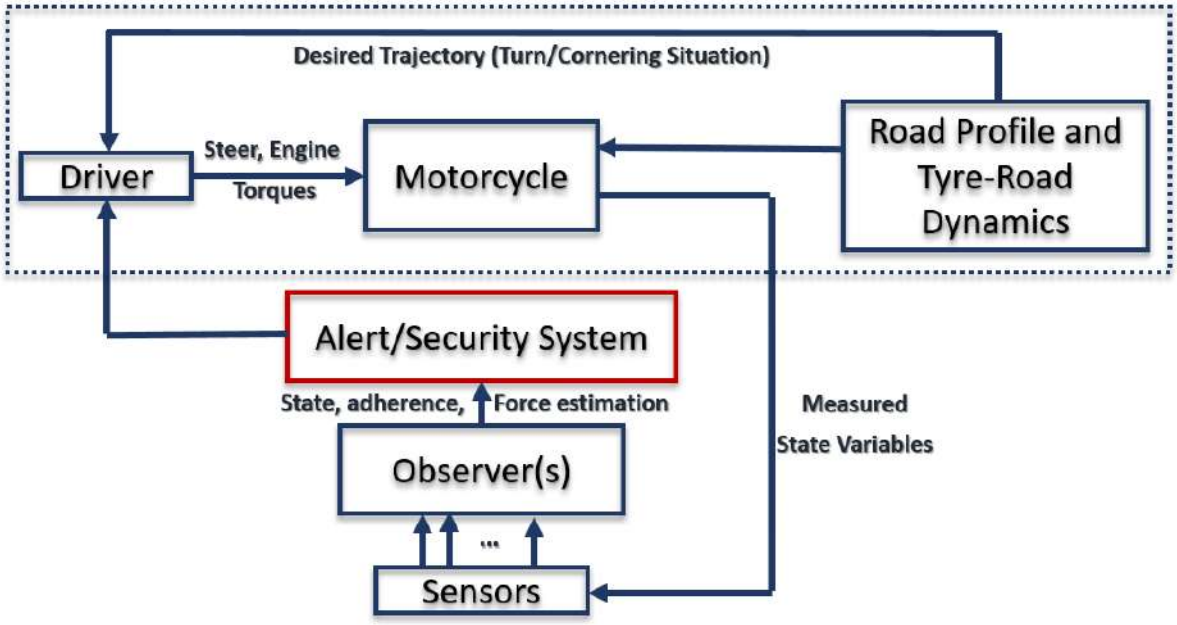

Figure 1.3: Architecture of the estimation system.

1.5 Outline and Structure of the report

The "autonomous motorcycle" model is a model that includes all the possible important degrees of freedom in a realistic motorcycle, and that is valid in all situations, even those involving corners and turns allowing for more efficacy when it comes to state estimation and stability analysis. In Chapter 1, an elaborate introduction to the problem dealt with in this report has been explained as well as the objective of this work.

Chapter 2 starts with a literature review. The literature review is divided in two main topics, namely motorcycle dynamics in cornering situations, which itself is divided into three parts : Motorcycle and tyre models, and stability in cornering situations.

Chapter 3 of this report explains the derivation of the equations of motion of a motorcycle. This involves the lagrangian method and includes Coriolis and all gyroscopic terms (made by W. Ooms BSc. [2].). The model, generalized coordinates as well as Tire-Road contact dynamics are explained, and the model's general architecture is given. The equations of motion are programmed in MATLAB/Simulink.

The criteria based stability is then studied in Chapter 4 for different planes and variables in multiple simulated cornering situations. The design of an elaborate observer is the main topic of Chapter 5. Chapter 5 starts with a discussion of several ways of observing and estimating the state variables and a solution that does not involve all parts of the motorcycle model for this sake has been studied as well.

CHAPTER 2
LITERATURE REVIEW

Introduction

The literature review is divided into two main topics. These topics are the motorcycle model, observers. A good starting point to learn more about motorcycle dynamics, is the book of V.Cossalter "Motorcycle Dynamics" [5].. Although this book does not explicitly cite a certain motorcycle model, it does provide a lot of insight in the kinematics and dynamics of motorcycles. It should be noted that for our case, controlling the motorcycle is not the focus point, but rather studying and estimating its stability using observers, driver-less motorcycle models were therefore targeted for study.

2.1 Motorcycle dynamics in Cornering Situations

As this work focuses on stability analysis of motorcycles in cornering situations, choosing, studying and establishing a model based on motorcycle dynamics that best describe and predict the vehicle's behaviour in such cases, is the objective. Many motorcycle models have been developed in literature, two parts need to be considered however, the motorcycle model and the tire model.

Although many models are available from literature as a set of first order differential equations, most of them are linear, and parameters used in these models can be fairly meaningless especially for stability analysis. Therefore, many other factors should be taken into account when establishing a model.

2.1.1 Motorcycle Models

From a modelling point of view, simplified motorcycle models are similar to simplified bike models (Modèles bicyclette), and can be used to represent either of the two. Therefore, bikes and motorcycles are treated as the same. Many models describing bike and motorcycle dynamics can be found in literature today. The simplest models that can still reveal some of the dynamics are second order. Examples of these models are [6] and [7]. These models stem from the beginning of the twentieth century.

These models are very simplistic and cannot be used for a realistic dynamic motion simulation. These models also do not predict a self-stabilizing velocity region for the motorcycle. A picture of a simple bicycle model is drawn in Figure 2.1, [6].

In the first half of the twentieth century, the investigation of the stability of bikes has lead to ever more complex mathematical descriptions of bikes and as time progresses, the order of

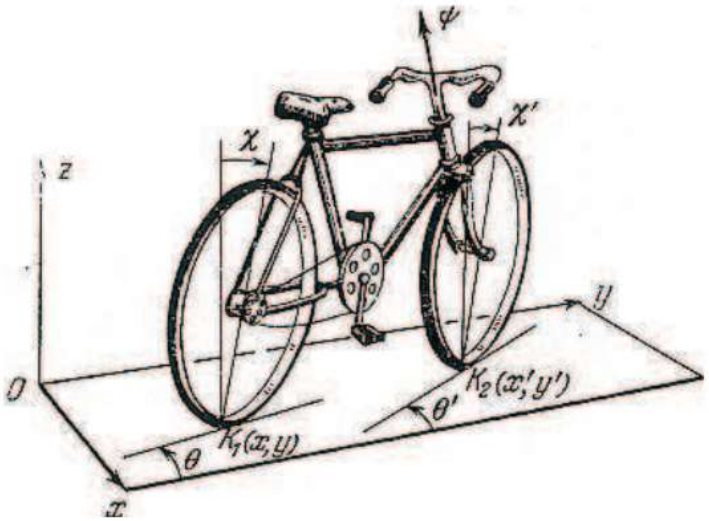

Figure 2.1: Simple bicycle model. [6]

.

these models increases as well.. A good example is the work of Döhring [8]. [9]'s description of Döhring is complex and accurate. However, in that time however, there was no possibility to evaluate the equations of motion, since there was no computer based verification available.

With an ever increasing complexity of models, also the number of parameters increases. These parameters have to be estimated and inaccurate parameters can lead to an inaccurate model. A good balance between model complexity and number of model parameters is thus important. A literature study reveals that different models require different sets of parameters. This has a large impact on the model size, but also on ease of measurement. Some variable definitions are easier to measure on a real bike than others. Another thing to mention is that the order of a bike model varies between two and almost infinite. The choice of the number of degrees of freedom is important since it defines which physical phenomena can be simulated and which cannot.

With the diffusion of computers, more advanced software packages arised as well, that made hand calculations old fashioned. With model based simulations an almost unlimited number of DoFs (degrees of freedom) can be utilized. Software packages can nowadays predict the motorcycle dynamics and motion without explicitly requiring the equations of motion. Although the motion itself may be sufficient, the equations of motion give more insight in the motorcycle behaviour.

In work of Oms [2] the minimal number of degrees of freedom were sought that can still predict the position of the motorcycle in three dimensional space as a function of time. A two degree of freedom motorcycle model is too simple to be used for stability analysis purposes. To be able to study the stability in turns, at least 6 degrees of freedom (DOF) are needed, namely to describe the position and orientation of the motorcycle as a rigid object in three dimensional space. Reference [5] summarizes the most important degrees of freedom in a motorcycle to be the rotation of the handlebar, the suspension and the rotation of the wheels and explains that the absolute minimum would be 7, 6 DoFs in a conventional 3D space and the rotation or steering of the handlebar. With suspension and rotation of both wheels, this adds up to 13 DoFs.

2.1.2 Tyre Models

The tyre is probably the single most important component of the motorcycle, which defines the largest part of the motorcycle dynamic behaviour, especially considering the fact that what matters to us the most here is stability analysis, meaning that adherence is important, and adherence is accurately simulated or calculated using an accurate tyre-road model. This is due to the tyre being the only component that delivers desired interaction forces with the environment of the motorcycle.

Several mathematical tyre models have been developed in the twentieth century. These models range from mainly theoretical descriptions to empirically derived descriptions. The goal of every model is to represent the tyre dynamic behaviour accuratily. The bike models developed at the beginning of the twentieth century did not include a tyre model at all and treated the tyre as a simple kinematic constraint. For example in Reference [10], the wheel in this model is a body fixed to the rear frame that is able to move in longitudinal direction, and not in lateral direction and the rolling of the wheel is not included.

Other advanced models such as the University of Arizona tyre model and the TNO-Delft tyre model [12], are able to slip in longitudinal direction, as well as sideways, these two models are basically the same, except for some minor slip definitions. They use the slip and camber angle in the contact patch between the tyre and the road in order to generate a force. Tyre force is believed to be a result of microscopic electromagnetical force. Therefore the force as a function of slip assumption is justified.

2.1.3 Stability and adherence in Cornering Situations

We have already established that a motorcycle is inherently and naturally unstable, even more in corners and turns, and even with an initial speed, a lot of reasons might lead to this instability, reasons that might or might not be under the control of the driver :

- Intersections : Due to anything that could obstruct the driver's line of sight (trees, parked vehicles, signs...).
- Roundabouts : They favour driving at excessive speeds, which is problematic in general, especially with a weak entry angle.
- Urban Areas : The design of rolling urban infrastructures, with a visual perspective with large and multiple pathways, favours overflows of queues.
- Pavement's or Roadway's adherence : To illustrate the importance of adherence, a study was conducted in the United States between 2001 and 2004, which accounts for no less than 97% of fatal accidents as a single vehicle on wet road [3], study in Britain reported that 2RMs are more likely that cars to drive on both dry roads (17.9% of landings versus 10.4% for cars) and wet (26.2% against 18.6% for cars), and are particularly vulnerable in the presence of mud or oil on the roadway (66.4% vs. 52.3%) [4].

All of these general and environment related factors might affect the stability of a motorcycle, in literature, the most valued factor in the one related to adherence, as in can in a way be controlled, but many other factors are analysed. In this work we have divided them into two parts, non numerical factors or factors relative to the driver's surroundings and uncontrollable factors, and numerical factors that can be programmed.

2.2 Observers

An observer is a dynamic system that can reconstruct or estimate in real time the current state of a real system from the available measurements, the inputs of the real system and a prior knowledge of the model. It then makes it possible to follow the evolution of the state of the system in real time. The observer also allows us to estimate other parameters related to the behaviour of the vehicle, such as tire / ground contact forces or the detection and isolation of faults or failures.

Initially the systems approached were the linear systems, for which the observers of Kalman and Luenberger gave good results. The Kalman filter is used in the case of stochastic systems by minimizing the covariance matrix of the estimation error, and the Luenberger observer has been used for deterministic linear systems.

In the case of non-linear systems, state observation is a little more delicate and there is currently no universal method for observer synthesis. The possible approaches are either an extension of linear algorithms or non-linear algorithms specific. In the first case, the extension is based on a linearisation of the model around an operating point. For the case of specific non-linear algorithms, the numerous researches carried out on this subject (cf. [13], [14]) gave birth to numerous algorithms of observation. We will present these algorithms in a later chapter.

1. Non-linear transformation methods: This technique uses a change of coordinates to transform a non-linear system into a linear system. Once such a transformation is made, the use of a Luenberger-type observer will be sufficient to estimate the state of the transformed system, and thus the state of the original system using the inverse coordinate change.

2. Extended observers: In this case, the observer's gain is calculated from the linearised model around an operating point. This is for example the case of the extended Kalman filter and the extended Luenberger observer.

3. Generalized Luenberger Observers (OLGs): This is a new type of observer that has recently been proposed for the class of monotonic systems. This new design consists in adding to the Luenberger observer a second gain inside the nonlinear part of the system.

4. High gain observers: First introduced in [15], this type of observers is generally used for Lipschitz systems. Its name is due to the fact that the gain of the chosen observer is sufficiently large to compensate for the non-linearity of the system.

5. Sliding Mode observers : This type of observer is based on systems with variable structure [20] (Emelyanov 1967). It has good robustness properties with respect to parametric errors and bounded disturbances. For this and other reasons, the sliding mode observer will be used later to estimate vehicle condition and tire / road contact forces.

6. Observers based on contraction theory : This type of observers (First introduced in [16], [17], [18] and [19]), as the name implies, is based on the theory of contraction used as a tool for analyzing convergence. This technique leads to new conditions of synthesis different from those provided by the preceding techniques.

2.3 Conclusion

In this chapter, every study element that can be potentially needed for our work has been reviewed from existing literature, from motorcycle models and the choice, tyre-road contact dynamics, stability and adherence and finally the observers. The next chapter discusses modelling of the motorbike.

CHAPTER 3

MODELLING AND SIMULATION

Introduction

In this chapter, the model that was picked is a thirteen degrees of freedom motorcycle model is derived. It is obtained by deriving the equations of motion, it is based on the reference [2], the base in his work that was done for an eleven degrees of freedom, being the derivation of the equations of motion, it is believed that the model is going to be accepted and exploited more easily (Fig. 3.1).

The chapter starts with an introduction to the model, a description of the bodies that make up the motorcycle, and the reason for this choice, the choice of generalized coordinates and parameters is also discussed here. The model is formulated on the so called Euler-Lagrange equations, for this, the forces (and thus works) exercised on the motorcycle are derived, the position vectors are needed for this, and are obtained as a mathematical function of the parameters (that have been chosen) and the generalized coordinates, the final system's architecture is given and simulation results are presented.

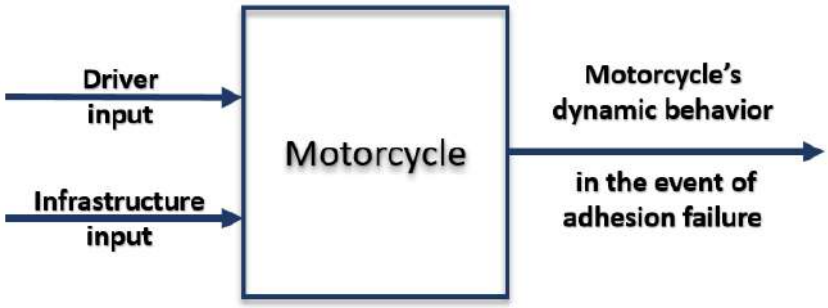

Figure 3.1: Motorcycle global model.

3.1 13 DoFs Motorcycle Lagrangian Model

Just as in [2], the motorcycle model presented here is a set of thirteen second order differential equations instead of just eleven. These equations are derived from classical mechanics and describe the motion of the motorcycle as a function of the forces acting on the separate bodies of the motorcycle. Therefore, these equations are also called the equations of motion. The basis

of the motorcycle motion equations are the Euler-Lagrange equations.
The Euler-Lagrange equations can be stated as :

$$M(q) \cdot \ddot{q} + C(q, \dot{q}) \cdot \dot{q} + P(q) = W(q, \dot{q}) \tag{3.1}$$

In the Lagrangian equation 3.1, q is a vector containing thirteen independent, called generalized coordinates. These coordinates are a bunch of variables that are independent of each other and that describe the system's positions (whether it be positions or angles). The first derivative with respect to time of the generalized coordinates is $\dot{q}$, and the generalized coordinates' second derivative with respect to time is $\ddot{q}$. These two vectors ($\dot{q}$ and $\ddot{q}$) are called generalized velocities and generalized accelerations respectively.
The meaning of the other terms is explained thoroughly in the next section. It is imporatant to note that the equations of motion in this form comes from robot modelling, (refer to [21], "Robot modelling and control").

3.1.1 Model description

Motorcycle bodies

The motorcycle is modelled as six rigid bodies represented in Fig. 3.2.. These rigid bodies are :

1. **Rear Wheel :** along with the front wheel are one of the most important parts of the motorcycle, as they define most of the generalized coordinates as we are going to see in subsection 3.1.1.

2. **Swingarm** : It is sometimes argued that the dynamics of the swingarm are neglected, the main reason for including it in the model however is to make a clear distinction between sprang and unsprung mass, by separating it from the front fork.
   The vertical dynamics can therefore be united with lateral dynamics, which is important for transient cornering dynamics even at large forward velocity and a sharp turn radius.

3. **Main body** : It contains the largest part of all mass. The engine, transmission, fuel tank, frame and seat are all parts of the main body, this is the most important component of the motorcycle.

4. **Steering head** : The steering head is connected to the main body and the front fork and the three positions is space of the motorcycle are defined by it.

5. **Front Fork** : is connected to the front wheel as well as the steering head, and represents the unsprung mass.

6. **Front Wheel** : same as the rear wheel, but is connected to the front fork.

The parts in this choice of division form a path starting at the rear wheel and ending at the front wheel. Expanding the model by separation of the main body into smaller bodies, it is thus easy to expand the current model, since the newly defined bodies are not part of this chain, but can be added on top of the main body.

It is also to be noted that the dynamics of the separate bodies have comparable timescales, each having a direct contribution to the overall dynamics of the motorcycle. High frequency

dynamics such as the valve train will need very small time steps, while the objective, is more on the global motion and in the lower frequency dynamics. It is surely better to model these dynamics as noise, or as disturbance force term.

These dynamics are neglected in this report and not considered, since it will not severely influence the overall dynamics of our model. The driver is also not included in the model since it is not part of the motorcycle as it is not a rigid body with respect to the other components of the motorcycle bodies and the motion that is executed by the driver is unpredictable and cannot be precisely controlled.

It is clear from 3.1, and meaning of the terms explained in subsection 3.1.1 that the position vectors of these bodies should be written as a function of the generalized coordinates q. To do that, the set of generalized coordinates should be defined first.

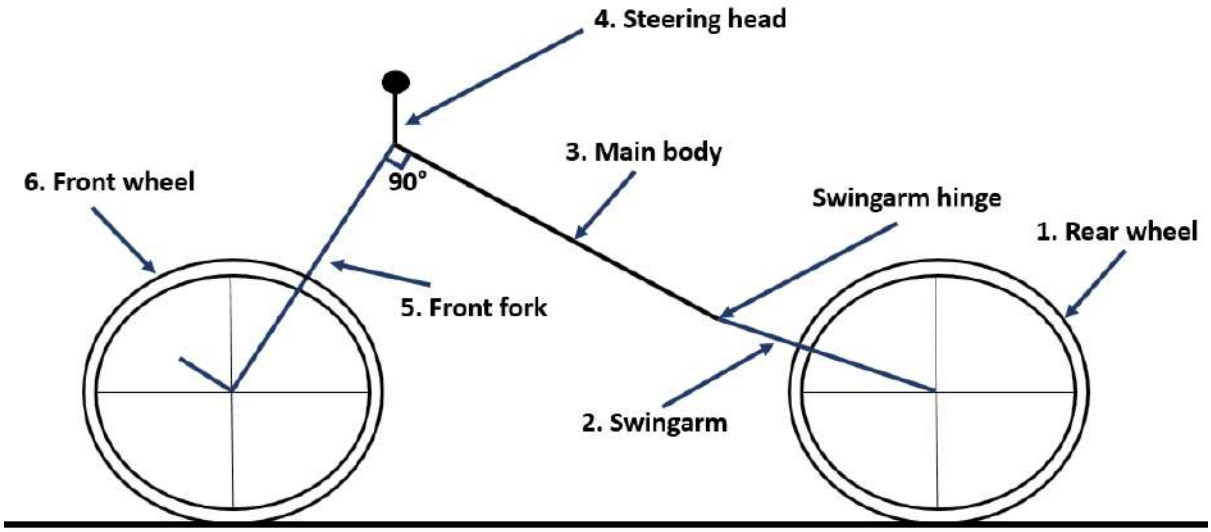

Figure 3.2: Body composition of the motorcycle model.

Generalized Coordinates

Choice of the generalized coordinates :

The motorcycle model presented has thirteen degrees of freedom (DoFs). These are defined as follows :

- The motorcycle as an object in 3D, three dimensional space has six degrees of freedom: three translational, and six rotational degrees of freedom, three of the front wheel and three of the rear wheel. **9**
- On top of these nine DoFs, there are two DoFs for the front and rear suspension deflection. **2**
- Two DOFs for the rotation of the wheels, front and rear. **2**

Table 3.1: List of generalized coordinates and their corresponding descriptions.

Generalized coordinate	Notation	Description	Unit
$q(1)$	q_x	x-coordinate	m
$q(2)$	q_y	y-coordinate	m
$q(3)$	q_z	z-coordinate	m
$q(4)$	q_0	Rear yaw angle	rad
$q(5)$	q_1	Rear pitch angle	rad
$q(6)$	q_2	Rear roll/camber angle	rad
$q(7)$	q_4	Front yaw angle	rad
$q(8)$	q_5	Front pitch angle	rad
$q(9)$	q_6	Front roll/camber angle	rad
$q(10)$	q_7	Swingarm angle	rad
$q(11)$	q_f	Fork length	m
$q(12)$	q_8	Rear wheel orientation	rad
$q(13)$	q_9	Front wheel orientation	rad

Together, this adds up to thiteen DOFs and are illustrated in figure 3.3. 13 DoFs means that thirteen independent generalized coordinates have to be defined. In the process of deriving the model equations, several iteration steps have led to different sets of generalized coordinates.

Each generalized coordinate has been given a name and notation so that it can easily be referred to. The coordinates and their names are summarized in Table 3.1. The order in which the generalized coordinates are stored in the vector q is the same as in Table 3.1.. These generalized coordinates will thoroughly be explained in the next section.

Description and meaning of the generalized coordinates :

q_x, q_y, q_z : x, y and z coordinates.

The first three generalized coordinates are translational and measured in meters. the freedom to translate is given to the motorcycle via these coordinates. The x coordinate, and the y coordinate are not the same as the lateral and longitudinal directions of the motorcycle.
These x-, y-, and z-coordinate together form a 3 dimensions vector, and define the position of the joint between the main body/frame and the steering head. This point is defined in a three dimensional space and are measured with respect to an inertial reference frame fixed to the earth and independent of any coordinate frame internal to the motorcycle.

q_0, q_4 : Rear and front wheel yaw angles

the Rear yaw angle is the vertical orientation of the main body of the motorcycle. It is the angle between the x axis of the global motorcycle's reference frame and the line of intersection between the ground plane and the plane of symmetry of the motorcycle. The rear wheel as well as the swingarm with the main body will experience the same yaw angle. the same can be said for the front wheel yaw angle except that it's the relative angle between the motorcycle main body and the steering head. a positive yaw angle means a rotation to the left.

No matter if the bike is standing straight, or laying on its side, the yaw is always a rotation around the axis (whichever) perpendicular to the plane spanned by the x and y coordinates. That is, Yaw maps the x coordinate of the global reference frame to the longitudinal coordinate of the motorcycle. The yaw coordinate is visualized in figure :

q_1, q_5 : Rear and front wheel roll/camber angles

The rear roll/camber angle is the same as the frame inclination angle, inclination of the main body. Therefore, it is also the inclination of the motorbike swingarm. In papers, this coordinate is - most of the time - interchangeably called roll or camber.

The font roll angle is defined in the same way, it is however affected by the steering joint, as the front wheel is consolidated with the front fork, contrary to the rear wheel which is considered to have the same roll as the main frame. This is the angle between a vector that is perpendicular to the steering axis and front wheel rolling direction, and the ground plane. It is the angle between the wheel plane of symmetry and the line normal to the road plane.

From this definition camber angle is the angle between the tire vertical plane and the absolute vertical plane. this means that on banked corners, it is theoretically possible to have a camber angle of 90 degrees or more.

Inclination is the angle that maps the absolute vertical axis to the motorcycle's vertical axis. This is visualized in figure 3.2.

q_2, q_6 : Rear and front wheel pitch angles

Pitch angles (front or rear) is the toughest generalized coordinate to explain. In fact, in a lot of texts about the subject, pitch is given as the angle between the horizontal ground plane and a vector fixed to the motorcycle in its plane of symmetry. This definition is not accurate enough. another definition would be that the pitch is the rotation around an axis perpendicular to the motorcycle plane of symmetry that is needed to keep the front wheel on the ground surface.

In the model studied and used in this work however, these angles need to be independent coordinates, and the definitions given above although correct, imply that these coordinates are dependent and thus cannot be used.

The best way to define this coordinate is to say that it is the rotation around whichever axis perpendicular to the motorcycle's plane of symmetry, that is there to give its main body its final DoF and allow it to obtain any orientation in space.

Note that when the camber/roll angle is 90 degrees, pitch coincides with yaw. For this, a camber angle of 90 degrees in normal operating conditions is considered to imply that the motorcycle is unstable, a maximum roll angle is later defined to avoid this.

q_3 : Steering angle

This angle is not a generalized coordinate but will be explained because of its importance, in fact, the steering angle is the relative angle between the motorcycle main body and the steering head. This angle is measured perpendicular to the steering axis that of the steering head.

q_7, q_f : Swingarm angle and front suspension

The coordinate q_7 (swingarm angle) is a rotation to map from the fixed world directly to the pitch angle of the swingarm. It has a similar meaning as the pitch angle q_2 for the main body, but then for the swingarm. This coordinate allows the swingarm to move with respect to the frame.

The front suspension translational degree of freedom of the front fork is called q_f. the notation f is used to refer to the front part of the suspension.

These two coordinates are important to the dynamics because they describe the relative motions of the wheel centre with respect to the frame.

q_8, q_9 : Rotation of the rear and front wheel

The coordinates q_8 and q_9 are the rotation of the rear and front wheel respectively. These coordinates are added to include the longitudinal slip from the tire model. The tire model that we're going to talk about in subsection 3.2, calculates forces applied on the tire because of the velocity differences between the road and the road-tire contact patch.

q_8 and q_9 also have a close meaning to the pitch angle q_2 for the main body, but this time for the wheel bodies. These angles are absolute angles.

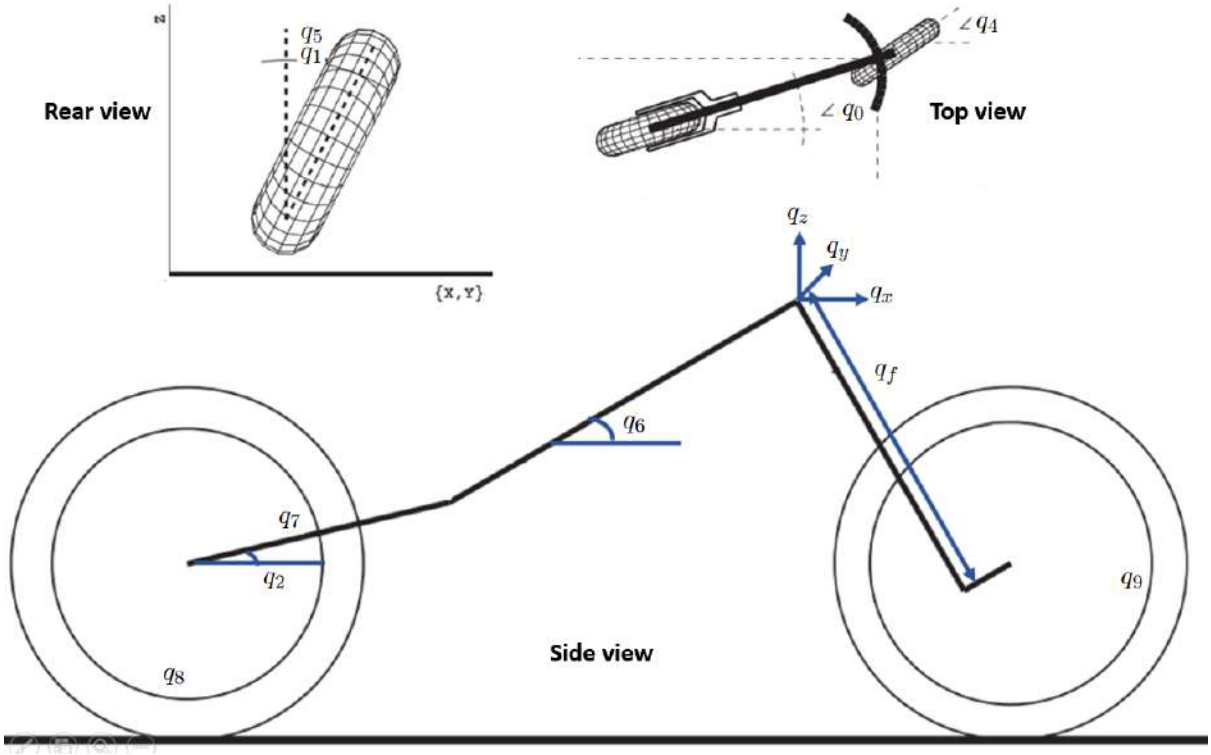

Figure 3.3: Illustrative representation of generalized coordinates.

Meaning of Lagrangian terms

Equation 3.1 describes the general architecture of the used model, this section explains each term of the terms used in the equation. But first it is important to define the joints that the motorcycle as a whole is comprised of, meaning the connection between the different components of the motorcycle, these are defined by local rotation frames, these are defined in subsection 3.1.2.

Acceleration term $M(q)$: The first term of 3.1 is the only term that contains the generalized accelerations. The matrix $M(q)$ is the dynamic mass matrix (a 13 by 13 matrix) and is a function of the generalized positions and the motorcycle parameters. Because the model doesn't contain any transport kinetic energy and mutual kinetic energy terms, the $M(q)$ can be formulated as :

$$M(q) = \sum_{i=1}^{n} \frac{m_i}{2} \cdot (\frac{\partial O_i}{\partial q})^T \cdot \frac{\partial O_i}{\partial q} + \sum_{i=1}^{n} \sum_{j=1}^{3} (\frac{I_{ji}}{2} \cdot \omega_{ji}^T \cdot \omega_{ji}) \tag{3.2}$$

The following remarks can be made :

- In equation 3.2 there are two terms :
  - The first term sums the translational kinetic energy of all bodies,
  - The second term sums over the rotational kinetic energy of all bodies.

  Therefore, the index $n = 6$, as the motorcycle is divided into six separate bodies.
- The mass of body i is m_i,and O_i (as explained further in the report) is the position of the center of mass of body i.
- The rotational inertia of body i around the jth axis of the inertial reference frame equals I_{ji}, and ω_{ji} is the angular velocity of the ith body around the jth axis of the inertial reference frame. They (I_{ji} and ω_{ji}) can be calculated as follows :

$$\begin{aligned} I_{1i} &= \tfrac{1}{2} \cdot (I_{yi} + I_{zi} - I_{xi}), & \omega_{1i} &= \tfrac{\partial}{\partial q} \cdot (R_i \cdot [0\ 0\ 1]^T), \\ I_{2i} &= \tfrac{1}{2} \cdot (I_{xi} + I_{zi} - I_{yi}), & \omega_{2i} &= \tfrac{\partial}{\partial q} \cdot (R_i \cdot [0\ 0\ 1]^T), \\ I_{3i} &= \tfrac{1}{2} \cdot (I_{xi} + I_{yi} - I_{zi}), & \omega_{3i} &= \tfrac{\partial}{\partial q} \cdot (R_i \cdot [0\ 0\ 1]^T). \end{aligned}$$

  In these equations :
  - R_i is the rotation matrix that maps the vectors of the inertial reference frame to the local orientation of body i,
  - I_{xi} Is the inertia around the body's local x axis,
  - I_{yi} is the inertia around the body's local y axis,
  - I_{zi} is the inertia around the body's local z-axis,
  - The body's local x, y, and z axis are the principal axes of the body.

Velocity term $C(q, \dot{q})$: The second term of equation 3.1 appears from differentiating the kinetic energy towards the generalized coordinates and generalized velocities. $C(q, \dot{q})$is a 13 by 13 matrix containing the contribution of the centrifugal and Coriolis forces to the equations of motion. In literature, $C(q, \dot{q})$ is usually called the Christoffel matrix. The Christoffel matrix can easily be calculated from the mass matrix.

$$C_{kj}(q, \dot{q}) = \sum_{i=1}^{13} \frac{1}{2} \cdot (\frac{\partial M_{kj}}{\partial q_i} + \frac{\partial M_{ki}}{\partial q_j} - \frac{\partial M_{ij}}{\partial q_k}) \cdot \dot{q}_i \tag{3.3}$$

The subscripts i, j and k in 3.4 refer to the elements of the mass matrix and the column of generalized coordinates and have nothing to do with the meaning of the subscripts in equation 3.2.

Gravitational term $P(q)$: The third term on the left side of equation 3.1, due to the fact that the system is located in the earth's gravitational field, arises from potential energy stored in the system . Other forms of potential energy could have been added to this term. For spring and damper terms of suspensions, however, since the non-conservative part of the force must be placed inside $W(q, \dot{q})$, it is easier to place both the conservative and non-conservative force inside $W(q, \dot{q})$. The potential energy due to the earth's gravity field can be calculated as :

$$P(q) = \sum_{i=1}^{6} \frac{\partial O_i}{\partial q} \cdot G \cdot m_i \tag{3.4}$$

- O_i is the position of the center of mass of body i.
- In 3.4, G represents the gravitational vector, and is given as : $[0 \quad 0 \quad -g]^T$.
- And g is the gravitation constant.

Force term $W(q, \dot{q})$: Finally, and as stated previously, the last part of Equation 3.1, consists of all applied forces minus the internal forces.

Internal forces are forces inside the system, that do not deliver work. This term here is called the external force term, and is a form of all virtual works done by all external forces. The virtual work done by the external forces can be calculated using equation 3.5.

$$W(q, \dot{q}) = \sum_{i=1}^{m} \frac{\partial O_i^T}{\partial q} \cdot F_i + \sum_{i=1}^{n} \frac{\partial^T}{\partial q} \cdot T_i \tag{3.5}$$

Once again, O_i is the position of the center of mass of body i, these terms will be further elaborated in the next subsection.

The virtual work term, $W(q, \dot{q})$, is divided into a sum of seven ($m = 7$) applied forces (F_i) and three ($n = 3$) applied torques (T_i).

- Three forces are acting on each wheel (Longitudinal, lateral and vertical for each wheel).
- The front suspension is treated as an applied force, but the rear suspension is handled as an applied torque.
- Two other torques are used as control variables (engine and steer).

All of these are given in more details in Section 3.2 (Model architecture), where the forces and torques are elaborated further.

Before this however, we need to distinguish between the separate bodies and develop expressions for positions and orientations of each of the component bodies, these being is dependent on the generalized coordinates vector (q) but also the motorcycle parameters, they will be defined first.

It is also noted that equation 3.1, and all of its terms is calculated using Maple before being implemented on Matlab.

3.1.2 The system parameters

The motorcycle model uses parameters that can be divided into three groups :

- Kinematic parameters,
- Inertia or dynamic parameters,
- Force parameters.

They are presented and explained in the following subsections.

Kinematic parameters

The kinematic parameters are here to describe the geometrical dimensions of the motorcycle as well as the wheels. They're also used to describe the position of the joints and rotation points.

These parameters are presented in the following table (3.2), and shown in Figure 3.4.

Table 3.2: List of Kinematic parameters.

Kinematic parameter	meaning	Unit
l_2	Swingarm length	m
l_3	Fork offset	m
l_4	Frame length	m
b_1	Rear tire roll radius	rad
b_6	Front tire roll radius	rad
a_1	Rear tire crown radius	rad
a_6	Front tire crown radius	rad

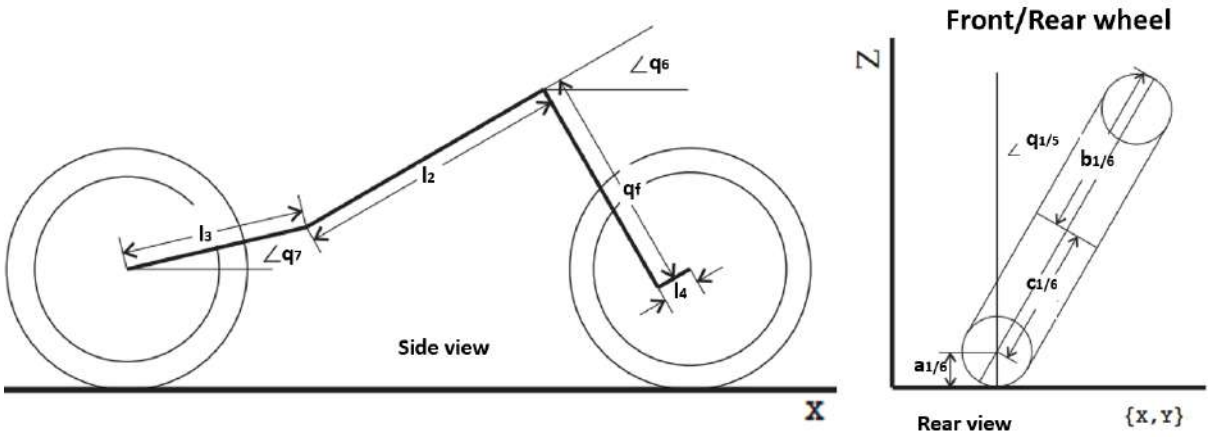

Figure 3.4: Illustration of kinematic parameters.

Where :

$$c_1 = b_1 - a_1, \qquad c_6 = b_6 - a_6$$

Dynamic/Inertia parameters

Dynamic parameters relate specifically to the mass and inertia properties of the different bodies the motorcycle is comprised of.

There are four dynamic/inertia parameters for each body. These are the mass m_i, and the inertia I_i (Table 3.3), the position relative to its nearest joint and the orientation relative to the orientation of the nearest joint, figure ..... shows the joints as well as the positions.

Table 3.3: List of dynamic parameters.

Dynamic parameter	meaning	Unit
m_i	Mass of body i	m
I_i	Inertia matrix of body i measured in mass center	m
p_i	Position vector pointing from the closest joint to the mass center	m

Force parameters

Force parameters described in table 3.4 represent characteristics like spring constant or tire stiffness. They are used in the formulation of the forces. Force parameters can however not be visualized in a figure.

Table 3.4: List of force parameters (Most of them are with no unit).

Force parameter	**meaning**
g	gravity constant
q_{70}	rear suspension neutral angle
q_{f0}	front suspension neutral length
k_1	rear tire vertical spring stiffness
k_2	rear suspension vertical spring stiffness
k_3	front suspension vertical spring stiffness
k_4	front tire vertical spring stiffness
b_1	rear tire vertical damping constant
b_2	rear suspension vertical damping constant
b_3	front suspension vertical damping constant
b_4	front tire vertical damping constant
b_{lr}	rear tire longitudinal damping constant
t_1	rear tire lateral (transversal) damping constant
b_{lf}	front tire longitudinal damping constant
t_6	front tire lateral (transversal) damping constant
d_{lr}	rear tire longitudinal relaxation constant
d_{tr}	rear tire lateral (transversal) relaxation constant
d_{lf}	front tire longitudinal relaxation constant
d_{tf}	front tire lateral (transversal) relaxation constant

Now that the generalized coordinates and the parameters we can write down the position and orientation of the joints and mass centers as those are the ingredients needed to formulate the position vectors and orientation matrices necessary for the equations of motion. They're explained in the next subsection.

Orientation matrices and position vectors :

In this subsection, expressions for particular points inside the motorcycle are given. Because a point inside the motorcycle is given by its x-, y- and z- coordinates with respect to the inertial reference axis, the expression for a point in the motorcycle is given by a vector equation. Rotation of a vector is easiest described with rotation matrices. To rotate a vector, it only has to be pre-multiplied with the right rotation matrix. Therefore, this section starts with the definition of the rotation matrices that are used in the expressions for the positions. The rotation matrices contain sine and cosine functions. For convenience, the sine of q_i is denoted as s_i, and the cosine of q_i is denoted by c_i.

$$s_i = sin(q_i) \tag{3.6}$$

$$c_i = cos(q_i) \tag{3.7}$$

Rotation matrices :

The rotation matrices are stated below. Each of these rotations is a basic rotation. Vectors are used for pointing to a specific joint or location inside the model. These rotation matrices are used to perform a rotation of a vector. The rotation matrix can be seen as a new set of unit length vectors, perpendicular to each other, that together form a new reference frame.

With rotation matrices, a vector can simply be rotated by pre-multiplying the column with the rotation matrix. Frames with multiple rotations can therefore be built from several

basic rotations, but the basic frames have no physical meaning when considered separately. They only mean something in combination with other frames.

In other words, a position is described by a vector which is represented by a column of length three. The matrix that is in front of the vector is the frame in which the vector is expressed.

$$R_0 = \begin{pmatrix} c_0 & -s_0 & 0 \\ s_0 & c_0 & 0 \\ 0 & 0 & 1 \end{pmatrix}, \qquad R_1 = \begin{pmatrix} 1 & 0 & 0 \\ 0 & c_1 & -s1 \\ 0 & s_1 & c_1 \end{pmatrix}$$

$$R_2 = \begin{pmatrix} c_2 & 0 & s_2 \\ 0 & 1 & 0 \\ -s_2 & 0 & c_2 \end{pmatrix}, \qquad R_4 = \begin{pmatrix} c_4 & -s_4 & 0 \\ s_4 & c_4 & 0 \\ 0 & 0 & 1 \end{pmatrix}$$

$$R_5 = \begin{pmatrix} 1 & 0 & 0 \\ c_5 & -s_5 & 0 \\ 0 & s_5 & c_5 \end{pmatrix}, \qquad R_6 = \begin{pmatrix} c_6 & 0 & s_6 \\ 0 & 1 & 0 \\ -s_6 & 0 & c_6 \end{pmatrix}$$

$$R_7 = \begin{pmatrix} c_7 & 0 & s_7 \\ 0 & 1 & 0 \\ -s_7 & 0 & c_7 \end{pmatrix}, \qquad R_8 = \begin{pmatrix} c_8 & 0 & s_8 \\ 0 & 1 & 0 \\ -s_8 & 0 & c_8 \end{pmatrix}$$

$$R_9 \begin{pmatrix} c_9 & 0 & s_9 \\ 0 & 1 & 0 \\ -s_9 & 0 & c_9 \end{pmatrix}$$

These matrices represent respectively :

- R_0 : Rear yaw basic rotation.
- R_1 : Rear roll basic rotation.
- R_2 : Rear pitch basic rotation.
- R_4 : Front yaw basic rotation.
- R_5 : Front roll basic rotation.
- R_6 : Front pitch basic rotation.
- R_7 : Swingarm angle basic rotation.
- R_8 : Rear wheel angle basic rotation.
- R_9 : Front wheel angle basic rotation.

Position vectors :

The position vectors pointing to the center of mass of a body, and the origin of a force or torque are expressed here. O_i is a rotation point. There are eight rotation points in the model and are summarized in table 3.5, and the expressions are given in equation 3.8 [2].

Joint position are expressed as :

Table 3.5: List of joint positions and their short descriptions

Joint position	meaning
O_0	Rear wheel contact patch
O_1	Lowest point in the rear wheel torus centerline
O_2	Center of the rear wheel hub
O_3	Joint between swingarm and main body
O_4	Steering joint: joint between main body and steering head
O_5	Center of the front wheel hub
O_6	Lowest point in the front wheel torus centerline
O_7	Front wheel contact patch
O_{m_i}	position of mass center of body i

$$
\begin{aligned}
O_0 &= O_4 + R_0 \cdot (R_1 \cdot (R_2 \cdot [-l_3 \quad 0 \quad 0]^T + R_7 \cdot [-l_2 \quad 0 \quad 0]^T + [0 \quad 0 \quad -b_1]^T) + [0 \quad 0 \quad -a_1]^T) \\
O_1 &= O_4 + R_0 \cdot (R_1 \cdot (R_2 \cdot [-l_3 \quad 0 \quad 0]^T + R_7 \cdot [-l_2 \quad 0 \quad 0]^T + R_8 \cdot [0 \quad 0 \quad -b_1]^T)) \\
O_2 &= O_4 + R_0 \cdot (R_1 \cdot (R_2 \cdot [-l_3 \quad 0 \quad 0]^T + R_7 \cdot [-l_2 \quad 0 \quad 0]^T)) \\
O_3 &= O_4 + R_0 \cdot (R_1 \cdot (R_2 \cdot [-l_3 \quad 0 \quad 0]^T)) \\
O_4 &= [q_x \quad q_y \quad q_z]^T \\
O_5 &= O_4 + R_4 \cdot (R_5 \cdot (R_6 \cdot [l_4 \quad 0 \quad -q_f]^T)) \\
O_6 &= O_4 + R_4 \cdot (R_5 \cdot (R_6 \cdot [l_4 \quad 0 \quad -q_f]^T + R_9 \cdot [0 \quad 0 \quad -b6]^T)) \\
O_7 &= O_4 + R_4 \cdot (R_5 \cdot (R_6 \cdot [l_4 \quad 0 \quad -q_f]^T + [0 \quad 0 \quad -b_6]^T) + [0 \quad 0 \quad -a_6]^T)
\end{aligned}
\tag{3.8}
$$

All vectors are explained and elaborated in equation 3.8, and previous tables.

3.2 Tire-Road contact dynamics and Adherence

A motorcycle has more or less grip on the wet road... Are the tires soft, medium or hard tires ? these terms are frequently used to define the behaviour and quality of tires and their expected performance vis-a-vis the road surface.

these "street" terms however mean nothing as they're not associated with any numerical values expressed in whatever unit.

The term grip, is commonly known as adherence or adhesion in literature, it is generated through a chemical liaison (like a glue), but also a mechanical deformation, this means that the bigger the contact patch, the greater the grip/adherence (Fig. (3.5).

The tire must perform two tasks :

- Allow the transfer of the driving force or braking force to the ground/road and,
- Generate the necessary lateral forces in order to maintain the equilibrium of the motorcycle in the curve or along a curvilinear path such as for example those generated to avoid an obstacle etc... this part is very important as we focus on stability in curvatures in this work.

At this point, it is also important to understand how the lateral force is generated and how much it needs to be when the bike is running in constant rotation at constant speed (stable condition) and which parameter depends on the force, the latter part is going to be explained in the chapter 4, reserved for stability analysis.

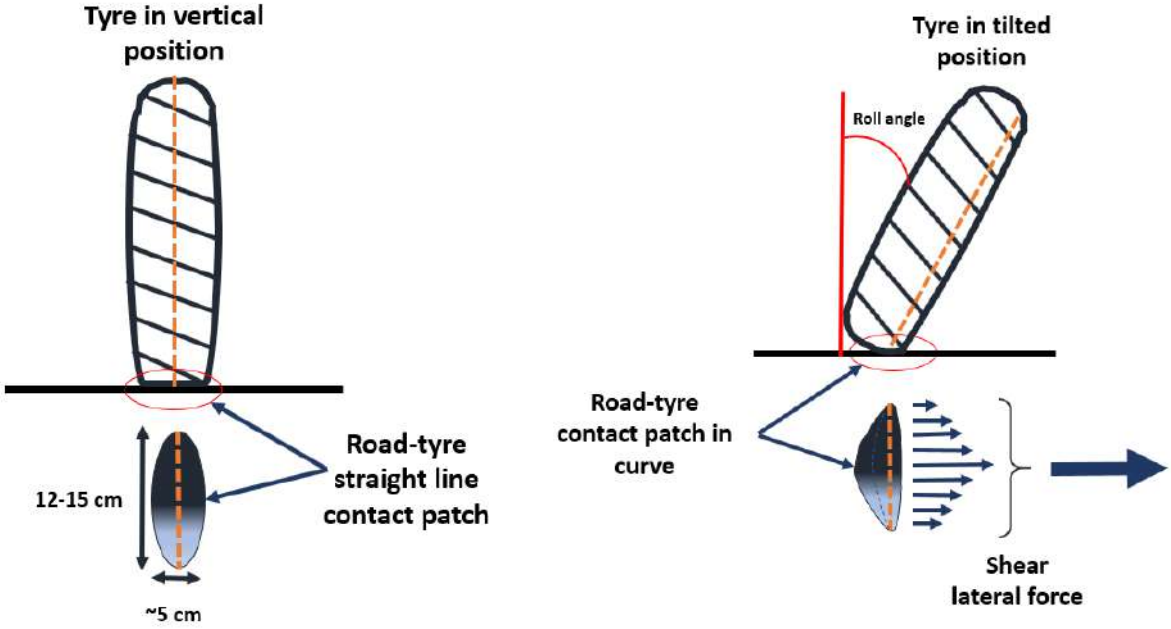

(a) Contact patch when in straight line

(b) Contact patch in curves

Figure 3.5: Illustration of how camber angle affects the contact patch.

It is easy to understand that the **lateral force depends on the normal vertical load** applied on the wheel. A high vertical load creates a high lateral force. Understanding the dependence of the lateral force on the camber angle and the skidding of the tire (tire slippage expressed by a skid angle that will be defined later) is less intuitive.

The lateral force also depends on two other parameters that bikers know very well : tire pressure and tire temperature in working condition, these depend on the tire type and will not by addressed thoroughly in this work.

We first consider the camber angle effect. In a vertical position, the tire footprint is elliptical and symmetrical; The tire footprint shown in Figure 3.5 is painted with shades of gray whose intensity is proportional to the pressure between the tire and the ground, it can clearly be observed form the figure 3.5, that when the wheel is tilted, the rubber particle that through the imprint doesn't follow the path that it would follow if there wasn't the contact between tire and ground. Because of there is contact with the ground the particle has to follow a different path, therefore the ground contact cause a deformation of tire carcass, this deformation generates a lateral force that increases when the camber angle increases.

Understanding better that phenomenon it is helpful to think about a shape-retaining tire, as if it was metallic, in that case the contact patch becomes like a point, there is not carcass deformation, hence the force due to the camber is null.

The camber force depends on shape and dimension of contact patch and the contact patch itself depends on tyre's geometric characteristics (rolling radius and cross section radius, Table 3.2 and carcass lateral/radial stiffness...

Lateral slip effect :

The side-slip angle is the angle between the forward direction and the central plane of the wheel. The contact patch is asymmetrical when the there is lateral slip. In the first part of contact patch the rubber particles tend to follow speed direction but, since the speed direction doesn't coincide to the wheel plane, the particles located inside contact patch are deformed with respect to tire carcass. This is the contact patch part with adherence. When the deformation is al little more, the elastic recall forces due to the deformation of the rubber are greater then the adherence force so the particles start to slider. This is the contact patch part with slide. The integral of contact patch pressure give the lateral force due to the side-slip (Fig. 3.6).

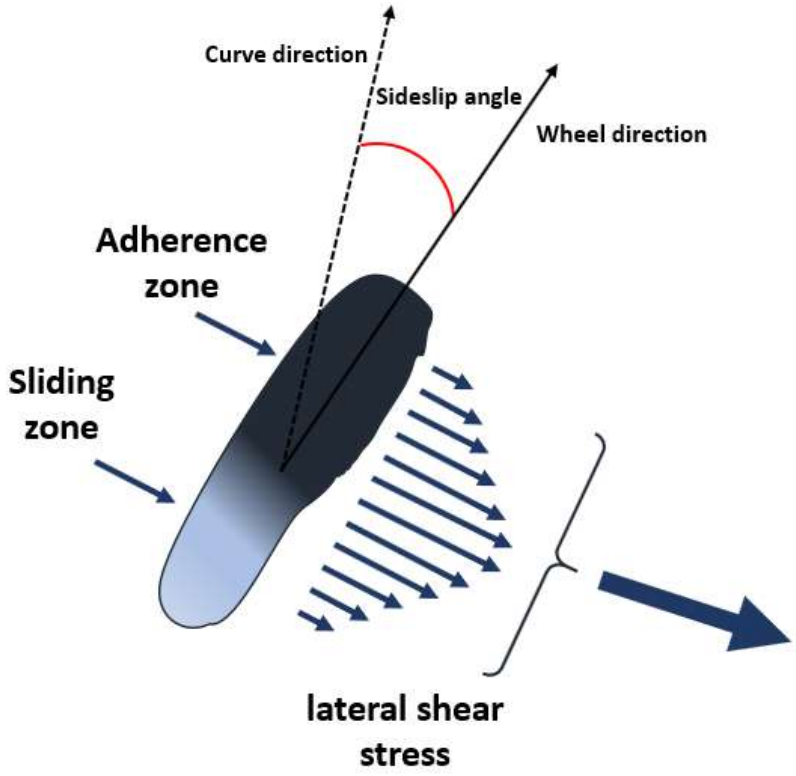

Figure 3.6: Resultant lateral force due to the side-slip angle.

to summarize, apart from the normal force, two main elements contribute to the lateral force : the side-slip angle and the camber angle, the longitudinal force however heavily depends on the engine torque (and obviously the normal force as well).

3.3 Model architecture

The final ingredient before the equations of motion can be derived are the forces and torques. The forces have been mentioned before. to complete the equations of motion two elements are still needed :

- **Forces acting on the motorbike :**
  Forces and torques are calculated in the next section.
- **Virtual work resulting from forces :**
  This is calculated using equation 3.5, since the forces and torques are given, Maple is used for this before it is implemented on Matlab.

It was said that there are seven forces and three torques. These torques are directly related to a specific degree of freedom. The next level are the virtual suspension work terms. Table 3.6 summarizes forces and their brief description, and table 3.7 the resulting virtual works.

Table 3.6: List of forces and torques applied to the motorcycle

Force/torque	**Meaning**
F_{rs}	Rear suspension torque
F_{fs}	Front suspension force
F_{zr}	Rear normal/vertical force
F_{zf}	Front normal/vertical force
F_{lr}	Rear longitudinal force
F_{lf}	Front longitudinal force
F_{tr}	Rear lateral/transversal force
F_{tf}	Front lateral/transversal force
F_{u1}	Input engine torque
F_{u2}	Input steer torque

Table 3.7: List of works resulting from forces/torques

Work	**Meaning**
Q_{rs}	Rear suspension virtual work
Q_{fs}	Front suspension virtual work
Q_{zr}	Rear normal/vertical virtual work
Q_{zf}	Front normal/vertical virtual work
Q_{lr}	Rear longitudinal virtual work
Q_{lf}	Front longitudinal virtual work
Q_{tr}	Rear lateral/transversal virtual work
Q_{tf}	Front lateral/transversal virtual work
Q_{u1}	Input engine virtual work (**2**)
Q_{u2}	Input steer virtual work

Virtual works and the corresponding forces/torques are calculated in the next two subsections.

3.3.1 Input Torques Fu_1 and Fu_2

The two control inputs are engine torque and steering torque, the braking torque is integrated into the engine torque, in fact, when the latter is negative, inferior to zero, it is considered as being a braking action.

3.3.2 Suspensions force and torque F_{fs} and F_{rs}

The suspension force includes some constants and velocities and are given by the equations 3.9.

$$\begin{aligned} F_{fs} &= k_2 \cdot (q_2 - q_6 - q_{70}) + b_2 \cdot (\dot{q}_2 - \dot{q}_6) \\ F_{rs} &= k_3 \cdot (q_f - q_{f0}) + b_3 \cdot \dot{q}_f \end{aligned} \tag{3.9}$$

The parameters needed for these forces are listed in table 3.8, and a short description of their meanings is given.

Table 3.8: Suspension parameters and their meaning

Suspension parameter	Meaning
k_2	Rear suspension spring stiffness
k_3	Front suspension spring stiffness
b_2	Rear suspension damping constant
b_3	Front suspension damping constant
q_{70}	Rear suspension spring neutral angle
q_{f0}	Front suspension spring neutral length

3.3.3 Vertical Forces F_{zr} and F_{zf}

The calculation of the tire vertical force requires information about the vertical position and velocity of the tire contact patch. they're given by equations 3.10. The parameters are explained in table 3.9.

$$\begin{aligned} F_{zr} &= -k_1 \cdot z_r - d_1 \cdot \dot{z}_r \\ F_{zf} &= -k_4 \cdot z_f - d_4 \cdot \dot{z}_f \end{aligned} \tag{3.10}$$

Table 3.9: Vertical force parameters and their meaning

Suspension parameter	Meaning
k_1	Rear tire vertical spring stiffness
k_4	Front tire vertical spring stiffness
d_1	Rear tire vertical damping constant
d_4	Front tire vertical damping constant

We can also integrate the profile of the road to these equations, specifically into z_r and z_f. Consider d an input containing the road profile (bumps etc), the new z_r and z_f expressions become :

$$\begin{aligned} z_r &= z_r - d \qquad \dot{z} = \dot{z}_r - \dot{d} \\ z_f &= z_f - d \qquad \dot{z} = \dot{z}_f - \dot{d} \end{aligned}$$

It is to be noted that when the d is a constant, its theoretical derivative in infinity, but in reality it should be null.

3.3.4 Lateral/transversal Forces F_{tr} and F_{tf}

The derivation of the tire lateral force used here is derived from the linear tire model used in [11]. F_{zr} and F_{zf} are the rear and front tire vertical forces as has been explained in the previous section. The rest of this term is called the slip angle just as in [11]. the longitudinal force parameters are presented in table 3.10.

$$\begin{aligned} F_{tr} &= F_{zr} \cdot \arctan(-v_{tr} / \mid -v_{lr} \mid) \\ F_{tf} &= F_{zf} \cdot \arctan(-v_{tf} / \mid -v_{lf} \mid) \end{aligned} \tag{3.11}$$

Table 3.10: Lateral force parameters and their meaning

Suspension parameter	Meaning
v_{tr}	Rear contact patch transversal (lateral) velocity
v_{lr}	Rear contact patch longitudinal velocity
v_{tf}	Front contact patch transversal (lateral) velocity
v_{lf}	Front contact patch longitudinal velocity

These velocities can be obtained using equations 3.12.

$$\begin{aligned} v_{tr} &= -sin(q_0) \cdot vx_r + cos(q_0) \cdot vy_r \\ v_{lr} &= cos(q_0) \cdot vx_r + sin(q_0) \cdot vy_r \\ v_{tf} &= -sin(q_8) \cdot vx_f + cos(q_8) \cdot vy_f \\ v_{lf} &= cos(q_8) \cdot vx_f + sin(q_8) \cdot vy_f \end{aligned} \tag{3.12}$$

Where (referring to 3.8) :

$$\begin{aligned} x_{r/f} &= O_{0/7} \cdot [I \quad 0 \quad 0]^T \\ y_{r/f} &= O_{0/7} \cdot [0 \quad I \quad 0]^T \end{aligned} \tag{3.13}$$

Velocities are derivatives of these positions referring to 3.13, and I is an identity matrix.

3.3.5 Longitudinal Forces F_{lr} and F_{lf}

The tire longitudinal force is also calculated from the equation in [11]. The velocities in this expression can be calculated with 3.12.The expression for the tire longitudinal force is given in 3.14. The last part of this term is the difference in velocity between the road and the tire contact patch and is called slip.

$$\begin{aligned} F_{lr} &= F_{zr} \cdot ((b_1 + a_1 \cdot \cos(q_1)) \cdot \dot{q}_8 - v_{lr}) \\ F_{lf} &= F_{zf} \cdot ((b_6 - a_6 \cdot \cos(q_5)) \cdot \dot{q}_9 - v_{lf}) \end{aligned} \tag{3.14}$$

3.3.6 Overall model architecture

In the previous sections all the ingredients needed to calculate the equations of motion were discussed and all variables and terms are defined, equations of motions can be calculated. The state space representation is then derived from the equations of motion, figure 3.7 shows the overall model architecture.

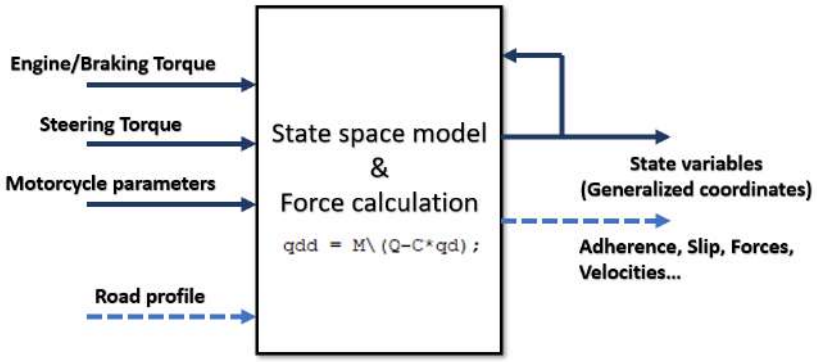

Figure 3.7: Overall model representation.

Figure 3.8 shows the structure of the complete model. The model of the motorcycle is the most important block. Around this block, there are three other blocks.

The name of these blocks should make it clear what is happening inside these blocks. The velocity vector of the contact patches. The contact patch velocities can also be obtained directly by measuring inside the motorcycle model block. The two blocks in the lower right corner called "rear wheel forces" and "front wheel forces" calculate the forces acting on the tire contact patches.

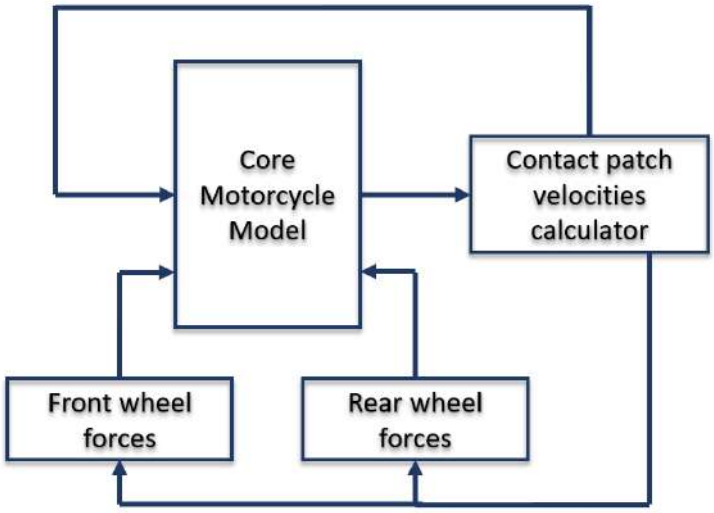

Figure 3.8: Motorcycle global model composition.

3.4 Simulation and Results

Figure 3.9 shows the structure of the complete model on Simulink. The model of the motorcycle is on a lower layer in the block called 'motorcycle'. That block is the most important block.

A real time input data for this motorcycle's parameters (See Appendix) has been recorded and used for simulation. Two cases are studied :

- The first is the 'straight line' case (Figure 3.10 and 3.12), where the motorcycle starts with an initial speed, then various engine manoeuvres are applied without a steering torque input.

  The engine input starts with a null value till t = 2 seconds, but since the motorbike starts with an initial speed, it keeps rolling, at 2 seconds though, a negative value is applied, this corresponds to a braking force, we notice that the speed starts to decrease consequently, and then increases at around 3.25 seconds, as the engine torque becomes positive (meaning that the motorcycle enters the acceleration mode).

- The second is the 'curve' case (Figure 3.13 and 3.15), where the motorcycle starts with an initial speed again, then various steering manoeuvres resulting in a curvature are applied without any engine torque input.

- A speed bump is simulated in both cases at around 3.5 seconds, this is done using the road profile entry, explained in the previous section.

Selected generalized coordinates are then given for both case, as well as the various forces and velocities for the rear and the front wheels. Appendix C shows the full set of generalized coordinates.

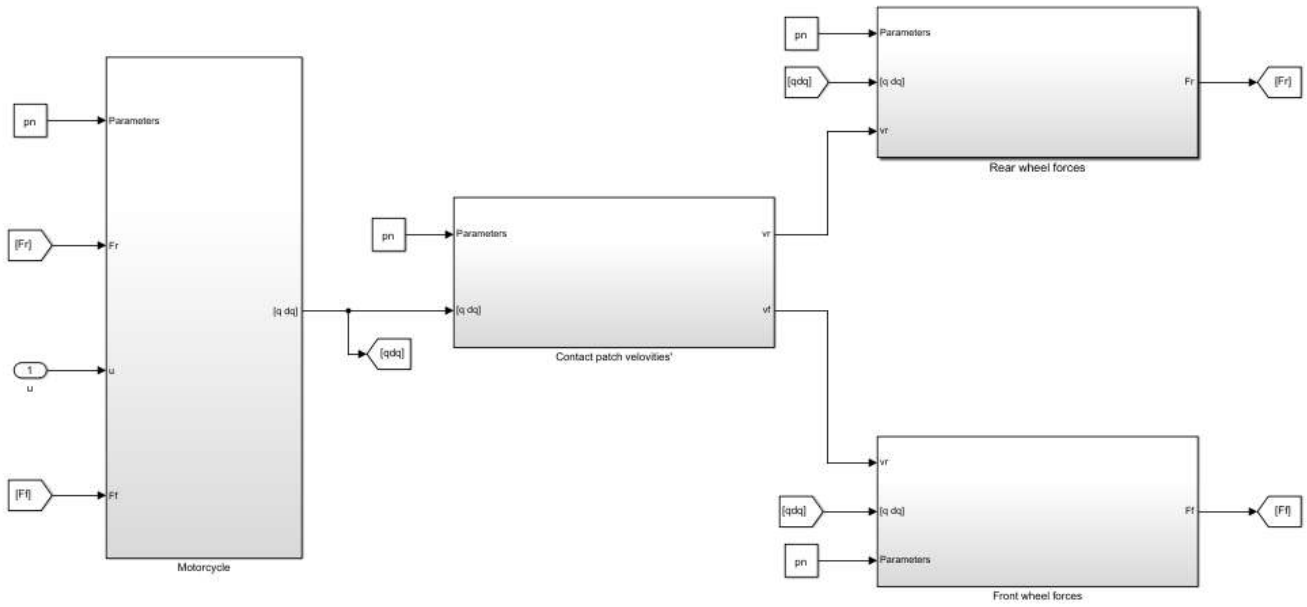

Figure 3.9: Motorcycle global model on Simulink.

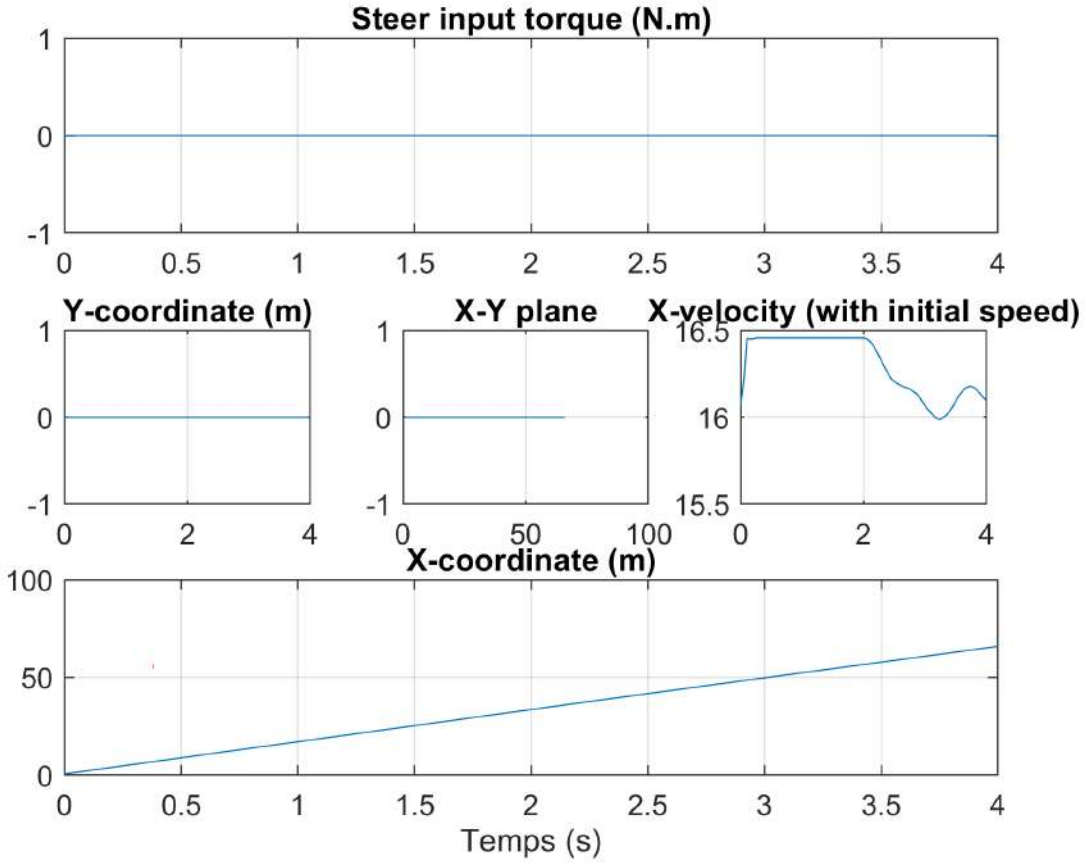

Figure 3.10: X-Y plane and engine torque in case of a straight line (No steer).

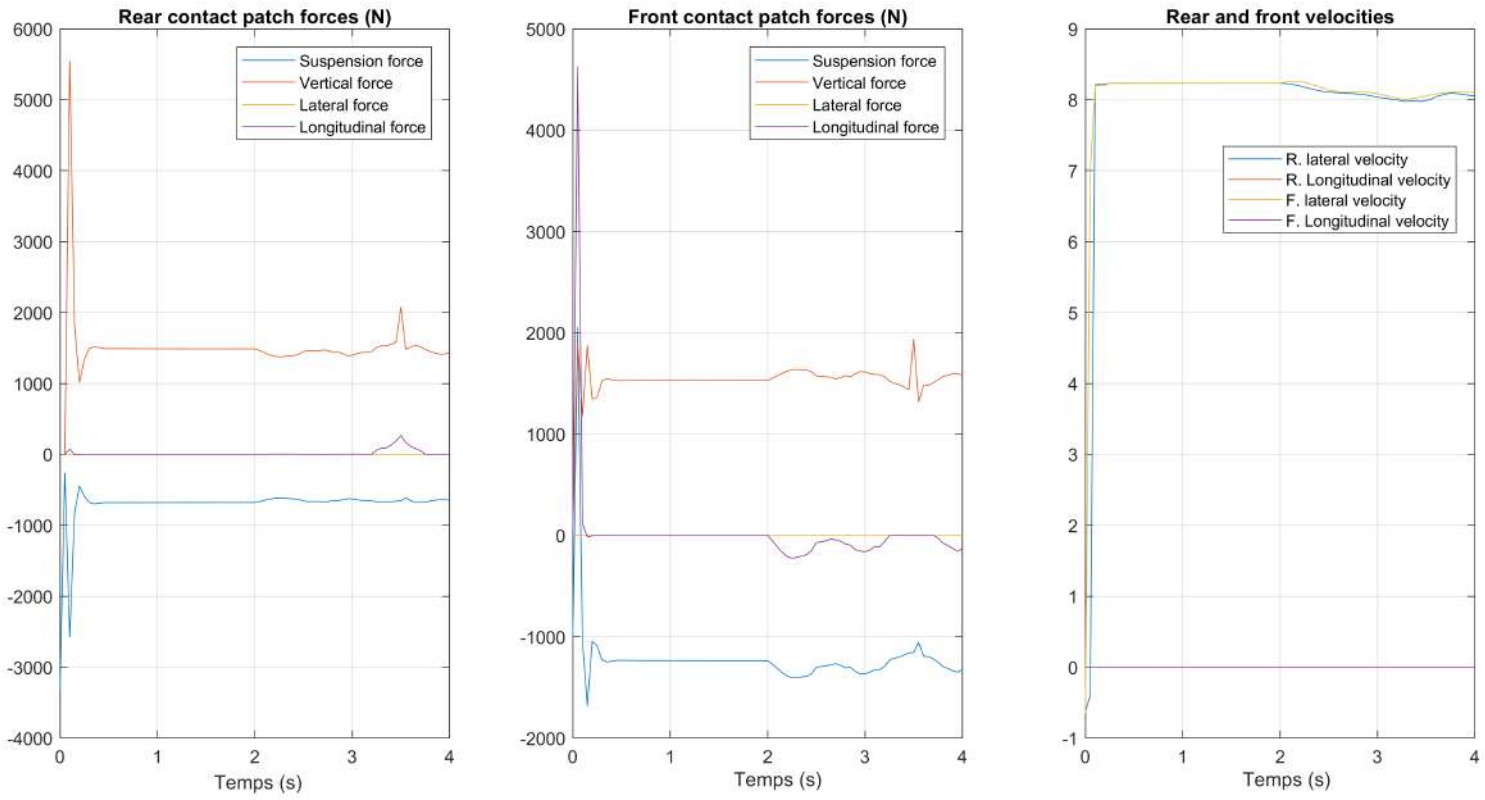

Figure 3.11: Forces and velocities in case of a straight line (No steer).

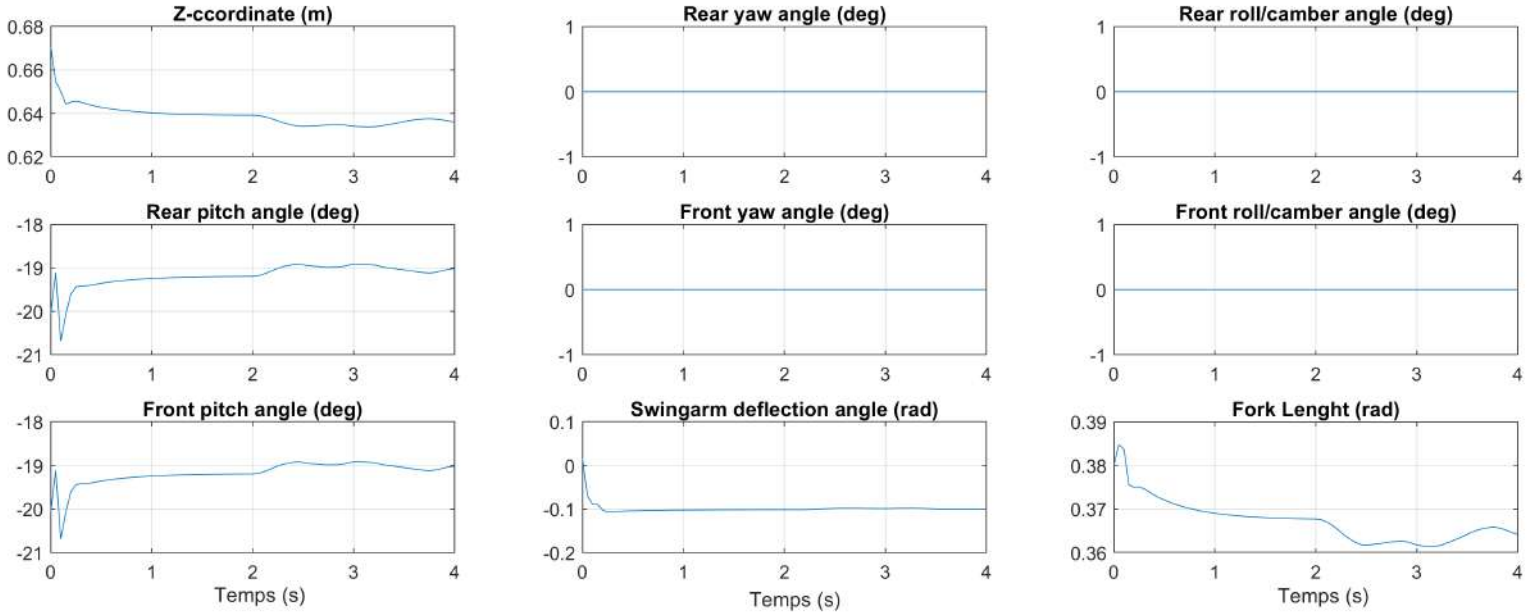

Figure 3.12: Selected generalized coordinates in case of a straight line (No steer).

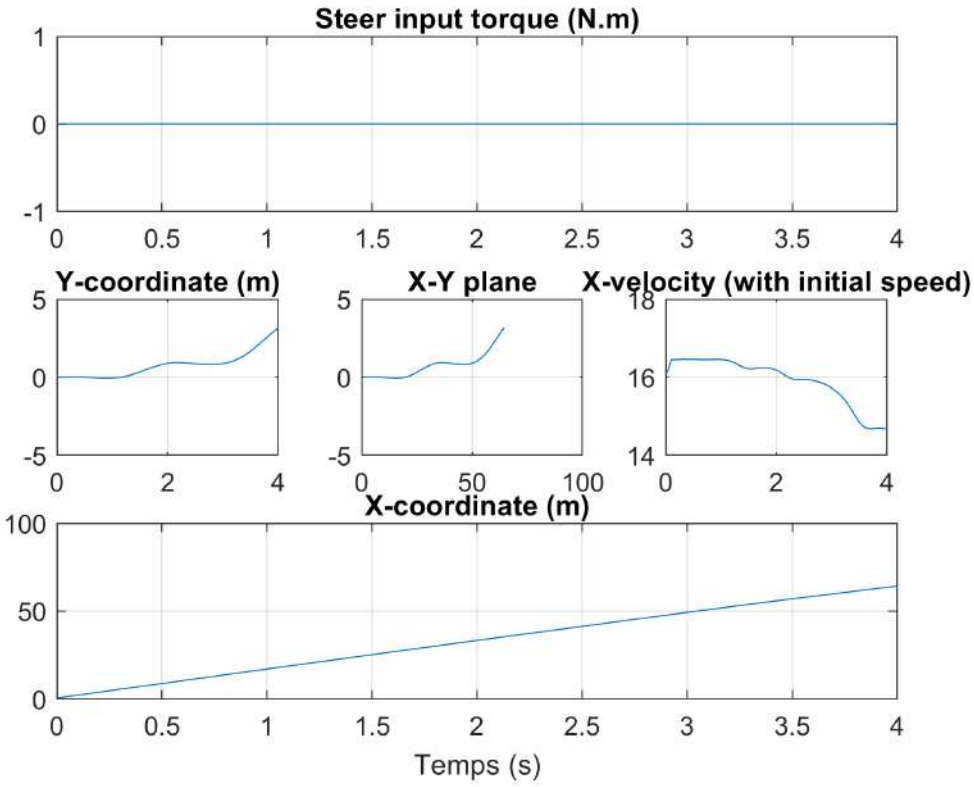

Figure 3.13: X-Y plane and steer torque in case of a curve (With initial speed and no engine torque).

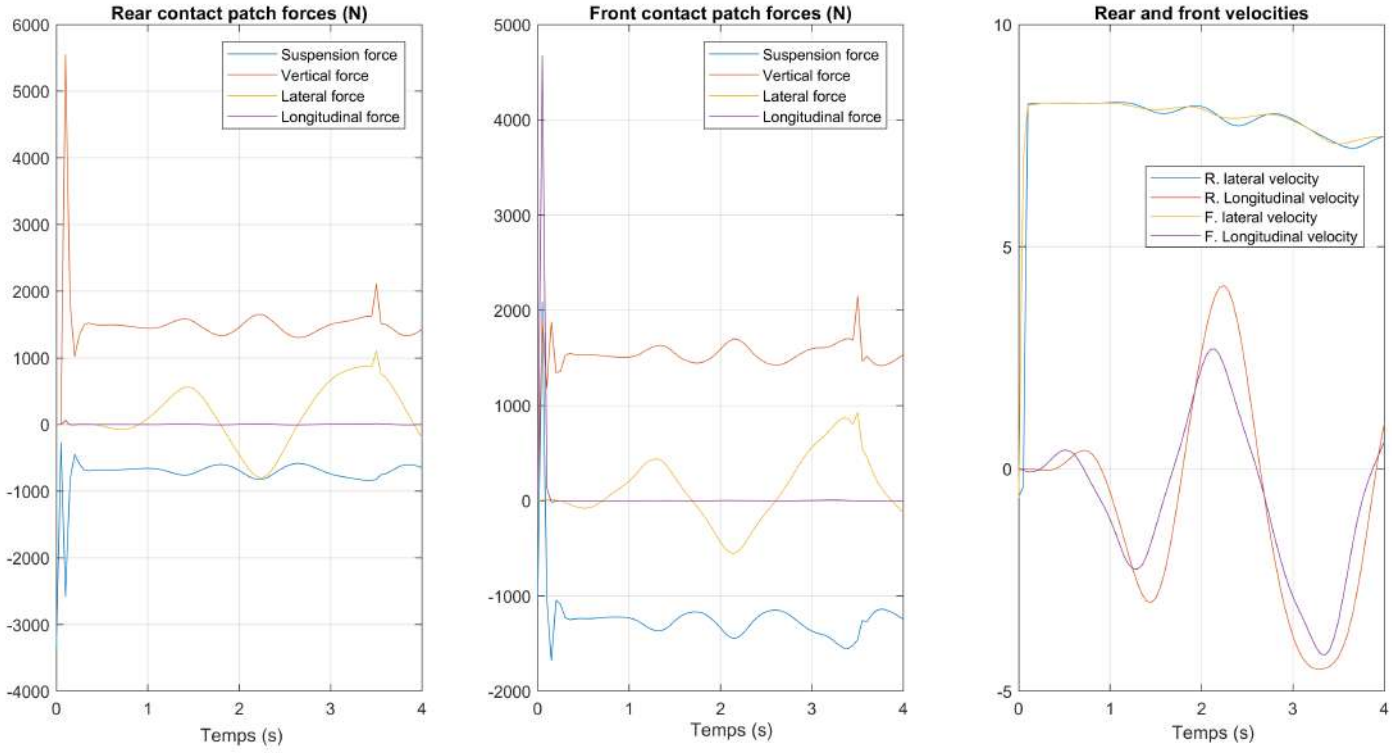

Figure 3.14: Forces and velocities in case of a straight line (No engine torque).

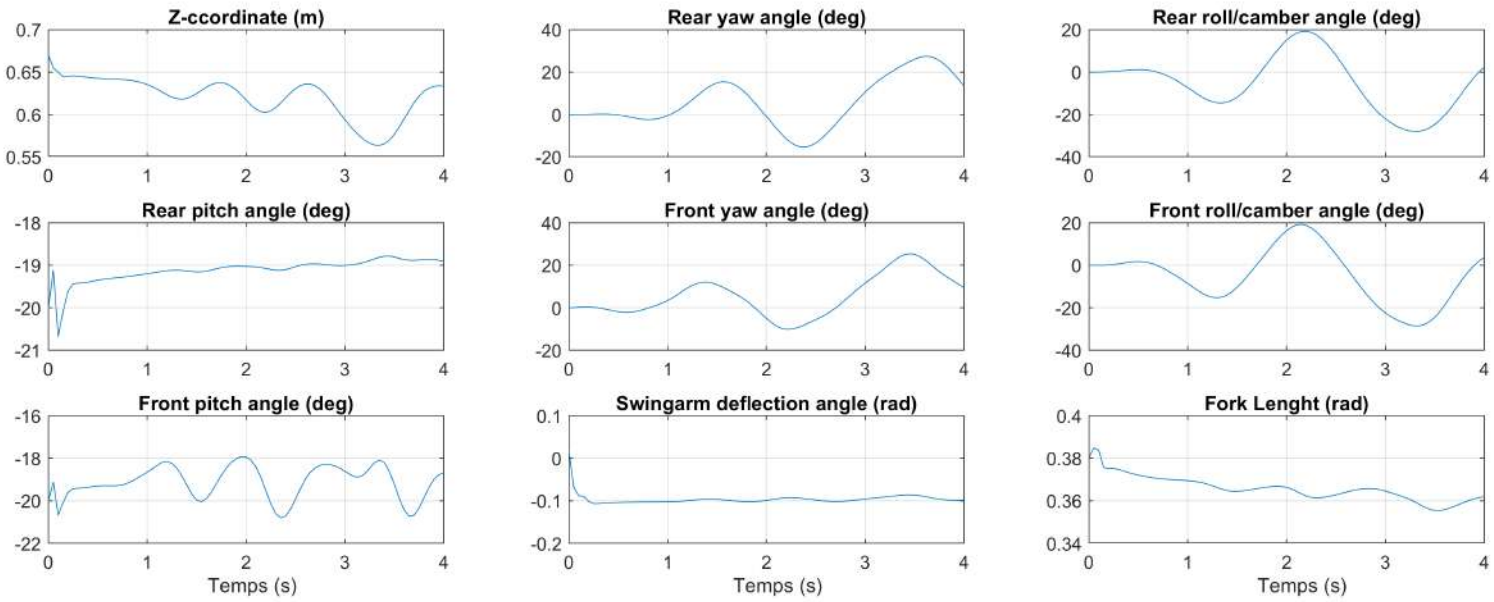

Figure 3.15: Selected generalized coordinates in case of a curve (No engine torque).

We notice, as expected, that in the case of a straight line, the lateral forces are null, this is normal as there is no steering torque and thus no camber, as explained in the previous section, no camber (and consequently no sideslip angle) means that there is no lateral force applied on the motorbike (at the contact patches).
Conversely, in the second case, that of a cornering situation, with no engine torque and an initial speed, lateral forces emerge and depend heavily on the vertical forces, but mostly velocities, affected by the camber angles, which are themselves affected by the steer torque. it is also noticed that the longitudinal forces are null, as there is no engine torque applied.

Front and rear rotations might look the same but there is an offset in amplitude and phase, this is normal as the two contact patches do not react at the same time to inputs.

3.5 Conclusion

In this chapter, a relatively complete 13 degrees of freedom model, in the three dimension, of the motorcycle was developed based on the work of [2], and Lagrangian formalism. Components of the Cristoffel and mass matrices were calculated using Maple, and given in Appendix A. Forces and resulting works where then calculated, again using Maple. The last section presented simulation results for different input scenarios, the important one being the second, as it is the scenario that describes a cornering situation.

CHAPTER 4

STABILITY ANALYSIS IN CORNERING SITUATIONS

Introduction

Our ultimate goal in this work is not to control the system but rather to study its stability in turns, and considering how our system is written some possibilities or options might be very time consuming. we have two possibilities/options, either we linearise the system and study its stability using "modes" in the traditional way, or we use what we would call criteria based stability analysis. And since our model is already complex enough and presents too many non-linearities, it was more fidelity and time efficient to opt for the latter option.

4.1 Criteria Based Stability in Cornering Situations

in a general way, the stability of the vehicles is conditioned by the dynamics of the tires which play a fundamental role. For motorized two-wheelers, this role seems even more important. Indeed, under the vertical load, the tire information gives birth to oval contact area (contact patch). When the wheel rolls, the properties of the wheel / ground adherence in this contact area, and the complex complexes of the whole carcass, influence the behaviour of tires. We can distinguish two types of stability criteria in curves :

- Non numerical : these cannot be represented by numerical values and equations.
- Numerical : are the criteria that can be calculated using equations, their numerical values are estimated as such.

The lateral thrust as explained previously is generated primarily by camber thrust and drift (or side-slip) thrust, this creates the lateral adherence in curves, and when the engine torque is applied (or a brake torque), a difference between tire speed and road speed emerges, this creates the longitudinal adherence. Figure 4.1 shows the composition of this element (noted μ) for both wheels, their sum gives the overall adherence, again, for both wheels.

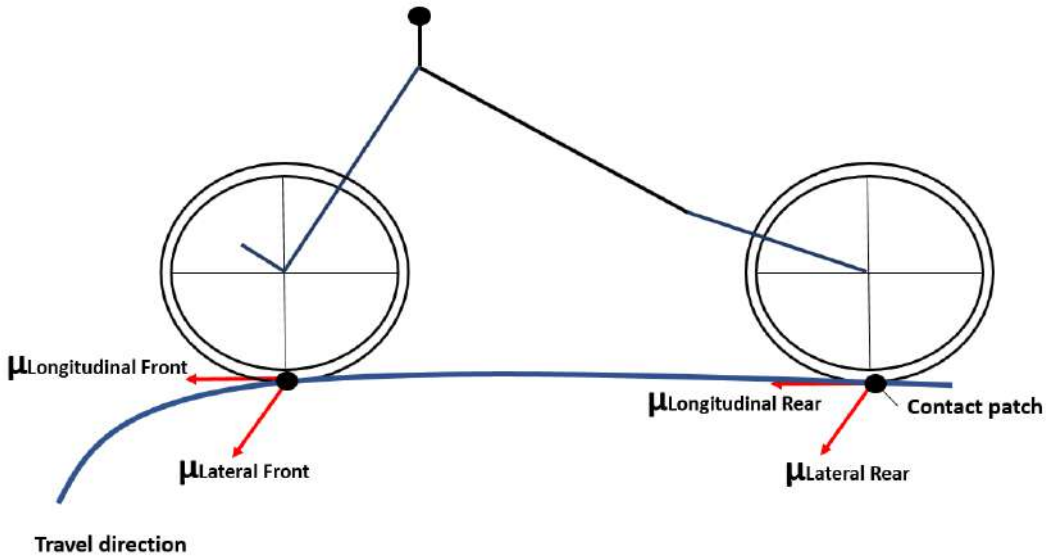

Figure 4.1: Front and rear wheel adherences.

This adherence (sometimes also called adhesion) insures the motorbike's travel safety on roads, it is the friction between the tire and the pavement. Enough friction (adherence) force is obviously needed between the tire and road for continuous stability.

4.1.1 Non numerical criteria

In turns, stability criteria that would potentially lead to instability if not managed well, and that are non measurable, as in, the motorcycle experiences any disturbance, which may be : unintentional movement of the pilot, a gust of wind, a degraded coating, a curtain or balancing of the wheels...

Whatever the disturbances, the transient behaviour of return to equilibrium depends on specific characteristics of vehicle stability that can be studied by specific, unfortunately complex studies.

The lateral behaviour in the neighbourhood of the straight line is altered by three instabilities (or unstable or unstable natural movements) encountered in certain speed ranges and that make the bike alone not stable :

- "**Capsize mode**" : a non-oscillating mode in which the wheel forward is deflected in the direction of the roll but not enough to avoid a fall. It is a vibratory mode, controllable by the driver if the speed is high enough, and by the foot on the ground if it is not.

- "**Wobble mode**" : a fast oscillating mode of the handlebar-front wheel assembly, well damped in low and medium speeds, and moderately damped in high speeds. It occurs when the handlebars begins to swing from one side to the other until the motorcycle falls.

- "**Weave mode**": a rather slow oscillatory mode unstable in low speeds, well damped at medium speeds and stable at high speeds. It affects the entire two-wheeled vehicle, and the trajectory undulates. In this mode.
  4.2 shows the wobble and the weave modes.

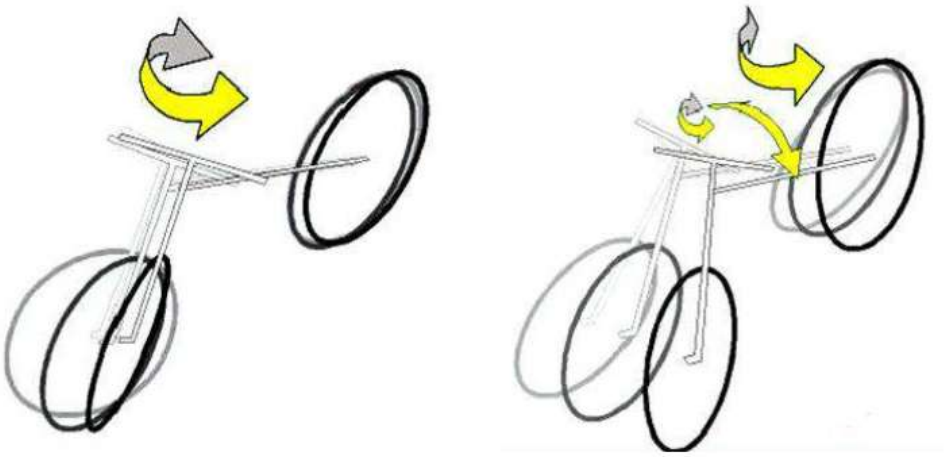

Figure 4.2: Wobble mode (right) and weave mode (left).

In open loop (without driver) and this for a wide range of longitudinal speed. This can be explained by the fact that any equilibrium requires three points of support. On the other hand, the damping of the associated poles is lower when the speed increases. Moreover, the action of the driver is very crucial to stabilize the motorbike, but is very unpredictable and limited by the characteristics of the oscillatory movement :

- **Equilibrium** : A two-wheeler maintains a state of equilibrium as long as the external forces (gravity, inertia, centrifugal and aerodynamic) cancel those of the tire / ground reaction. In a straight line driving, this stability is provided by the driver by controlling the longitudinal speed. On the other hand, in a bend/curve, the biker applies a torque to the handlebar, or even a lateral movement of his bust to control the roll angle of the motorcycle. At high speeds, a small angle of the handlebar moves laterally and quickly, the tire-ground contact point, while large handlebar movements are needed for the same effect at low speed.

- **Counter steering** : The counter steering consists of turning the steering, by a small movement, in the opposite direction of the turn. At low speed, obviously, the equilibrium of a motorcycle is precarious, in this case it is necessary to turn the handlebars in the desired direction to manoeuvre.

- **Gyroscopic effect** : When an object is in its own rotation, it tends to remain balanced around its axis of rotation, we speak at that time of a gyroscopic effect. In the case of the motorcycle, this effect is proportional to the speed of rotation of the wheels. This physical phenomenon ensures the bike stays balanced when driving. It should be noted that the amplitude of the gyroscopic effect is relatively small compared to the other moments, although its character transient is crucial in cornering situations.

4.1.2 Numerical criteria

In general, the emergence of forces and moments during a turn as shown in Figure 4.3, where for a roll angle the relevant forces (frictional, lateral and longitudinal, centrifugal and gravitational) acting of the motorbike, the torque of the centrifugal force balances the torque of the weight around the contact axis. Therefore, given a certain vertical load (weight), more camber angle means more speed, but even more lateral force!

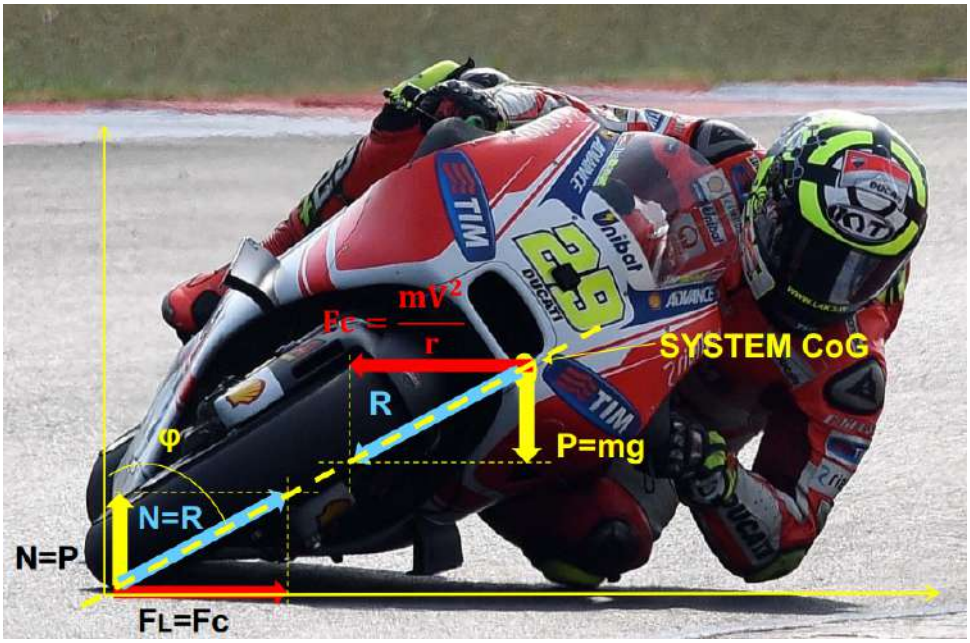

Figure 4.3: Equilibrium of forces resulting from leaning in a curve.

Figure 4.4: Forces acting on wheels (both front and rear).

Their balancing yields the value of the lateral force F_y ou F_L needed to maintain in equilibrium of the vehicle in a curve that is equal to $F_z tan\phi$, where F_z is the vertical load. However, falls and critical conditions cannot be captured under the aforementioned assumptions when

strong acceleration or braking occur.

The maximum safe-speed in a curve depends on the road geometry, the surface conditions, the driver's skills as mentioned in the previous subsection (or tolerance for discomfort) and the roll-over stability of the vehicle, another main effect is the gyroscopic effect.

The gyroscopic effect occurs when the wheel equipped with a rotational movement about its own axis, with a speed $\dot{q}_{8/9}$, is also rotated about a second axis, perpendicular to the previous one, with a speed v_x. The gyroscopic effect is manifested by a couple acting around an axis perpendicular to the previous ones. In the dynamics of the bike, there are different gyroscopic effects, but the most important in curves is the gyroscopic yaw effect, it is generated by the rotation of the wheels, in the stationary movement of the curve. The value of the gyroscopic moment is equal to the product of the polar moment of inertia of the wheel, with the rotation speeds.

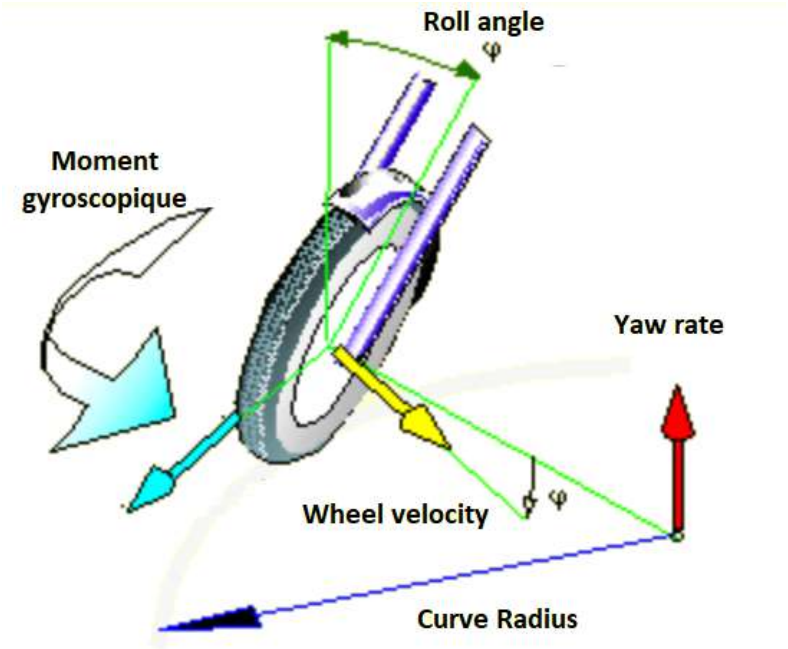

Figure 4.5: Gyroscopic yaw effect.

Consider a front or rear wheel, which rotates around its own axis at a speed $\dot{q}_{8/9}$, while the motorcycle runs along a radius curve R with a yaw rate $\dot{q}_{0/4}$. The movement of the wheel in the curve generates a gyroscopic moment around the horizontal axis, which tends to straighten the bike:

$$M = I \cdot v_x \cdot \dot{q}_{8/9} \cdot \cos(\phi) \tag{4.1}$$

where I indicates the moment of polar inertia of the wheel relative to its own axis, with the speed of rotation about the same axis, $\dot{q}_{0/4}$ (that we can also call v_x) the speed of yaw rotation, equal to the ratio between the forward speed of the motorcycle and the radius of the curve (R, Figure **??**). Now let's look at the effect of the two wheels. The gyroscopic moment results :

$$M = (I_r + I_f) \cdot v_x \cdot \dot{q}_{8/9} \cdot \cos(\phi) \tag{4.2}$$

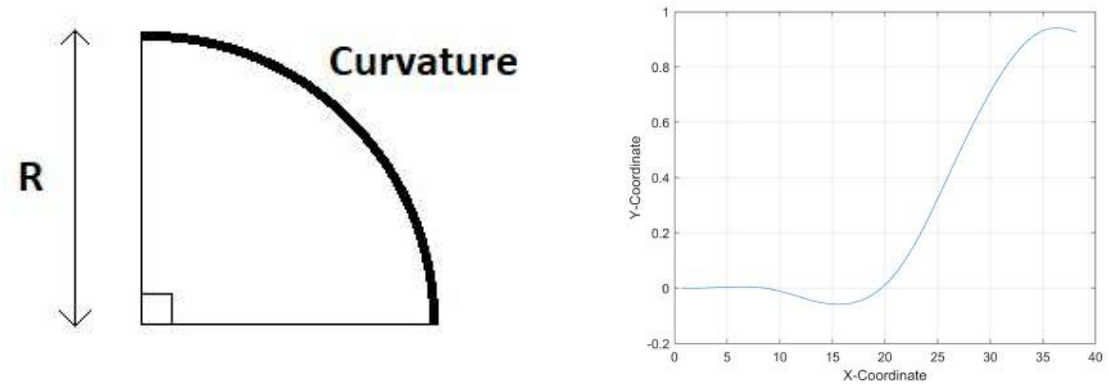

Figure 4.6: Curvature radius (calculated using max and min functions).

Where I_f and I_r indicate the moments of inertia of the front and rear wheels. If the gyroscopic effect is assumed to be zero, and if it also neglects the effect due to the thickness of the tires, the equilibrium condition in the curved stationary bike (speed of travel and the radius of the constant curve) imposes the resultant of the force of weight and the centrifugal force crosses the line which connects the points of contact of the two wheels. In this ideal case, the angle of roll of the motorcycle is ensured by the simple relation 4.3.

In a turn, a two-wheeled vehicle is essentially subjected to four major forces : centrifugal force, gravitational force, vertical load, and lateral sliding force. The condition of equilibrium is reached when the external torsor/sum of all these efforts is zero. This condition is ensured when the motorcycle is inclined by a roll angle presented in equation 4.3, a function of the square of the longitudinal velocity v_x and the curvature of the turn R, as follows :

$$\phi = \arctan(\frac{R \cdot v_x^2}{g}) \tag{4.3}$$

It is important to note that in the model used in this work, and as opposed to many models studied and used [22] in literature, steady state cornering condition is not assumed, meaning that in cornering situations adherence varies as well.

4.3 is a necessary but not sufficient condition, to integrate the road surface to the equation the following condition must also be satisfied :

$$v_x^2 < R \cdot g \cdot l \tag{4.4}$$

Where $l = \tan \Phi$ in 4.4, represents the road condition, $l = 0.8$ when it's normal, and $l = 0.4$ when it's wet (Fig. 4.9).

Obviously this is an estimation and is not completely accurate, as the road condition affects the forces, the forces in the model used, however, are represented in a linear form. But for the sake of this study we consider that these two conditions are sufficient. The next sections try to analyse the stability in curves.

4.2 Speed - Steer Stability Analysis

The strategy here is based on an algorithmic approach, two loops are used, the first loop represents the steering force (the force in $N.m$ applied on the steering head), this force is controlled using a coefficient M. The curve is then simulated, the different parameters derived, and the conditions studied above verified (also, when the the roll angle exceeds a certain value, the simulations stops and the system is considered to be unstable). the motorcycle is stable if they are respected and unstable when they are not.

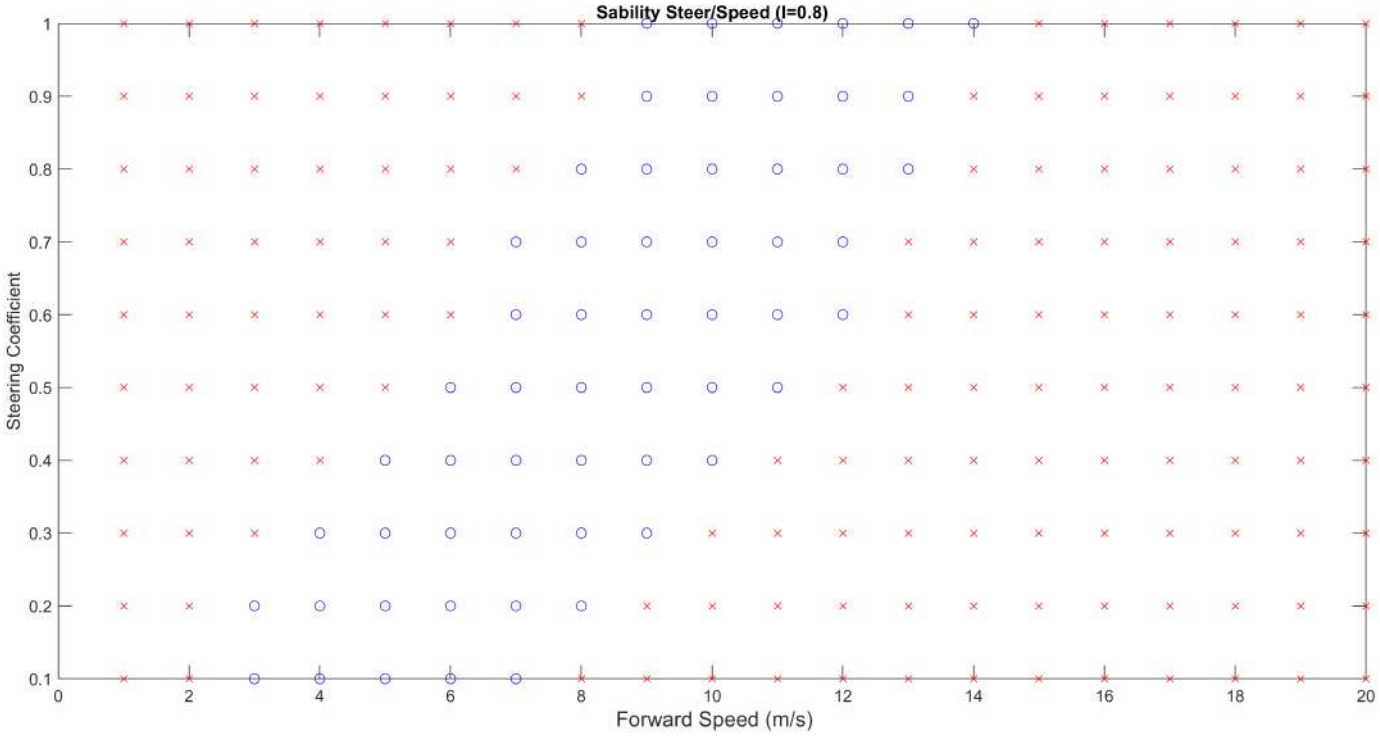

Figure 4.7: Forward speed - Steer stability when the road is dry ($l = 0.8$).

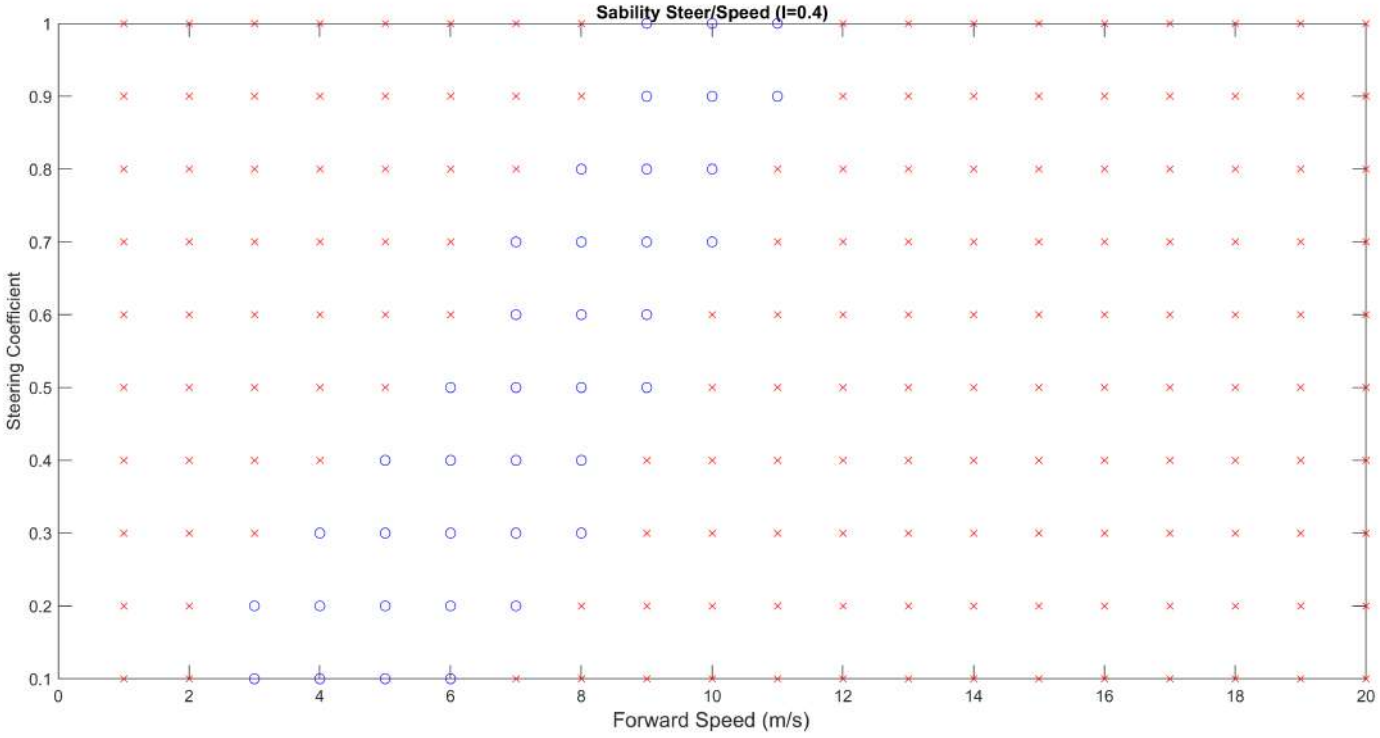

Figure 4.8: Forward speed - Steer stability when the road is wet ($l = 0.4$).

The blue part (circles) represent the stability region, and the red part (Xs) represent the

unstable region, this goes for all other figures. Obviously the steering force (and consequently the roll angle) is variable and not constant, this means that we had to measure the resulting roll angles at a specific point of the curve, we choose the the middle of the curve, the point in which the roll angle is at its maximum, the radius of the curve is then calculated using the max and the min of the X-Y plane (Fig. 4.5).

Figure 4.7 shows the stability region in terms of forward speed and steering force when the road is dry ($l = 0.8$), we notice that when the steer force increases, the speed needed to maintain stability increases as well. When the speed is too low what ever the steer force (and angle) the motorcycle falls, the same can be said when it's too high, in a curve this is normal, as the speed must imperatively be high enough for the steer force applied by the driver to have a gradual turning effect, when it is too high however, the steer needed becomes high as well, here only stability for certain values of the weighing coefficient are presented $(0.1 - 1)$ and their consequent steer forces as shown in Table 4.1, (resulting angles heavily depend on the speed and cannot be represented in the table) we can however go beyond, but when it becomes too high we fall into instability again.

Figure 4.8 analyses stability the same way but this time, on a wet road ($l = 0.4$), we observe that the stability region diminishes, this is normal as the adherence or the friction coefficient becomes weaker and thus the speed must not be too high or there will be a risk of sliding (instability), in fact the driver must be able to measure this adequately knowing the impact of the speed on the steer.

Table 4.1: Resulting steer input force for each value of the weighing coefficient M.

Value of coefficient M	0.1	0.2	0.3	0.4	0.5	0.6	0.7	0.8	0.9	1
Corresponding steer force $(N.m)$	2,96	5,92	8,87	11,83	14,79	17,74	20,7	23,66	26,62	29,58

It is also important to observe and analyse the evolution of the lateral forces, notably the difference between the front wheel and read wheel's lateral forces Fy_r and Fy_f.

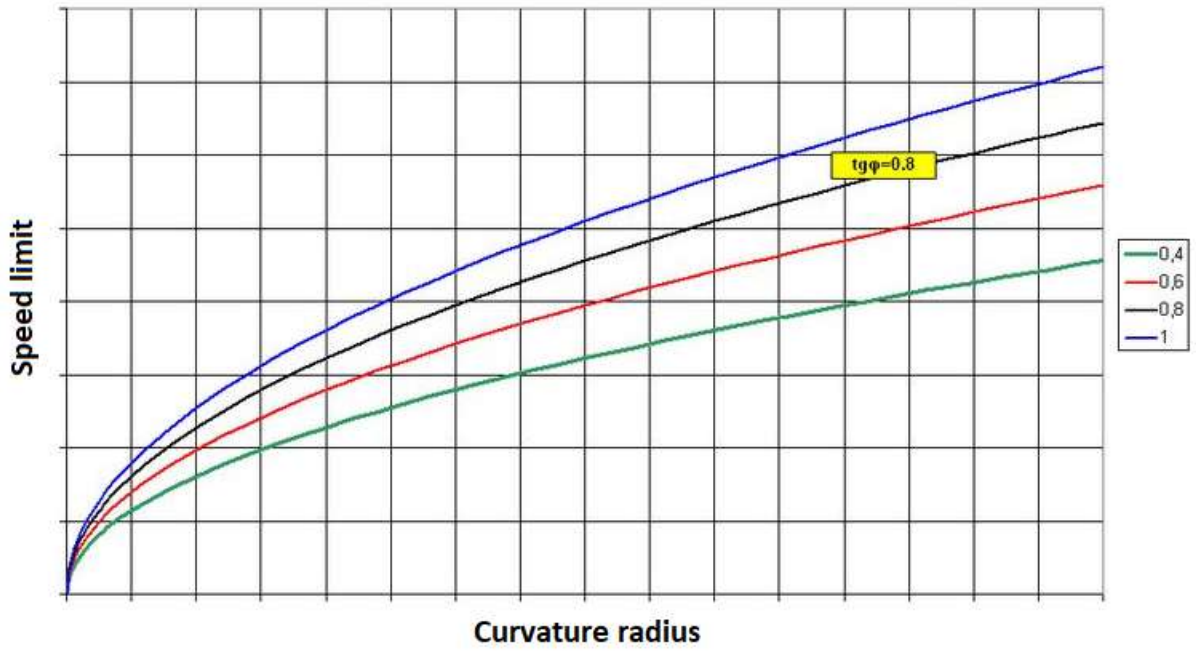

Figure 4.9: Speed limit in terms of curve radius and the coefficient $l = \tan\Phi$ [28].

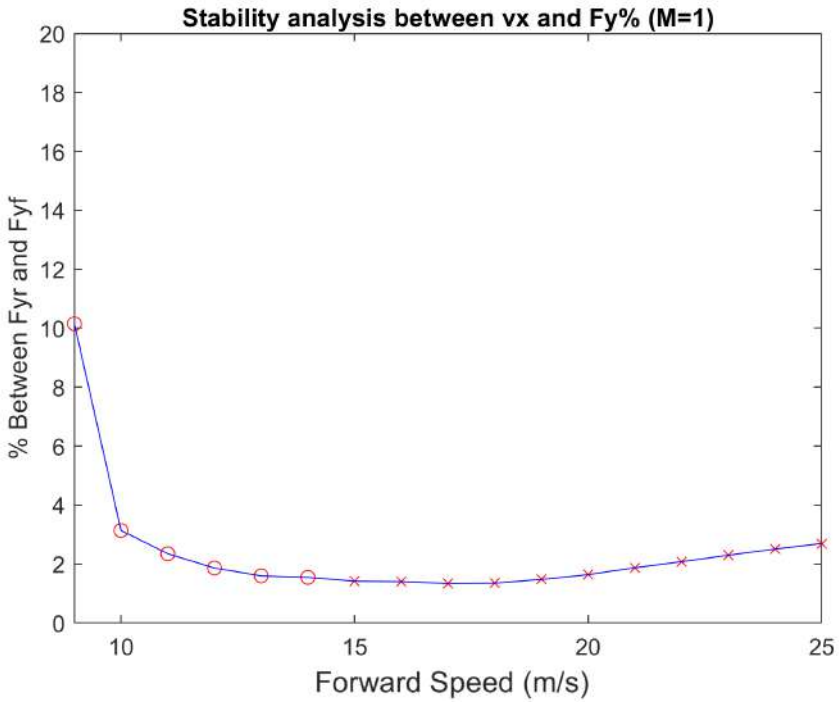

Figure 4.10: Stability in terms of the percentage between the rear/front forces ($l = 0.8$ and $M = 1$).

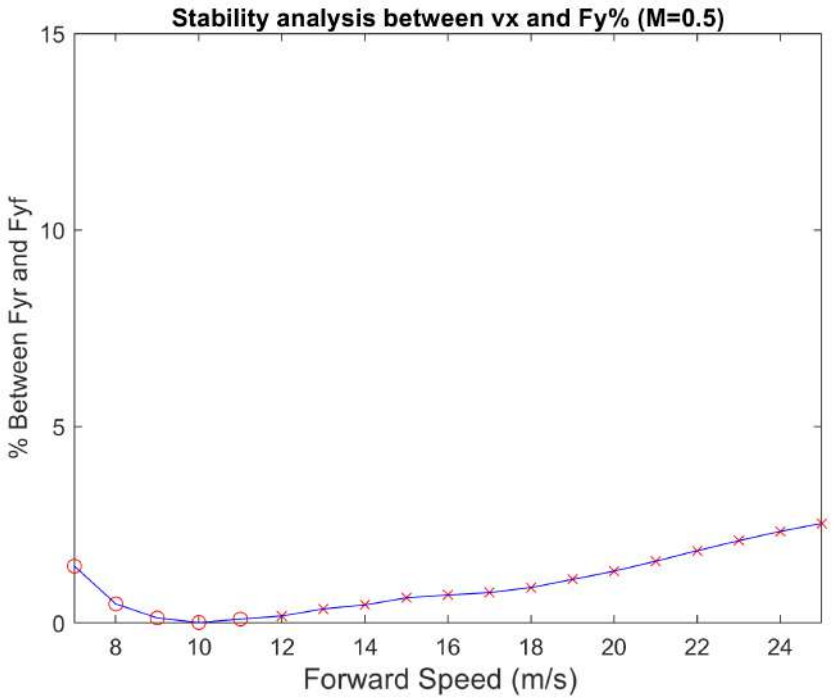

Figure 4.11: Stability in terms of the percentage between the rear/front forces ($l = 0.8$ and $M = 0.5$).

For this we chose a steer coefficient, and for each speed (starting from the one where the system is stable) and then calculated the difference (in %) between the lateral forces.

Figure 4.10 shows that of a dry road $l = 0.8$ and a steer weighing coefficient $M = 1$ and figure 4.11 that of a dry road and a steer weighting coefficient $M = 0.5$, we observe in both cases that at first the system is stable and that $Fy_{\%}$ decreases until it reaches a minimum, this occurs as the steer force become insufficient for the speed and the % is not sufficient, and after that the system becomes unstable, and $Fy_{\%}$ starts to increase again, this is where the speed is too high. and intuitively, more the steer force is high (and the speed too) more percentage between the lateral forces is high as well. This means that $Fy_{\%}$ has a heavy impact on the stability.

4.3 Speed - Lateral Forces Stability Analysis

In this section we try to interpret the impact noticed previous on stability by the difference between the front and rear lateral forces. in fact, this can be caused by different factors, a hit of a wind blow or even a small rock can cause a brusque change in lateral forces.

Figure 4.12 shows how much for a weighing coefficient of the steering input force $M = 1$ the difference between the two lateral forces in % can affect stability, this is done by taking into account only the range of speeds in which the system was originally stable.

For this we fix M and force vary $Fy\%$ from 0 to 100%, and then stop when the motorcycle keeps falling into instability, we then see the region in which it is stable, and the region in which it is not.

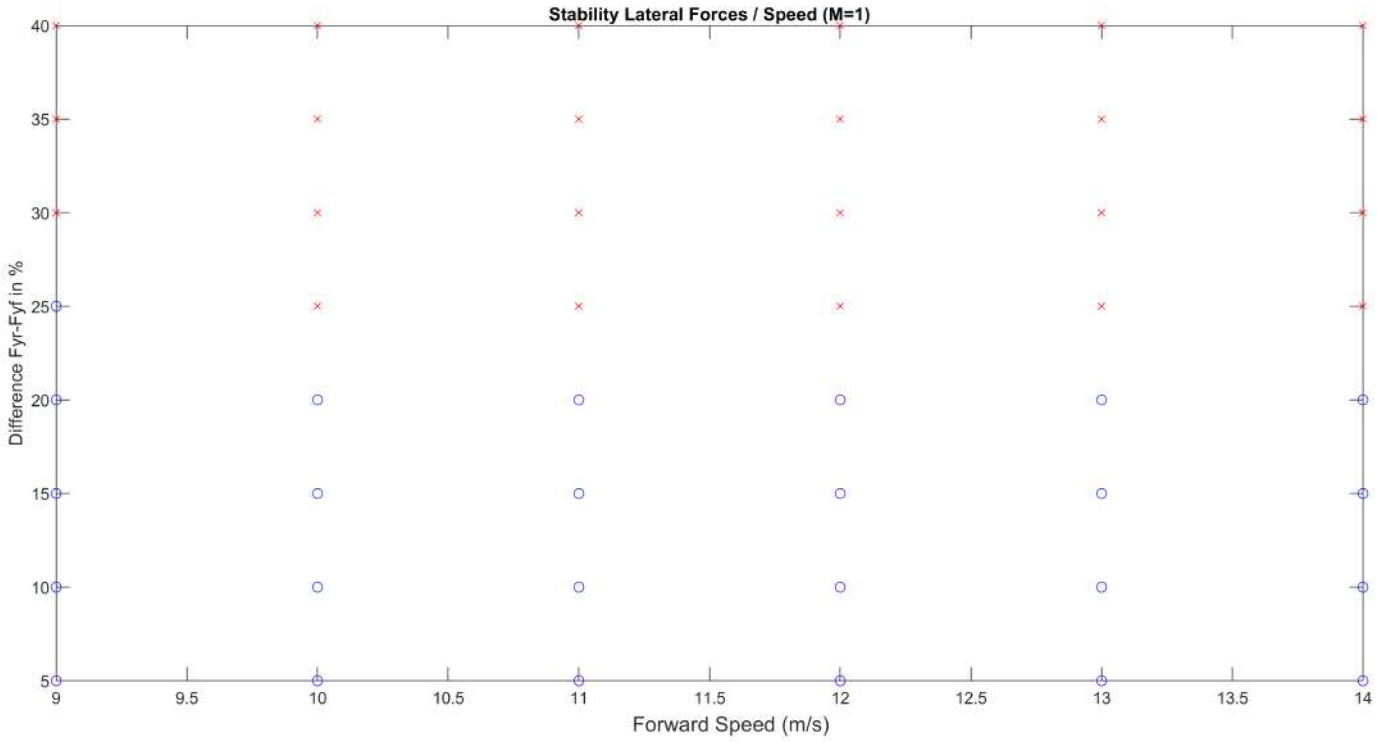

Figure 4.12: Stability in terms of the percentage between the rear/front forces and forward speed when $M = 1$.

Figure 4.13 depicts the same thing as Figure 4.12, but this time for a steer input weighing coefficient of $M = 0.6$.

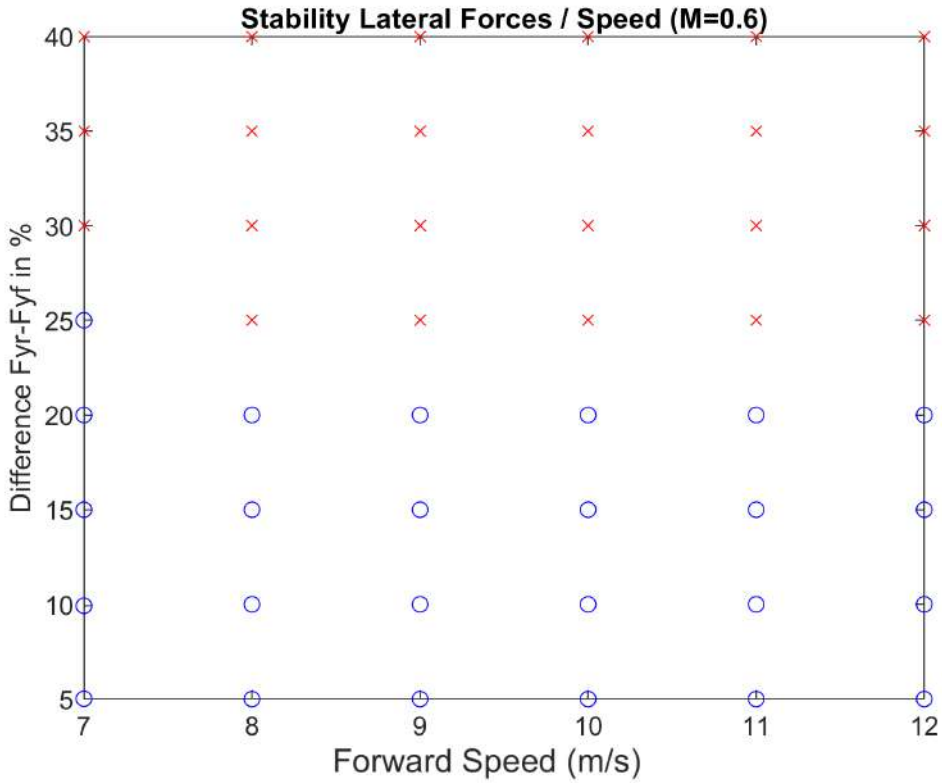

Figure 4.13: Stability in terms of the percentage between the rear/front forces and forward speed when $M = 0.6$.

We can easily deduct that in both cases, and for the stability range of speeds, the motorcycle falls into instability when $Fy_{\%}$ exceeds 25%, this means that when the lateral force at the front wheel's contact patch is 25% higher than that of the rear wheel's contact patch, and even with the correct steering force, the motorbike falls.

This is mostly important, when studying the impact of disturbances on the motorbike, in fact, and as stated before, a blow of a wind can cause an uneven distribution of lateral impact on different parts of the vehicle, and thus increase $Fy_{\%}$. Even more impactful in a turn would be running into a rock or a sudden road elevation, as in a curve the front wheel is almost always the wheel that runs into such an obstacle first, so it would be eventually interesting to study the effect of these kind of obstacles, considered as disturbances in our model, on the lateral forces and consequently, on $Fy_{\%}$.

4.4 Speed - Adherence Stability Analysis

This section studies the adherence's, or friction coefficient's, as it is frequently called in literature, influence on stability, with respect to the adherence. Intuitively the friction coefficient is very crucial for the motorbike's stability, especially in curves and cornering situations, the motorcycle's tire-road contact patch is not big enough to assure continuous adherence to the road, and in curves, it leans, which means there is a risk, if the speed, or any other variable that affects adherence for that matter, is not correct, an adhesion failure occurs, this means instability.

Figure 4.14 shows our system's stability region, when varying adherence for each forward speed incrementation. The coefficient E is varied between the values 0.5 and 1.5 and then the transversal forces of the two contact patches are weighed with this coefficient, the adherence is

then measured (Table 4.2) and stability is tested using the criteria previously described.

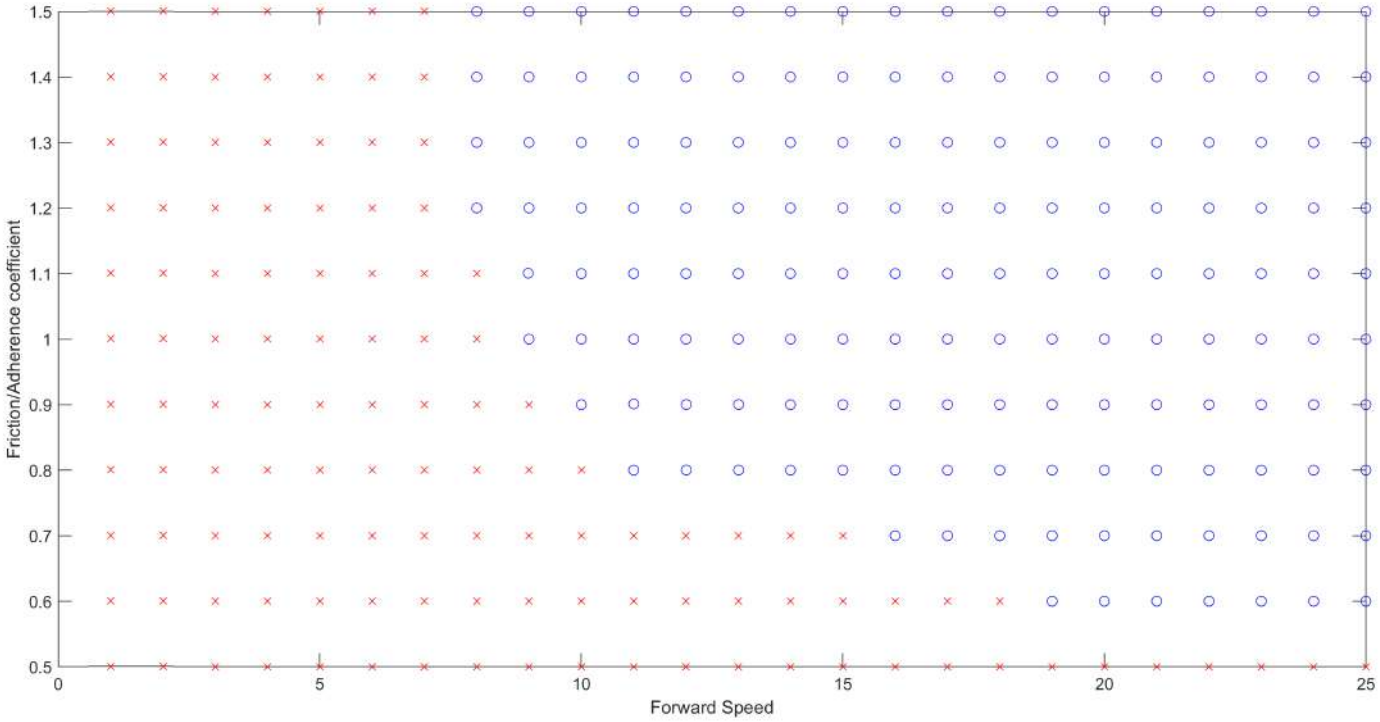

Figure 4.14: Stability - adherence analysis for a normal steering coefficient.

We notice that, at low speeds, the system is unstable even when adherence is high, this is normal as when the speed is not high enough even with sufficient friction, the bike eventually falls, for correct speeds however, the bike stabilizes only when the friction is high enough.

Table 4.2: Resulting steer input force for each value of the weighing coefficient M.

Value of coefficient E	0.5	0.7	0.9	1.1	1.3	1.5
Corresponding max adherence	0.23	0.32	0.45	0.52	0.66	0.88

4.5 Conclusion

In this chapter, the stability of the motorcycle has been studied for different variables and various conditions taking into account criteria based stability, all involving the forward speed, we have first studied stability regions for speed with respect to steer force, then speed with respect to the lateral forces, and finally speed with respect to adherence.

Figure 6.1 depicts the idea behind this study, in fact, once the speed stability regions of a motorcycle are defined for difference conditions in accordance with the most influencing parameters, namely the steer force, the lateral forces and the adhesion/friction coefficient, a real time algorithm can be conceived to use the state observers that are going to be studied in **Chapter 5** in order to construct a viable alert system for the driver, or an acting alert system for the motorcycle. The next chapter, studies the state observers, and the estimation of vertical, lateral and longitudinal forces, and eventually the adherence.

CHAPTER 5

MODEL OBSERVERS AND SIMULATION

Introduction

The use of observers for motorcycle state estimation, (estimation of state variables/motorcycle dynamics) has been a focus point for researchers for decades, an observer is usually picked for its simplicity, ease of establishment (whether it be theoretical or practical) but also for its performances, but a compromise between these factors should be found for practical convenience as not all state variables are measurable in reality or sensors might be too expensive.

5.1 State Space Representation and System Observability

Before presenting the non-linear observers, it is essential to study the observability of the system. Since the seventies, the theory of the observability of non-linear systems is under construction. In general, real processes have unavoidable non-linearities.

Thus, in some cases, linear methods are sometimes no longer suitable. In this sense, several studies have been devoted to the study of the observability of non-linear systems such as [25]. For the study of the observability of a non-linear system, we can use the derived from Lie [Diop 1991]. The system is locally observable if the observability rank condition is satisfied, ie the observability matrix (O) defined below is of rank n :

$$O = \begin{pmatrix} dh(x) \\ dL_f h(x) \\ : \\ dL_f^{n-1} h(x) \end{pmatrix} \tag{5.1}$$

Where :

$$\begin{cases} dh = (\dfrac{\partial h}{\partial x_1}, \dfrac{\partial h}{\partial x_2}, \cdots, \dfrac{\partial h}{\partial x_n}) \\ L_f \cdot h(x) = \dfrac{\partial h}{\partial x} \cdot f(x) \end{cases} \tag{5.2}$$

The condition of observability is the following :

$$rang(O) = n \tag{5.3}$$

In chapter 3, where we have modelled the system using the Lagrangian formalism, we have seen that the dynamics of the vehicle is described by the differential equation below :

$$\ddot{q} = M^{-1}(q)(W(q,\dot{q}) - C(q,\dot{q})\dot{q} - P(q,\dot{q})) \tag{5.4}$$

Where W, M, C, and P are work term (containing all forces and torques including input torques), the mass matrix, the cristoffel matrix and the gravitational term respectively.

To be able to estimate the overall state of the system, it is interesting to write the model 5.4 in a canonical form, choosing the state vector x as follows :

$$x = (x_1, x_2)^T = (q, \dot{q})^T \tag{5.5}$$

Equation 5.5 becomes :

$$x_2 = -M^{-1}(x_1) \cdot [C(x_1, x_2) \cdot x_2 + P(x_1, x_2)] + M^{-1}(x_1) \cdot W(x_1, x_2) \tag{5.6}$$

We then get the shape of the complete vehicle model.

$$\begin{cases} \dot{x}_1 = x_2 \\ \dot{x}_2 = f(x_1, x_2, F) + U(x_1) \\ y = h(x_1) \end{cases} \tag{5.7}$$

$f(\cdot)$ is a function, and $U(x_1) = M^{-1}(x_1) \cdot u(x_1)$ is the part of $W(x_1, x_2)$ containing inputs and F are the forces.

The proposed vehicle model has three properties :

- The matrix $M(x_1)$ is symmetric definite positive (passivity, see next section),
- The difference $M(x_1) - 2C(x_1, x_2)$ is antisymmetric,
- $C(x_1, \hat{x}_2) = C(x_1, x_2)$, $V(x_1, \hat{x}_2) = V(x_1, x_2)$, where $\hat{x}_2$ denotes the estimate of x_2.

5.2 Sliding Mode Observer

As presented in chapter 2 (literature review) many observers were presented, but the sliding mode observer presents more advantages and robustness (due to its sliding modes). Two main observers are mainly used in most literature, 1st order sliding mode and 2nd order sliding mode (also called higher order sliding mode observer).

To estimate the overall condition of the motorcycle using sliding mode observers, we must have important information about the measurements. So the output vector composed of measurements from the sensors must be well chosen. We can define the following hypotheses :

- We assume that the position vector is fully measurable : $y = x_1$

$$y^T = [q_x, q_y, q_z, q_0, q_1, q_2, q_4, q_5, q_6, q_7, q_f, q_8, q_9]$$

- The forces are in fact variable, (not only the steady state is considered), this means that for driving situations in a straight line with almost constant speed, such as on a highway, we assume that the tire / road contact forces F are constant only in steady state situation, obviously if the vehicle is travelling on a road that is not deformed and without bumps. In cornering situations however, it is variable in both states.

The state space model is presented in equation 5.7 We use here the algorithm proposed by Levant [26] to generate sliding modes of any order. In our case, the order of the observer is taken equal to 2 :

$$O : \begin{cases} \hat{x}_1 = \hat{x}_2 + z_1 \\ \hat{x}_2 = f(t, \hat{x}_2, u) + z_2 \end{cases} \tag{5.8}$$

where $\hat{x}_1$ and $\hat{x}_2$ are respectively the estimate of x_1 and x_2 and u is the input. z_1 and z_2 are calculated by the super-twisting algorithm as described in [26], equation 5.9.

$$\begin{cases} z_1 = -\alpha \cdot |\hat{x}_1 - x_1|^{\frac{1}{2}} \cdot sign(\hat{x}_1 - x_1) \\ z_2 = -\beta \cdot sign(\hat{x}_1 - x_1) \end{cases} \tag{5.9}$$

$sign(\hat{x}_1 - x_1)$ is a vector composed of sign functions of errors between the estimated state vector and the measured one.

$\alpha = [\alpha_1, \alpha_2, ...]$ and $\beta = [\beta_1, \beta_2, ...]$ are vectors containing weighing/gain coefficients used to ensure convergent/stability, these are determined while studying the stability of errors.

[27] cites that assuming :

$$||f(t, x_1, x_2, u) - f(t, x_1, \hat{x}_2, u) + \xi(t, x_1, x_2)|| \geq f^+$$

f^+ is a constant that does not depends on the elasticity terms, α and β satisfy the inequalities :

$$\begin{aligned} &\alpha > f^+ \\ &\beta > \sqrt{\frac{2}{\alpha - f^+}} \cdot \frac{(\alpha + f^+)(1+q)}{1-q} \end{aligned} \tag{5.10}$$

Where q a chosen constant between 0 and 1. Taking $\tilde{x}_1 = x_1 - \hat{x}_1$ and $\tilde{x}_2 = x_2 - \hat{x}_2$, the error terms, they can be written in the following form :

$$\ddot{\tilde{x}}_1 = g(x_1, x_1, \hat{x}_2, u, F) - \frac{\beta}{2} \cdot \dot{\tilde{x}}_1 |\tilde{x}_1|^{-1/2} - \alpha sign(\tilde{x}_1) \tag{5.11}$$

Where $g(\cdot) = f(\cdot) - f(\hat{\cdot}) + \xi$ and $\frac{d}{dt}|x| = \dot{x} sign(x)$:

$$\ddot{\tilde{x}}_1 \in [-f^+, f^+] - \frac{\beta}{2} \cdot \dot{\tilde{x}}_1 |\tilde{x}_1|^{-1/2} - \alpha sign(\tilde{x}_1) \tag{5.12}$$

In 5.12 and in the case of $\tilde{x}_1 > 0$ and $\dot{\tilde{x}}_1 > 0$ the trajectory is confined between the axis $\tilde{x}_1 = 0$, $\dot{\tilde{x}}_1 = 0$ and the trajectory of the equation $\ddot{\tilde{x}}_1 = -(\alpha - f^+)$. Let $\tilde{x}_{1M}$ be the intersection of this curve with the axis $\dot{\tilde{x}}_1 = 0$. Obviously $2 \times (\alpha - f^+) \cdot \tilde{x}_{1M} = \tilde{x}_{10}^2$. It is easy to see that for $\tilde{x}_1 > 0$, $\dot{\tilde{x}}_1 > 0$:

$$\ddot{\tilde{x}}_1 \leq f^+ - \alpha sign(\tilde{x}_1) - \frac{1}{2} \cdot \beta \cdot \frac{\dot{\tilde{x}}_1}{|\tilde{x}_1|^1/2} < 0 \tag{5.13}$$

This implies that :

$$\frac{|\dot{\tilde{x}}_{1M}|}{|\dot{\tilde{x}}_{10}|} < \frac{1-q}{1+q} < 1 \tag{5.14}$$

These insure the convergence of the state $(\tilde{x}_{1i}, \dot{\tilde{x}}_{1k})$ to $\tilde{x}_1 = \dot{\tilde{x}}_1 = 0$, to prove the finite time of convergence consider the dynamics of $\tilde{x}_2$. $\tilde{x}_2 = \dot{\tilde{x}}_1$ when $\tilde{x}_1 = 0$ taking into account :

$$\dot{\tilde{x}}_{2j} = g_j(\cdot) - \alpha sign(\tilde{x}_{1j})$$

and :

$$0 < \alpha - f^{+} \leq |\dot{\tilde{x}}_2| \leq \alpha + f^{+}$$

Holds in small vicinity of the origin, this : $|\dot{\tilde{x}}_{1k}| \geq (\alpha - f^{+})t_k$ Where t_k is the time interval between the successive intersection of the trajectory with the axis $\tilde{x}_1 = 0$. Hence :

$$t_k \leq \frac{|\dot{\tilde{x}}_{1k}|}{\alpha - f^{+}}$$

The total convergence time is given by equation 5.15.

$$T \leq \Sigma \frac{|\dot{\tilde{x}}_{1k}|}{\alpha - f^{+}} \tag{5.15}$$

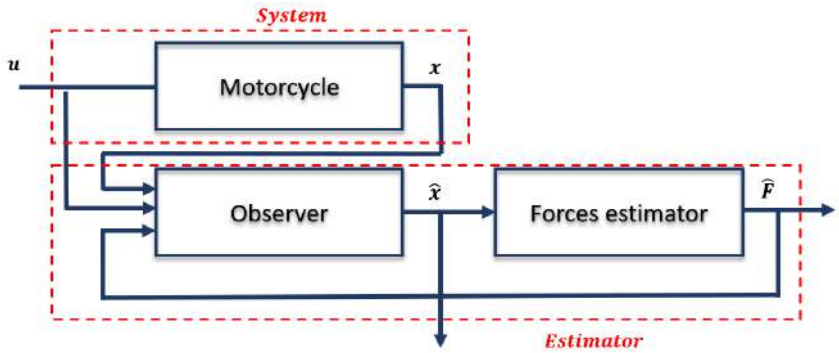

Figure 5.1: State and force estimation structure.

The next section, the simulation results obtained are presented.

5.3 Simulation

Simulation is done for the same input used in Fig. 3.10. Figure 5.2 shows selected real elements of the position vector $x_1 = q$ comparing them with their estimates. 5.3, compares some selected velocity elements of velocity vector $x_2 = \dot{q}$ with their estimates. Figures 5.4 and 5.5 show real front and rear contact patch forces and suspension force/torque and compares them with their estimated values.

We notice that the performance ie. convergence of estimates towards the real values, is fairly good, in fact, they converge in the 0.2 seconds mark, which is very fast considering the motorcycle dynamics. And lastly, Figure 5.6 depicts the real front and rear adherence, calculated using the following equations :

$$\mu_{ry} = F_{tr}/F_{zr}, \quad \mu_{rx} = F_{lr}/F_{zr}, \quad \mu_{fy} = F_{tf}/F_{zf}, \quad \mu_{fx} = F_{lf}/F_{zf}$$

From left to right are the rear and front, lateral/transversal and longitudinal adherences, these are obtained using the z-y or z-x forces (vertical-lateral or vertical-longitudinal). The global adherences are obtained using :

$$\mu_r = \sqrt{\mu_{ry}^2 + \mu_{rx}^2}, \qquad \mu_f = \sqrt{\mu_{fy}^2 + \mu_{fx}^2}$$

Their estimates are calculated using the estimated forces, and it's these estimates that are used to evaluate stability in accordance with the road/pavement conditions, adherence, security norms etc...

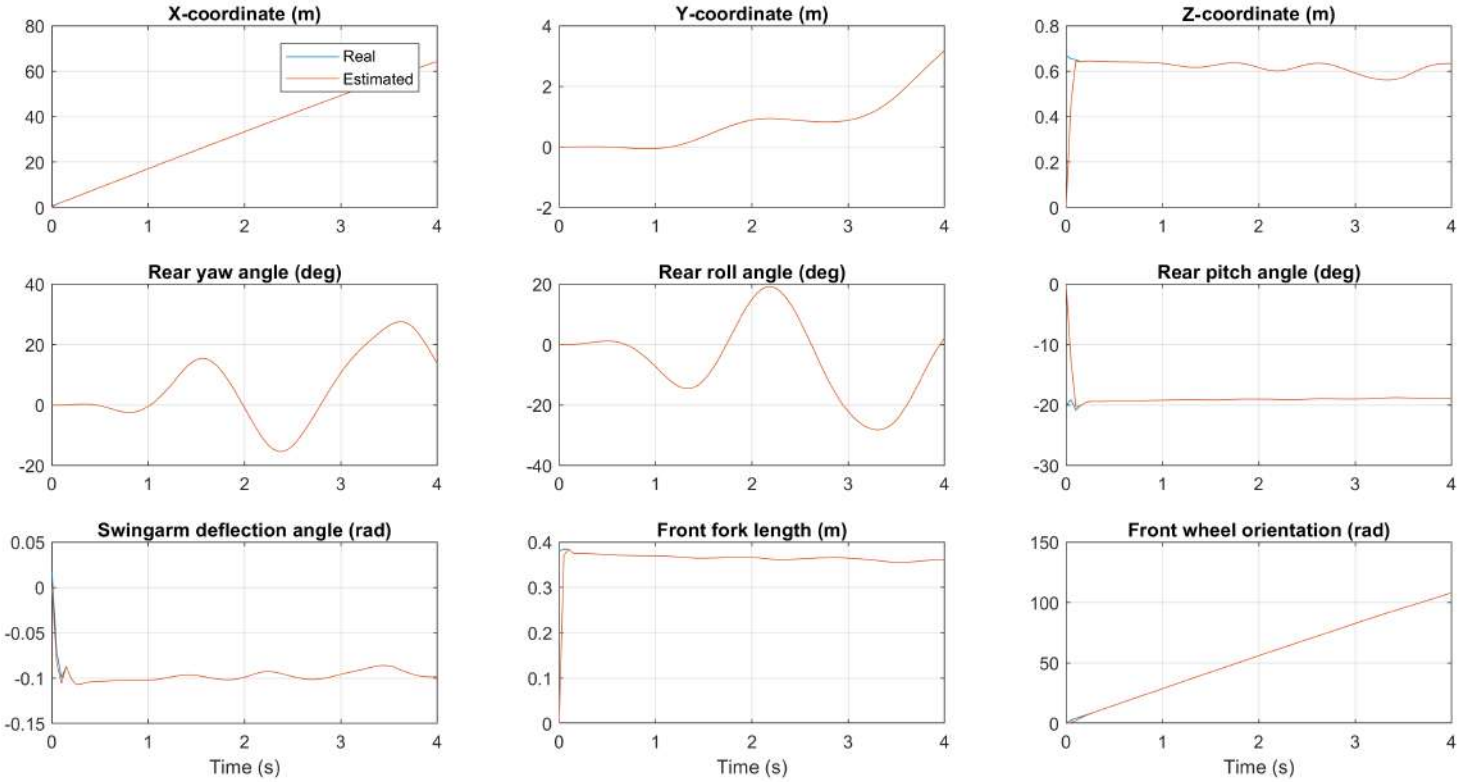

Figure 5.2: Selected angles and positions and their estimates.

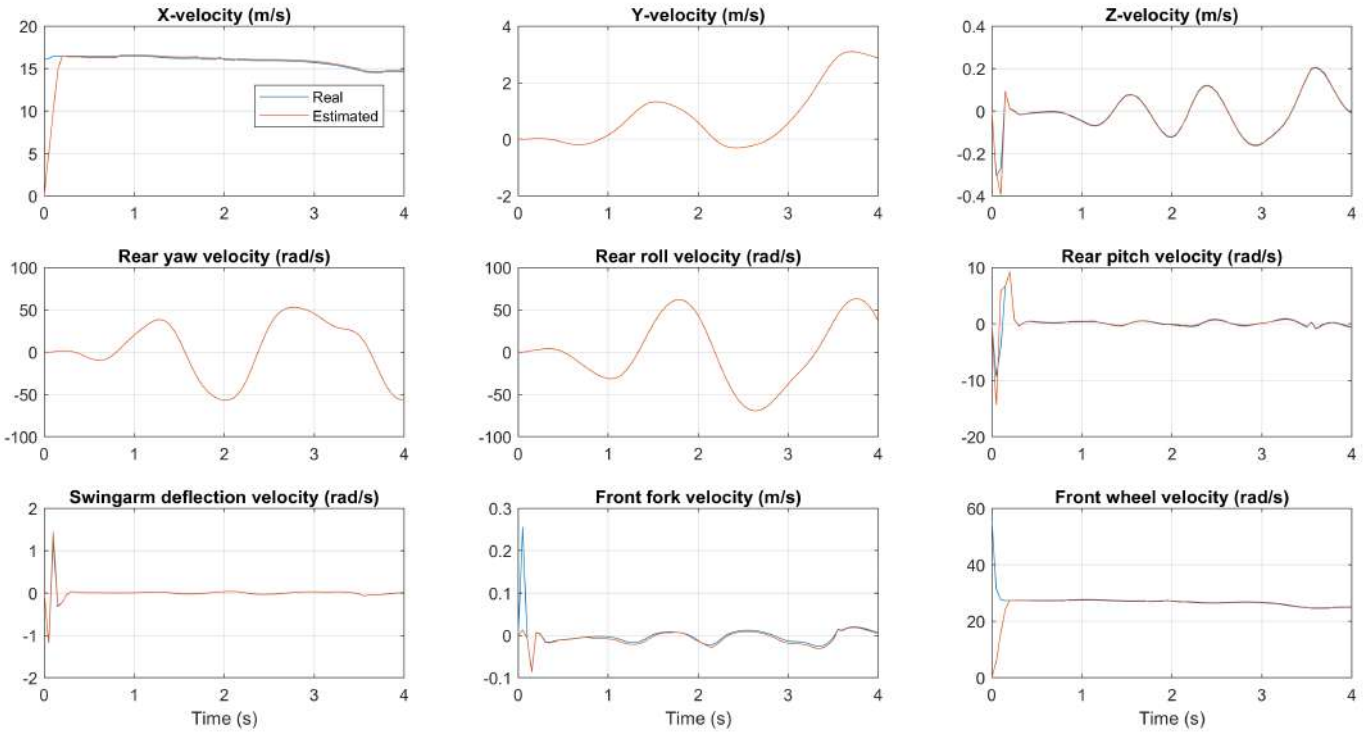

Figure 5.3: Selected velocities and their estimates.

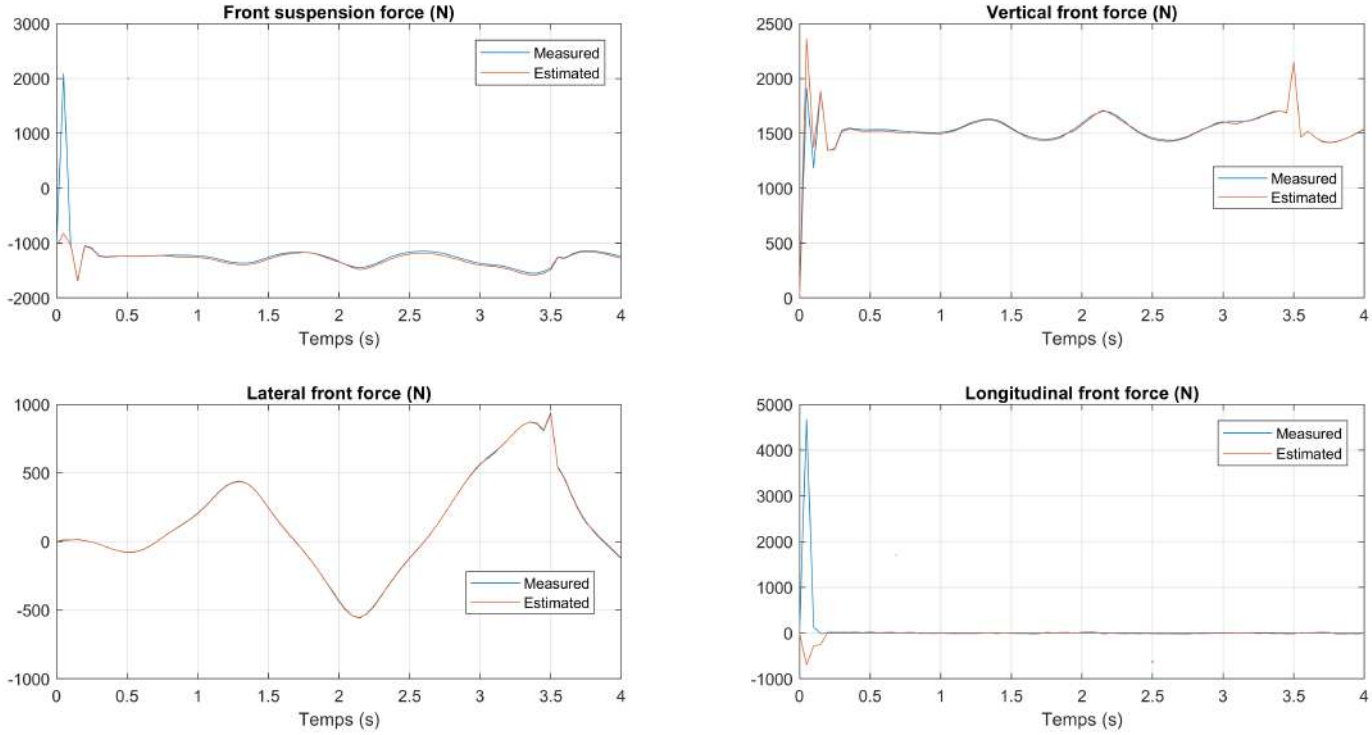

Figure 5.4: Front wheel real forces with their estimates.

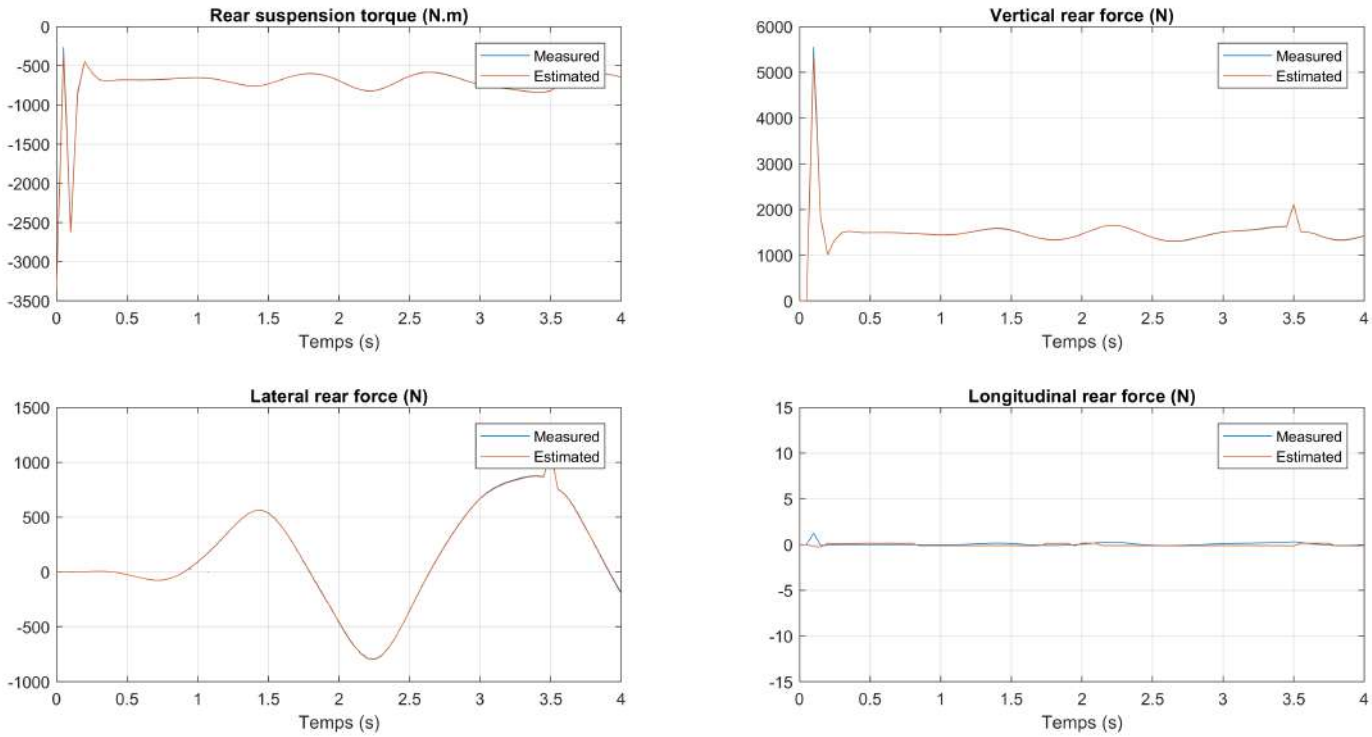

Figure 5.5: Rear wheel real forces with their estimates.

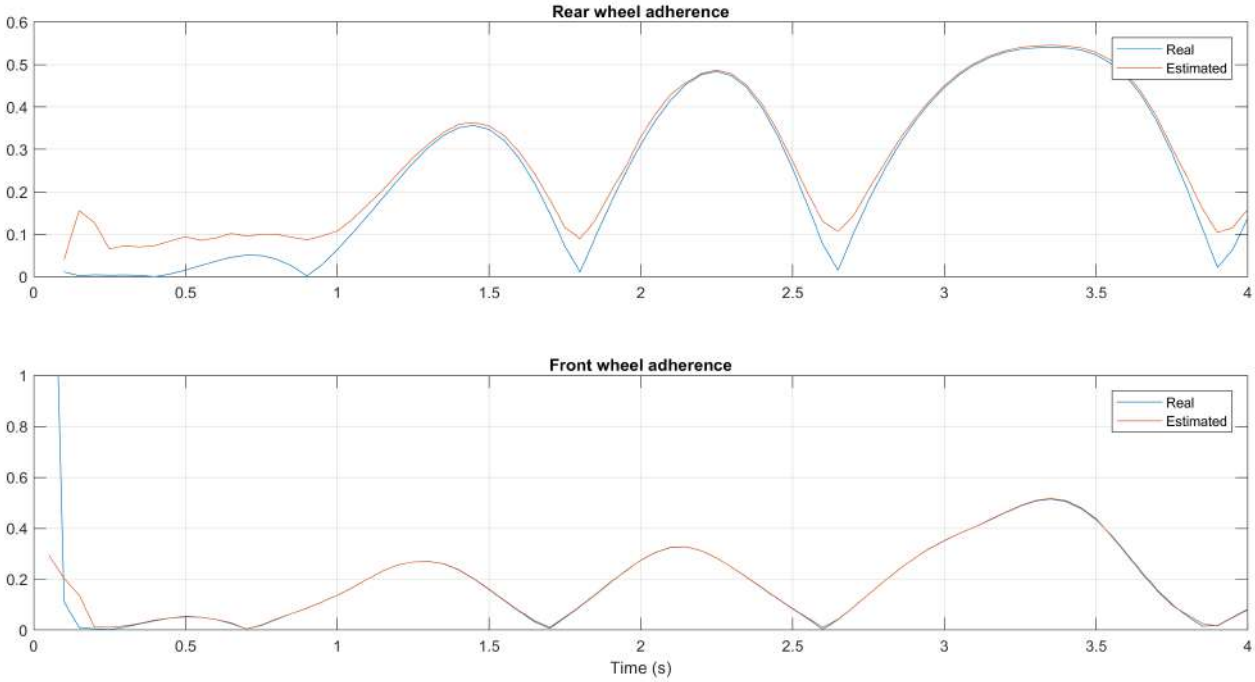

Figure 5.6: Real rear and front contact patch adherences with their estimated values.

5.4 Passivity Based Decoupling of the Model

The dynamics of motorcycle has been studied in [2]. However, the properties of the model are not always detailed and studied, especially the property of passivity. In the complete dynamic model with 13 degrees of freedom of the vehicle detailed in chapter 3, we find several passive components coupled together, namely the body, the front wheel, the rear wheel and the suspensions.

The objective of here is to study the property of passivity and the division of the dynamic model of the motorcycle into four subsystems, which are the translations of the bike according to the three axes x, y and z, the angles of turning of both the front and the rear wheel as well as their rotation angles, and finally the turns of two suspensions.

These four subsystems are subsequently grouped into four blocks. This division is justified by calculating and tracing the different coupling terms that connect the four blocks. The interest of cutting and its usefulness lies in the possibility of using models partially (only 1 block for instance) neglecting the other blocks. For this, two properties are important: the **preservation of passivity** of the block or sub-model, and the **effect of the couplings** coming from the other blocks must be negligible. Using Matlab-Simulink, we can illustrate the usefulness of this division. This is done later in this chapter.

5.4.1 Passivity theorem and properties

In order to show the passivity of the model, it is essential to present some definitions of passivity as well as theorems related to this property. Recall that a passive system satisfies the following property (described in [23]) :

$$E(t_1) = E(0) + E_s(0, t_1) - E_L(0, t_1) \tag{5.16}$$

where $E(t_1)$, $E(0)$ are respectively the energy of the system at time t_1 and at the initial moment $t = 0$, $E_s(0; t_1)$ is the energy supplied to the system during the interval of time $[0; t_1]$, $E_L(0; t_1)$ is the energy lost by dissipation in friction in the time interval $[0; t_1]$. Definition: A system with an input u and an output y where $u(t)$, $y(t) \in R^n$ Rn is passive if there is a strictly positive constant β such that (Inequality of Popov) **[Brogliato 2000]**

$$\int_0^T y^T(t) \cdot \quad u(t)dt \geq \beta \tag{5.17}$$

And that viable for any function u, and any $T \geq 0$.

Now suppose there is a continuous positive function $V(t)$ such that :

$$\int_0^T y^T(t) \cdot u(t) \quad dt \geq V(t) - V(0) \tag{5.18}$$

for all functions u, and all $T \geq 0$ and all $V(0)$, then the input system $u(t)$ and output $y(t)$ is passive.

Presented in a similar manner in [24], we recall that by using Lagrange's formalism, the dynamic model of the motorcycle is given as follows:

$$\tau = \frac{d}{dt}(\frac{\partial E_c}{\partial \dot{q}}) - \frac{\partial E_c}{\partial q} + \frac{\partial E_p}{\partial q} \tag{5.19}$$

Where $E_c = 0.5 \cdot (\dot{q}^T M(q)\dot{q})$ represents the kinetic energy, E_p the potential energy, and τ couples and external forces. After calculating the potential and kinetic energies we we can establish the dynamic model from Lagrange's equations. This gives us :

$$\tau = M(q) \cdot \ddot{q} + C(q, \dot{q}) \cdot \dot{q} + V(q, \dot{q}) + C_0(t, q, \dot{q})) \tag{5.20}$$

We can from equations 5.20 and 5.19, deduce :

$$\dot{q}^T M(q)\ddot{q} = \dot{q}^T \cdot (\tau - V(q, \dot{q}) - C_0(t, q, \dot{q})) \tag{5.21}$$

by integrating we find (assuming $q_0 = q(0)$):

$$\int_0^t \dot{q}^T \cdot (\tau - V(q, \dot{q}) - C_0(t, q, \dot{q})) \quad dt = \frac{1}{2} \cdot (\dot{q}^T(t_1) \cdot M(q)(t_1) \cdot \dot{q}(t_1)) \tag{5.22}$$

So our system checks Popov's inequality.

For the motorbike if we consider for input $u = (\tau - V(q, \dot{q}) - C_0(t, q, \dot{q}))$ and for output $y = \dot{q}$, then the transfer of $u = \tau - V(q, \dot{q}) - C_0(t, q, \dot{q})$, is passive.

Interconnection between passive systems

Generally, we find three types of interconnections of two passive systems S_1 and S_2. The first interconnection is said to be parallel, illustrated by Figure 3.1. As its name suggests, with this interconnection both systems have the same input $u = u_1 = u_2$ (no feedback) and the output $y = y_1 + y_2$.

- The combination of two or more passive systems in parallel gives us a passive system.

$$\int_0^{t_1} y^T(t) \cdot u(t) \quad dt = \int_0^{t_1} y_1^T(t) \cdot u_1(t) \quad dt + \int_0^{t_1} y_2^T(t) \cdot u_2(t) \quad dt \tag{5.23}$$

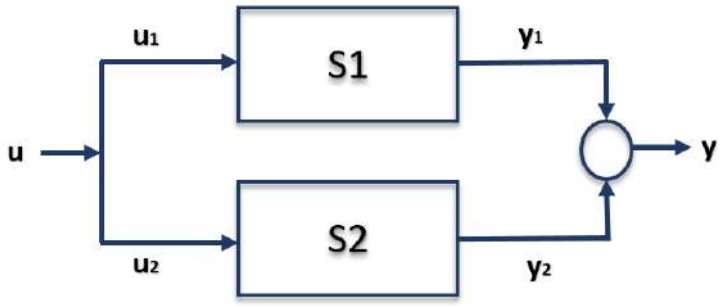

Figure 5.7: Parallel interconnection.

- The interconnection of two or more passive systems into feedback gives us a passive system.

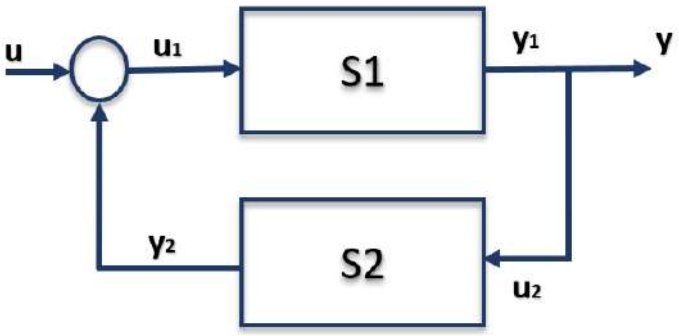

Figure 5.8: Feedback interconnection.

5.4.2 Decoupling of the global model

In this subsection, we present a proposal to split the complete dynamic vehicle model into four subsystems. This decomposition is based on the passivity property, presented previously, of the dynamic model. the generalized coordinates vector q, is going to be divided into 4 parts as stated previously, at the level of the box, we find three translation movements $q_A^T = [q_x \quad q_y \quad q_z]^T$ and three rotational movements for each wheel in addition to their orientations. $q_B^T = [q_0 \quad q_1 \quad q_2 \quad q_8]^T$ for the rear wheel, and $q_C^T = [q_4 \quad q_5 \quad q_6 \quad q_9]^T$ for the front wheel. The suspensions give us two de-beats along the vertical axis $q_D^T = [q_7 \quad q_f]^T$. So we can write the generalized coordinate vector q as follows :

$$\begin{aligned} q^T &= [q_A \quad q_B \quad q_C \quad q_D]^T \\ q_A^T &= [q_x \quad q_y \quad q_z]^T \\ q_B^T &= [q_0 \quad q_1 \quad q_2 \quad q_8]^T \\ q_C^T &= [q_4 \quad q_5 \quad q_6 \quad q_9]^T \\ q_D^T &= [q_7 \quad q_f]^T \end{aligned} \tag{5.24}$$

Meanings of q_i are described in Table 3.1.

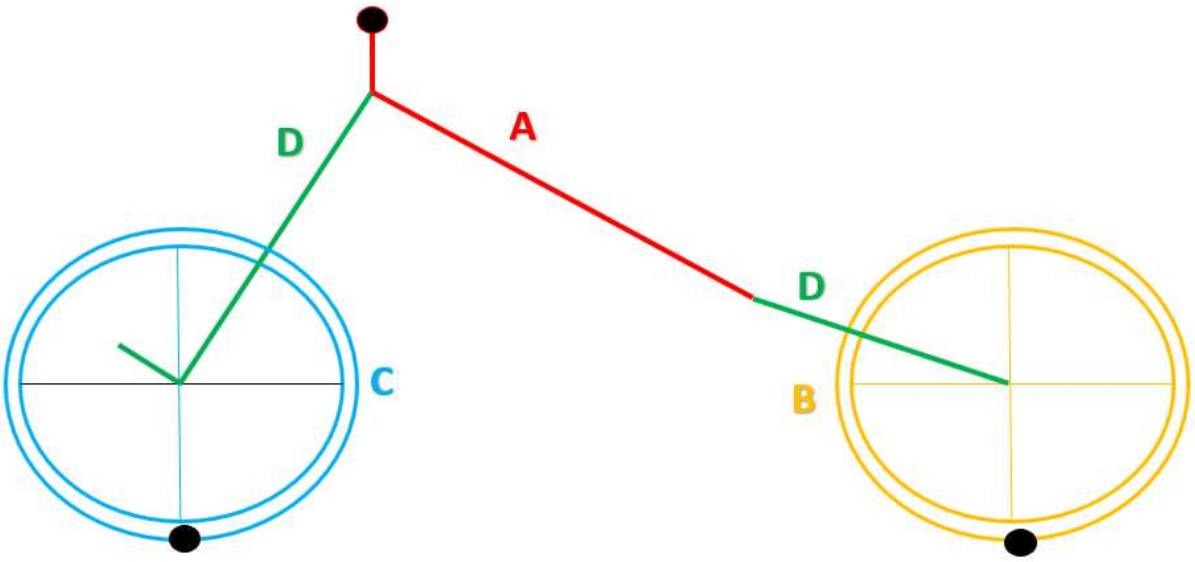

Figure 5.9: Wheel decoupling into four blocks.

Decoupling shown in figure 5.9, that is based on the decomposition in equation 5.24.

We can then split the complete dynamic vehicle model into four subsystems, assuming that the inertia matrix $M(q)$ and the Coriolis and Centrifuge matrix $C(q, \dot{q})$ are originally 13 by 13 matrices, and are composed of four rows and four columns.

$$M(q) = \begin{bmatrix} \hat{M}_{11}^{3\times3} & \hat{M}_{12}^{3\times4} & \hat{M}_{13}^{3\times4} & \hat{M}_{14}^{3\times2} \\ \hat{M}_{21}^{4\times3} & \hat{M}_{22}^{4\times4} & 0_{23}^{4\times4} & \hat{M}_{24}^{4\times2} \\ \hat{M}_{31}^{4\times3} & 0_{32}^{4\times4} & \hat{M}_{33}^{4\times4} & \hat{M}_{34}^{4\times3} \\ \hat{M}_{41}^{2\times3} & \hat{M}_{42}^{2\times4} & \hat{M}_{43}^{2\times4} & \hat{M}_{44}^{2\times2} \end{bmatrix} \tag{5.25}$$

Where $\hat{M}_{ij}^{k\times l}$ is the sub matrix, according to the chosen decomposition, of the mass matrix $M(q)$, of dimensions $k \times l$ and position ij.

$$C(q, \dot{q}) = \begin{bmatrix} 0_{11}^{3\times3} & \hat{C}_{12}^{3\times4} & \hat{C}_{13}^{3\times4} & \hat{C}_{14}^{3\times2} \\ 0_{21}^{4\times3} & \hat{C}_{22}^{4\times4} & 0_{23}^{4\times4} & \hat{C}_{24}^{4\times2} \\ 0_{31}^{4\times3} & 0_{32}^{4\times4} & \hat{C}_{33}^{4\times4} & \hat{C}_{34}^{4\times3} \\ 0_{41}^{2\times3} & \hat{C}_{42}^{2\times4} & \hat{C}_{43}^{2\times4} & 0^{2\times2} \end{bmatrix} \tag{5.26}$$

Where $\hat{C}_{ij}^{k\times l}$ is the sub matrix, according to the chosen decomposition, of the Coriolis matrix $C(q, \dot{q})$, of dimensions $k \times l$ and position ij. $\hat{0}_{ij}^{k\times l}$ is a matrix of dimensions $k \times l$ containing only zeros.

Our work matrix $W(q, \dot{q})$ is equal to a Jacobian times the force vector $J(q) \cdot F$, however, we are not going to decompose it as such for simplicity purposes.

$$W(q, \dot{q})^T = \begin{bmatrix} \hat{W}_1^{1\times3} & \hat{W}_2^{1\times4} & \hat{W}_3^{1\times4} & \hat{W}_4^{1\times2} \end{bmatrix} \tag{5.27}$$

Where $\hat{C}_{ij}$, $\hat{M}_{ij}$ and $\hat{W}_{ij}$ are components of matrices C, M and W, and are matrices themselves.

Expressions of sub-models A, B, C and D are given by matrix equation 5.28.

$$W = M \cdot \ddot{q} + C \cdot \dot{q} - P \tag{5.28}$$

Assuming that the couplings terms $Co_{A,B,C,D}$ are bounded $C_{ji} < k_i$, the five subsystems can be written in the following the form in equations 5.29, 5.30, 5.31, and 5.32.

$$\Sigma_A : \ddot{q}_A = f_A(q_A, W_A, P_A) + Co_A \tag{5.29}$$

$$\Sigma_B : \ddot{q}_B = f_B(q_B, W_B, P_B) + Co_B \tag{5.30}$$

$$\Sigma_C : \ddot{q}_C = f_C(q_C, W_C, P_C) + Co_C \tag{5.31}$$

$$\Sigma_D : \ddot{q}_D = f_D(q_D, W_D, P_D) + Co_D \tag{5.32}$$

We have presented here the various subsystems Σ_A, Σ_B, Σ_D and Σ_D which correspond respectively to the translations and rotations of the wheels, and the suspensions, equations 5.33, 5.34, 5.35, and 5.36 give the expressions of the coupling terms. Figure 5.10 shows the different blocks of the dynamic vehicle model.

$$Co_A = M_{12} \cdot \ddot{q}_B + M_{13} \cdot \ddot{q}_C + M_{14} \cdot \ddot{q}_D + C_{12} \cdot \dot{q}_B + C_{13} \cdot \dot{q}_C + C_{14} \cdot \dot{q}_D \tag{5.33}$$

$$Co_B = M_{21} \cdot \ddot{q}_A + M_{24} \cdot \ddot{q}_D + C_{24} \cdot \dot{q}_D \tag{5.34}$$

$$Co_C = M_{31} \cdot \ddot{q}_A + M_{34} \cdot \ddot{q}_D + C_{34} \cdot \dot{q}_D \tag{5.35}$$

$$Co_D = M_{41} \cdot \ddot{q}_A + M_{42} \cdot \ddot{q}_B + M_{43} \cdot \ddot{q}_C + C_{42} \cdot \dot{q}_B + C_{43} \cdot \dot{q}_C \tag{5.36}$$

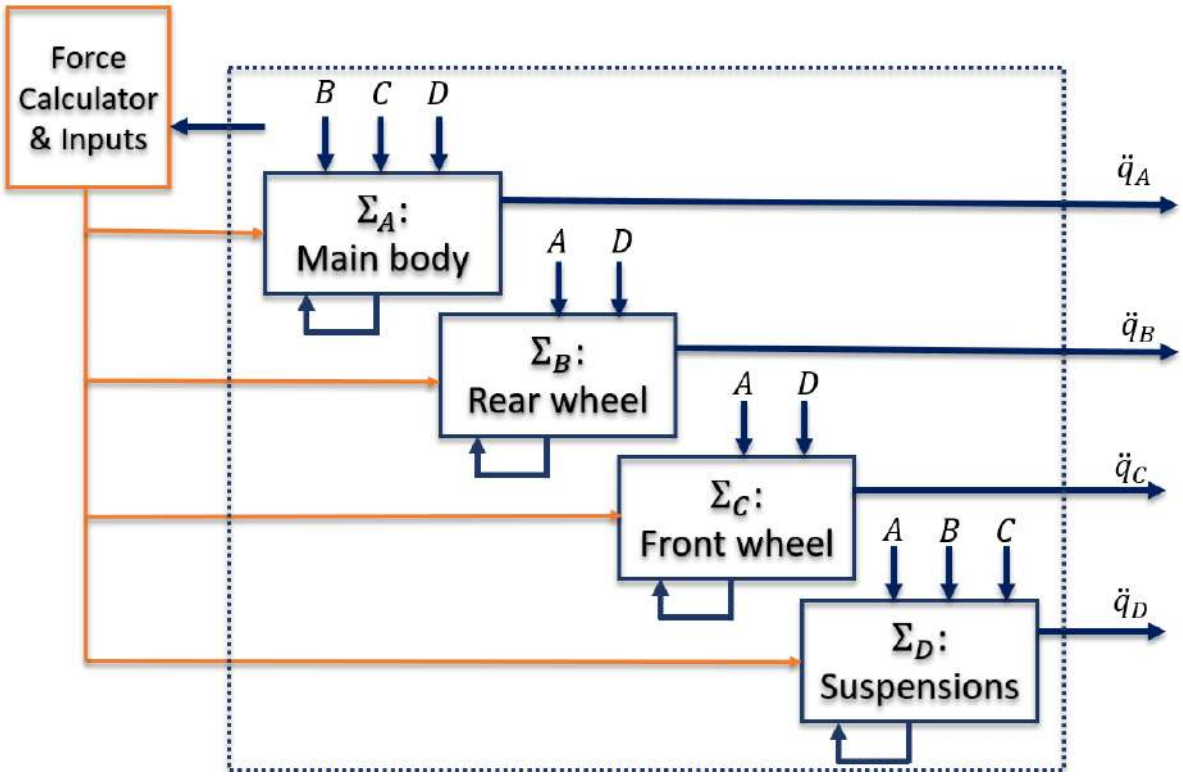

Figure 5.10: The four submodels of the global model.

5.4.3 State space representations of the Submodels

Sub-model Σ_A

Based on equation 5.29 and by choosing $x_{1A} = q_A$ and $x_{2A} = \dot{q}_A$, the state space representation is equivalent to the subsystem's and can be written as in equation 5.37.

$$\begin{cases} \dot{x}_{1A} = x_{2A} \\ \dot{x}_{2A} = f(t, x_{1A}, x_{2A}) + C_A \\ y_A = h(x_{1A}, x_{2A}) \end{cases} \tag{5.37}$$

Sub-model Σ_B

Equation 5.30 and given that $x_{1B} = q_B$ and $x_{2B} = \dot{q}_B$, the state space representation is equivalent to the subsystem's and can be written as in equation 5.38.

$$\begin{cases} \dot{x}_{1B} = x_{2B} \\ \dot{x}_{2B} = f(t, x_{1B}, x_{2B}) + C_B \\ y_B = h(x_{1B}, x_{2B}) \end{cases} \tag{5.38}$$

Sub-model Σ_C

Given that $x_{1C} = q_C$ and $x_{2C} = \dot{q}_C$, and according to equation 5.31, the state space representation is equivalent to the subsystem's and can be written as in equation 5.39.

$$\begin{cases} \dot{x}_{1C} = x_{2C} \\ \dot{x}_{2C} = f(t, x_{1C}, x_{2C}) + C_C \\ y_C = h(x_{1C}, x_{2C}) \end{cases} \tag{5.39}$$

Sub-model Σ_D

Again, from Equation 5.32, and choosing $x_{1D} = q_D$ and $x_{2D} = \dot{q}_D$, the state space representation is equivalent to the subsystem's and can be written as in equation 5.40.

$$\begin{cases} \dot{x}_{1D} = x_{2D} \\ \dot{x}_{2D} = f(t, x_{1D}, x_{2D}) + C_D \\ y_D = h(x_{1D}, x_{2D}) \end{cases} \tag{5.40}$$

Passivity of the sub-models

In order to justify this decomposition it is essential to prove the passivity of each subsystem by checking the **Popov** inequality presented previously. The dynamic subsystem **j**, the dynamic equation is given by equation 5.41.

$$M_j(x_{1j}) \cdot \ddot{x}_{1j} = W_j - C_j(x_{1j}, x_{2j})\dot{x}_{1j} - P(x_{1j}, x_{2j}) - C_j \tag{5.41}$$

Where j = A, B, C, or D. $M_j(x_{1j})$, W_j, $C_j(x_{1j}, x_{2j})$, $P(x_{1j}, x_{2j})$ and C_j are the Mass matrix, the Work term, Cristoffel matrix, Gravitational term and the Coupling term respectively (for each subsystem).

Following the same approach presented in the previous subsection, kinetic energy Ec_j of subsystem Σ_j is equal to :

$$Ec_j = \frac{1}{2} \cdot (\dot{x}_{1j}^T \cdot M_j(x_{2j}) \cdot x_{2j}) \tag{5.42}$$

The integral in 5.22 is applied here on equation 5.42, we find :

$$\frac{1}{2} \cdot (\dot{x}_{1j}^T(t_1) \cdot M_j \cdot \dot{x}_{1j}(t_1)) - \frac{1}{2} \cdot (\dot{x}_{1j0}^T \cdot M_j \cdot \dot{x}_{1j0}) \tag{5.43}$$

Where $x_{1j0} = x_{1j}(0)$. It can thus be concluded that the subsystems are passive.

5.4.4 Simulation and comparison

Figure 5.11 shows the implementation of the subsystems studied previously, on Simulink,

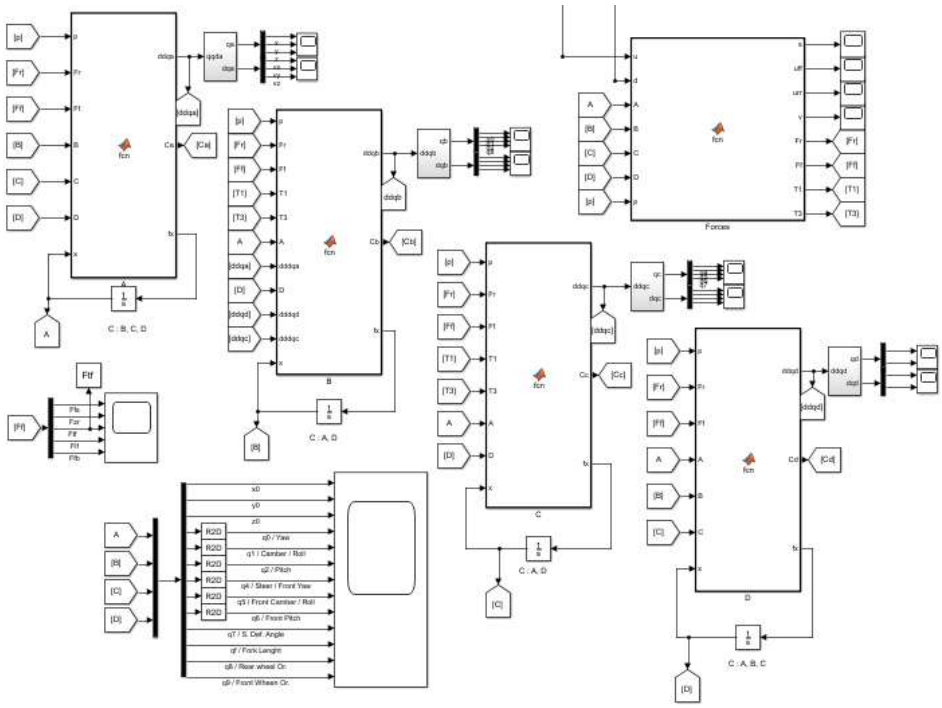

Figure 5.11: Sub-models in Simulink.

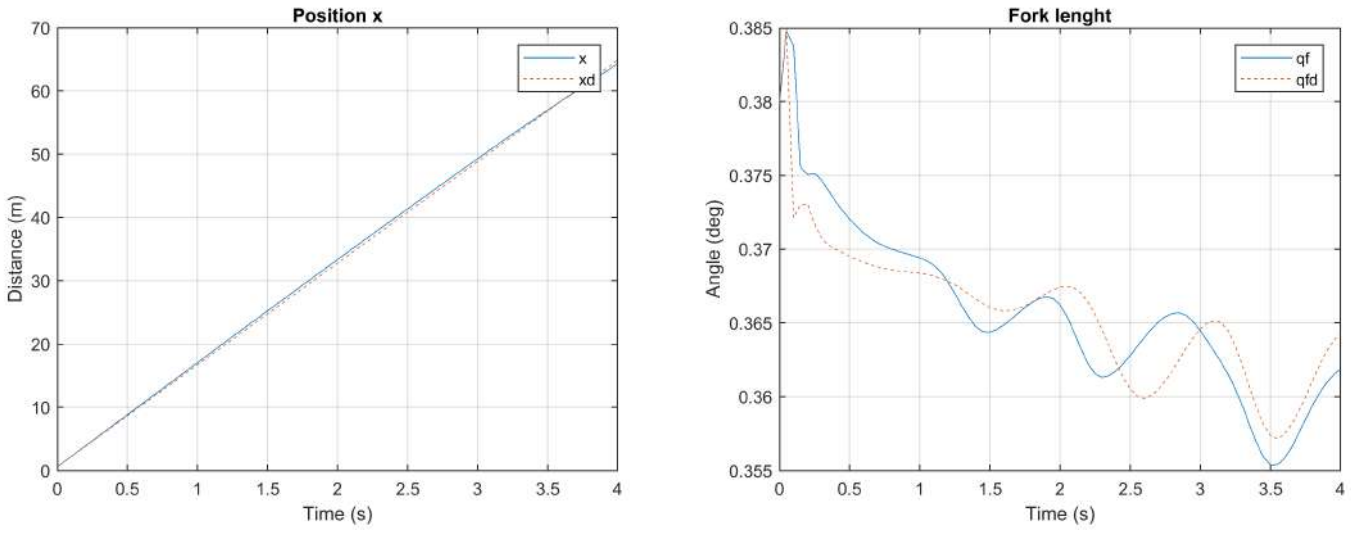

Figure 5.12: Position x and fork length of the original model versus the decoupled model.

Figures 5.12 to 5.14 show comparison between the original model, and the decoupled model.

It can clearly be seen that there are visible differences (error), in fact, some simulation problems have been encountered during this, some coupling terms were derived before other needed information were provided, this problem needs to be remedied for more precision. Therefore this should be investigated and developed further for more precision and a null error.

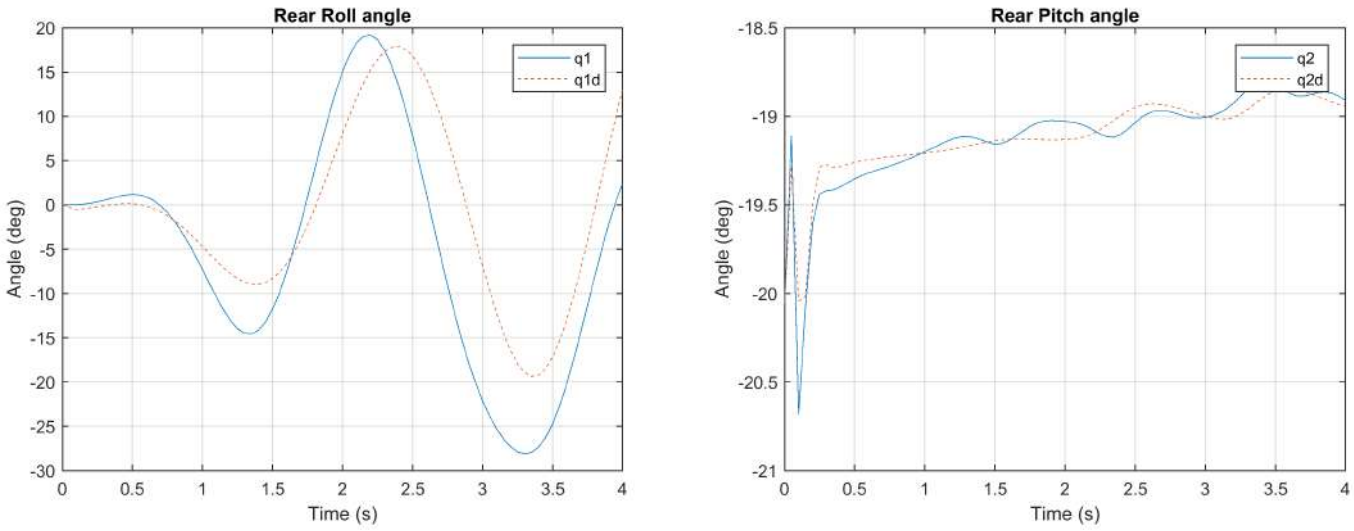

Figure 5.13: Rear roll and pitch angles of the original model versus the decoupled model.

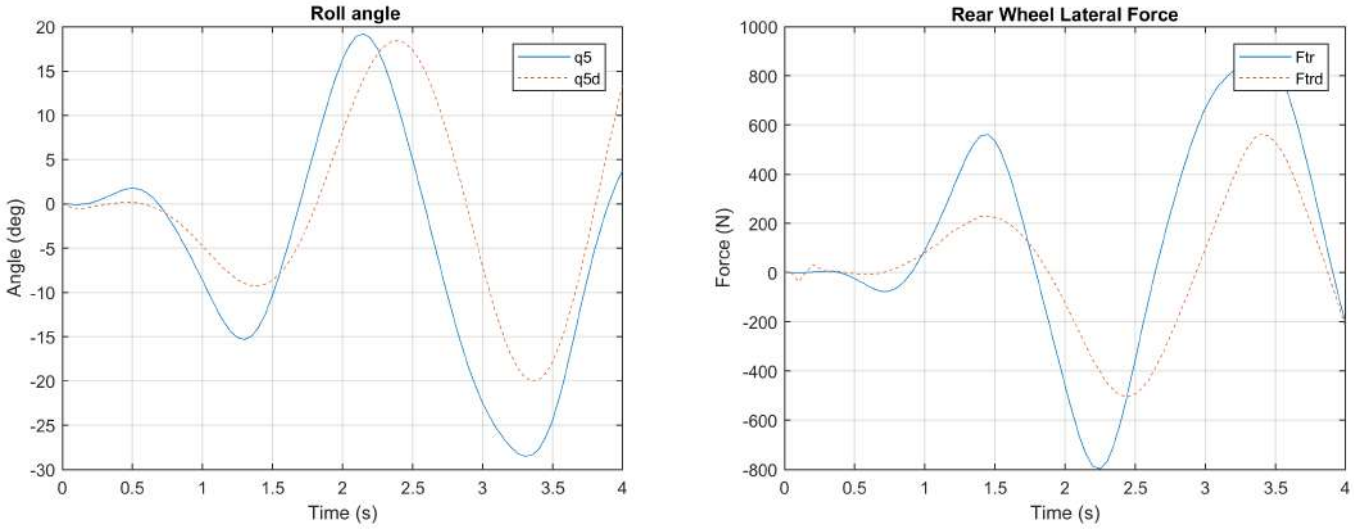

Figure 5.14: Front roll angle and transversal force of the original model versus the decoupled model.

For the sake of this study, we are going to consider that the results are good enough for us to be able to use the decoupled model for observer synthesis.

5.5 Partial state observers and Combination of Observers

Up until now, the observers were synthesised considering that the entire position vector is measurable, this in fact, is an ideal case, but not always possible in reality, as it unrealistic to consider that variables such as camber/roll and yaw angles are measurable. Table 5.1 shows the actually measured variables, and variables that are not.

In this section, this problem is treated using partial state observers. In vehicle dynamics, in order to study a particular phenomenon, it is useful to look at certain state variables. Thus, in the case of the study of braking, only the wheel / ground contact forces and the states concerning the wheels are interesting, likewise, in the case of the study of passenger comfort, only the states corresponding to the orientation and positioning of the body are interesting. In this regard, a partial observation of the system may be sufficient, hence the idea of designing partial observers. For this, we will use the decomposition of the dynamic model of vehicle presented in the previous section. In this context, we are interested in the **high gain observer** as it presents many advantages, advantages that cover the obligation to use the sliding mode observer for situations where it would be complicated to.

As it was presented in section 1, equations 5.5 and 5.7 are used to describe the variables in table 5.1.

Table 5.1: Resulting steer input force for each value of the weighing coefficient M.

Positions	**Measurable (Yes/No)**	**Velocities**	**Measurable (Yes/No)**
$x_{11} = q_x$	Yes	$x_{21} = \dot{q}_x$	Yes
$x_{12} = q_y$	Yes	$x_{22} = \dot{q}_y$	No
$x_{13} = q_z$	Yes	$x_{23} = \dot{q}_z$	Yes
$x_{14} = q_0$	No	$x_{24} = \dot{q}_0$	Yes
$x_{15} = q_1$	No	$x_{25} = \dot{q}_1$	Yes
$x_{16} = q_2$	No	$x_{26} = \dot{q}_2$	Yes
$x_{17} = q_4$	No	$x_{27} = \dot{q}_4$	Yes
$x_{18} = q_5$	No	$x_{28} = \dot{q}_5$	Yes
$x_{19} = q_6$	No	$x_{29} = \dot{q}_6$	Yes
$x_{110} = q_7$	Yes	$x_{210} = \dot{q}_7$	Yes
$x_{111} = q_f$	Yes	$x_{211} = \dot{q}_f$	Yes
$x_{112} = q_8$	No	$x_{212} = \dot{q}_8$	Yes
$x_{113} = q_9$	No	$x_{213} = \dot{q}_9$	Yes

5.2 shows the dependency of the different forces needed to calculate the adherences, this information is needed, as the variables that are not measurable are replaced with their estimates.

Table 5.2: Force-generalized coordinates / velocity dependence.

Forces	**Function of**
Front suspension	$f(x_{16}, x_{110}, x_{26}, x_{210})$
Rear suspension	$f(x_{111}, x_{211})$
Front vertical	$f(x_{23}, x_{14}, x_{15}, x_{110}, x_{24}, x_{25}, x_{210})$
Rear vertical	$f(x_{23}, x_{18}, x_{19}, x_{111}, x_{28}, x_{29}, x_{211})$
Front lateral	$f(F_{zr}, x_{14})$
Rear lateral	$f(F_{zf}, x_{17})$
Front longitudinal	$f(F_{zr}, x_{15}, x_{212})$
Rear longitudinal	$f(F_{zf}, x_{18}, x_{213})$

As a reminder, our system is written as :

$$\begin{cases} \dot{x}_1 = x_2 \\ \dot{x}_2 = f(t, x_1, x_2, u, F) \\ y = h(x_1, x_2) \end{cases} \tag{5.44}$$

Where F are the forces and u is the input. Figure 5.15 represents the schematic diagrams of our observers, since in the first subsystem, we need to observe the y velocity, that can be calculated by differentiation, sliding mode observer is used. This, however, is not possible for subsystems B and C, as it's the positions, or rather angles that cannot be measured, this is why the high gain observer is used in this case.

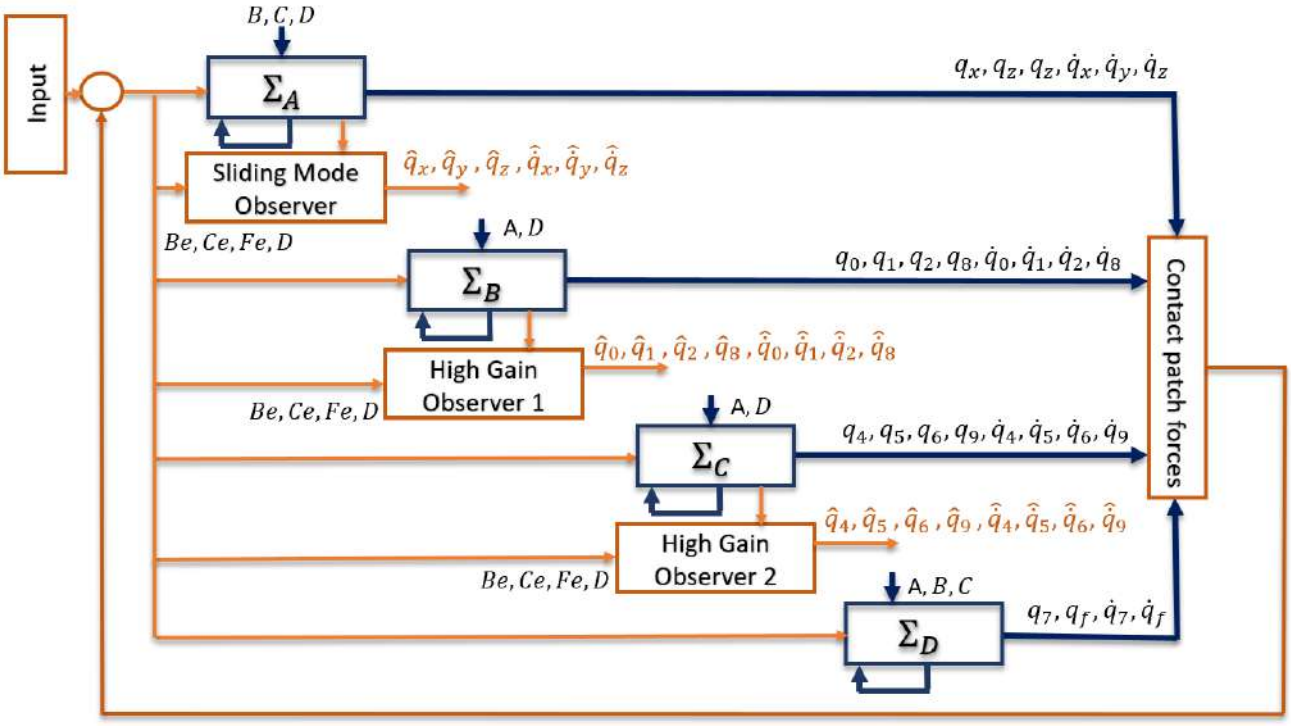

Figure 5.15: Combination of observers/sub-observers.

5.5.1 High Gain Observer

In the previous subsection, 3 observers were used, the first one is a higher order sliding mode (second order) observer discussed earlier in the report. The two other observers used are high gain observers, the principle of these is explained here. These observers have some advantages that can be summarized as follows :

- High-gain observers are relatively simple to design as it is not needed to solve complex differential equations nor use complicated formulae. Determining a suitable value for the gain is typically done through experimentation.
- For large class of non-linear systems, they can provide global or semi-global stability results for large class of systems. This means that their use can provide stability guarantees for any arbitrarily chosen initial conditions.
- They can be relatively fast.
- They can be robust to modelling uncertainty and external disturbances...

The big disadvantage of these observers is that a high gain can amplify noise as well, but so long as we don't have very much of noise in measurements (e.g., small noise power) or process disturbances (a very good models as in vehicle dynamics which is the case for our study), high gain observers do much better, as the state estimate converges to the actual state rapidly.

For multi-input multi-output systems, the general form is :

$$\begin{cases} \dot{x} = f(x) + g(x) \cdot u \\ y = h(x) \end{cases} \tag{5.45}$$

Where : $x \in R^n$, $g \in R^m$ and $y \in R^p$, $n = 26$ is the number of state variables, $m = 2$ number of inputs and $p = 17$ is the number of outputs/measured state variables. A use of a change of variables is needed, we put $z = \Phi(x)$, where :

$$z^T = [z_1, z_2, ..., z_p] \tag{5.46}$$

$$z_j^T = [z_{j1}, z_{j2}, ..., z_{jj}] \tag{5.47}$$

Where $dim(z_j) = n_j$ and $\sum_{i=1}^{p} n_j = n$. The system can be then rewritten as :

$$\begin{cases} \dot{z}_j = A_j z_j + \varphi(z_1, z_2, ..., z_j, y, u) \\ y_j = C_j z_j \end{cases} \tag{5.48}$$

So, synthesising the observer is done in the following manner :

$$\begin{cases} \dot{z}_j^i = A_j \hat{z}_j + \varphi_j(\hat{z}_1, ..., \hat{z}_j, y, u) - S_{\theta j}^{-1} C_j^T (C_j \hat{z}_j - y_j) \\ \theta_j S_j + A_j^T S_{\theta j} + S_{\theta j} A_j = C_j^T C_j \\ \theta_j > 0 \end{cases} \tag{5.49}$$

Where :

$$A_j = \begin{bmatrix} 0 & 1 & 0 & ... & 0 \\ 0 & 0 & 1 & ... & 0 \\ \vdots & \vdots & & & \vdots \\ 0 & ... & ... & & 0 \end{bmatrix} \tag{5.50}$$

$S_{\theta j}$ is calculated next, in equation 5.52. Consider our system :

$$\begin{cases} \dot{x}_1 = x_2 \\ \dot{x}_2 = f(x_1, x_2, u) \\ y = [C_1 \quad C_2] \cdot [x_1 \quad x_2]^T \end{cases} \tag{5.51}$$

Where $[x_1 \quad x_2]^T = [q \quad \dot{q}]$ and $C_{1/2}$ are output matrices of dimensions 1×13 containing zeros and ones, zeros for variables that are not measurable, and ones for those that are. Replacing the equations, we have :

$$\begin{cases} \theta S_{\theta 1} = C_1^T C_1 \\ \theta S_{\theta 2} + S_{\theta 1} = C_1^T C_2 \\ \theta S_{\theta 3} + S_{\theta 1} I = C_2^T C_1 \\ \theta S_{\theta 4} + S_{\theta 2} I + S_{\theta 3} = C_2^T C_2 \end{cases} \tag{5.52}$$

I is an identity matrix, the gain matrices are found by regulating the term θ, one of the many advantages of the high gain observer, it's the only term we need to fix to ensure convergence.

5.5.2 Simulation

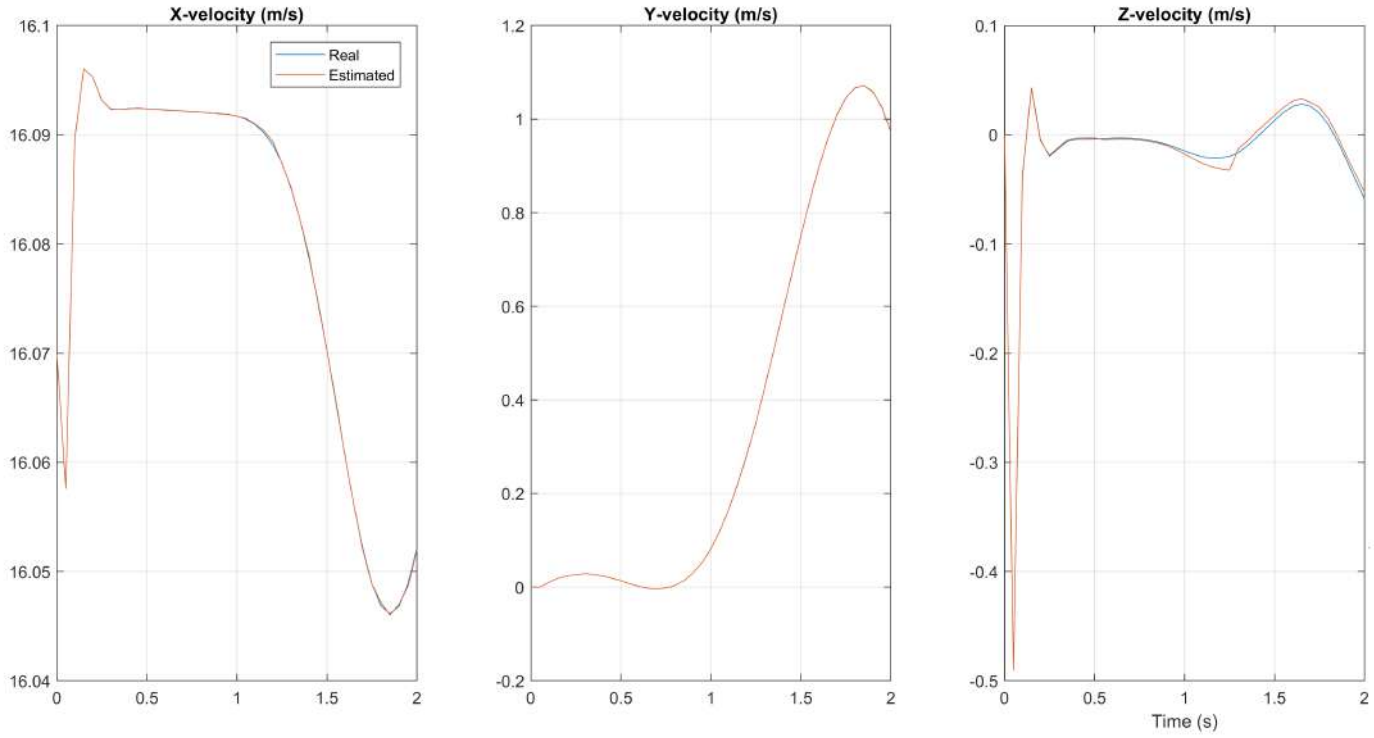

Figure 5.16: X, Y and Z coordinates ($q_x, q_y \quad and \quad q_z$) and their estimates.

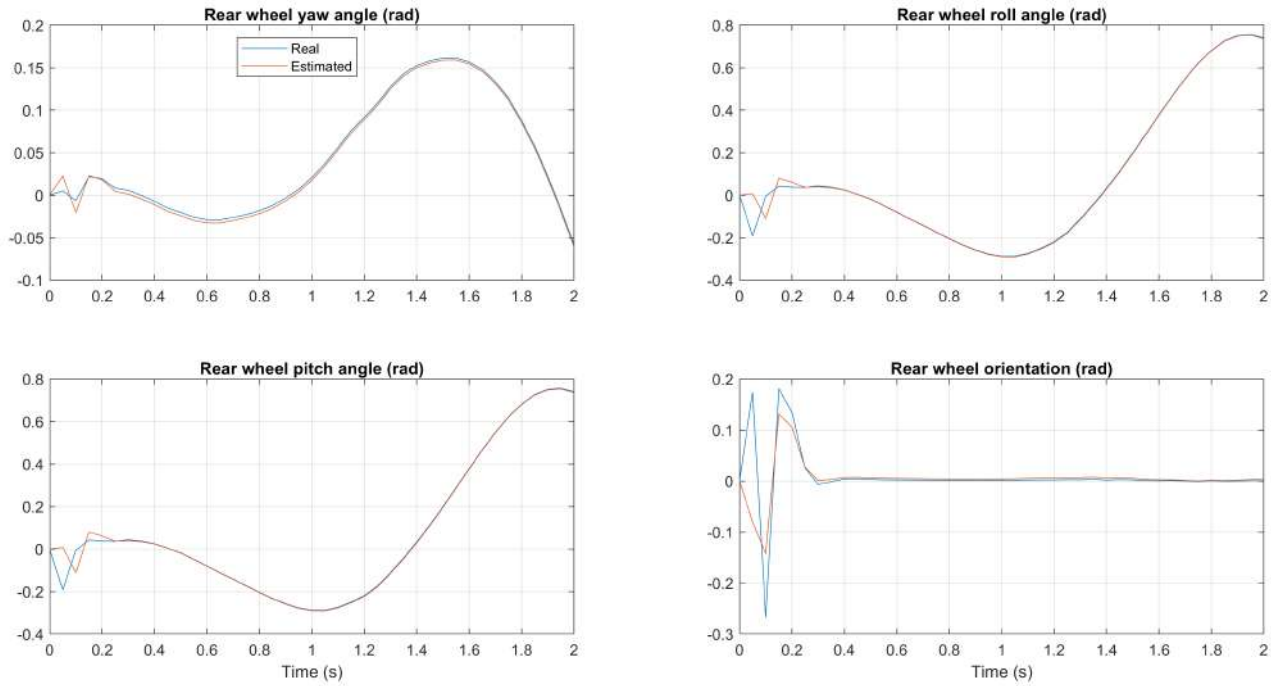

Figure 5.17: Rear yaw, roll, pitch and orientation ($q_0, q_1, q_2 \quad and \quad q_8$) and their estimates.

A selection of elements and their estimates are presented in this section, the simulation is done on the basis of what has been studied previously, sub-observers were used for different subsystems. A sliding mode observer for translational positions/velocities, and two high gain observers for rear and front wheel angles/velocities. For the sliding mode observer the 6 gains were regulated until convergence was reached, and for the high gain observers only one gain each was modified and convergence took less time to be found, but with more simulation time, as the entire vectors had to be used even the measured values.

Figure 5.16 compares translational coordinates $q_x, q_y \quad and \quad q_z$ with their estimates $\hat{q}_x, \hat{q}_y \quad and \quad \hat{q}_z$. Figure 5.17 compares rotational positions of the rear wheel $q_0, q_1, q_2 \quad and \quad q_8$ and their estimates $\hat{q}_0, \hat{q}_1, \hat{q}_2 \quad and \quad \hat{q}_8$. Figure 5.18 on the other hand shows the force estimations of the rear wheel forces. These forces are used to calculate or rather estimate the adherences.

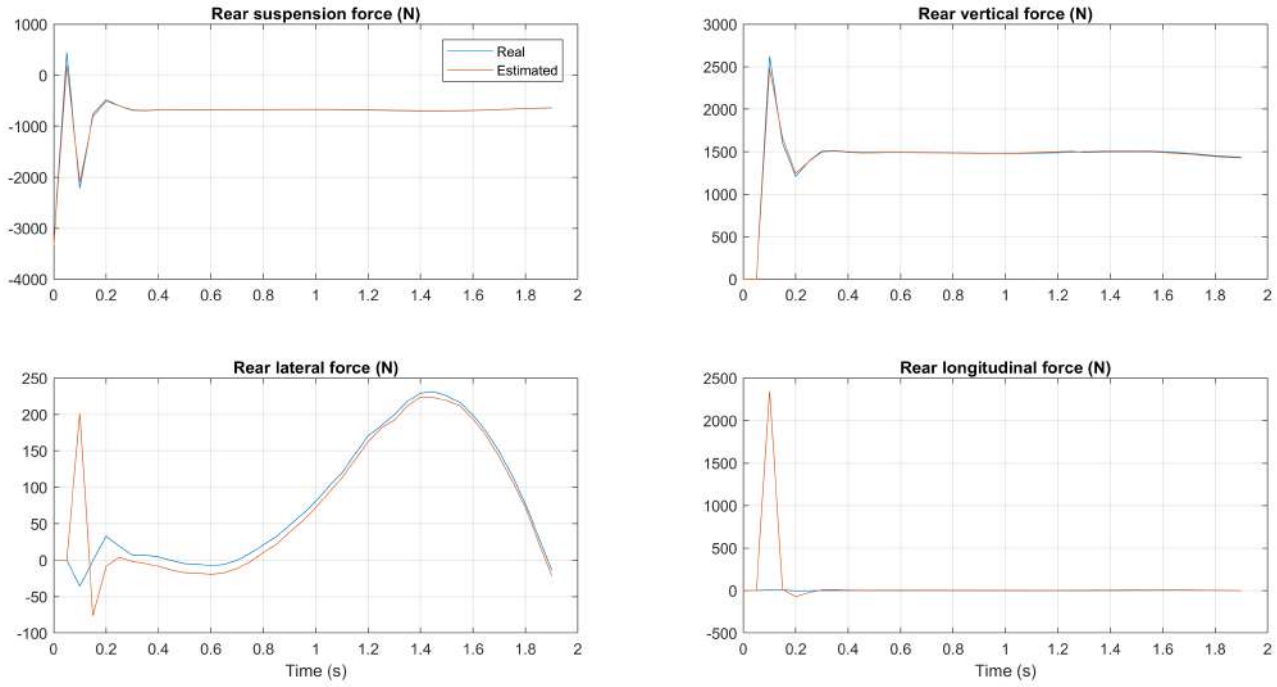

Figure 5.18: Rear forces and their estimates.

5.6 Conclusion

In this chapter, the state representation of the system has been formulated from the Lagrangian formalism of the modelled motorcycle, this was necessary for the synthesis of a state observer. A sliding mode observer has then been used to estimate the velocities and other state variables assuming the hypothesis where the position vector is entirely measurable (can be measured using sensors), this indeed is unrealistic. A more realistic case was studied, where not all positions and not all velocities are measurable, for this, the model was then decoupled, using the passivity theorem, into multiple subsystems, and multiple observers were used for each subsystems, namely, one 2^{nd} order sliding mode observer, and two high gain observer, simulation results and performance of the observers were then explained and commented.

CHAPTER 6

CONCLUSION AND RECOMMENDATIONS

6.1 Study Conclusion

In this work, a 13 degrees of freedom motorcycle model has been adapted to the study of stability in curves and corners, meaning that all the parameters and variables needed for stability analysis are integrated into the model namely the vertical, lateral and longitudinal forces, a simulation of this model with different inputs has been shown, validation is done intuitively however. Different stability criteria have then been studied, namely numerical based and non numerical based, the difference is that numerical ones can and have been used in our stability analysis algorithm that is based on loops with different condition verifications based on a specific variable and forward speed. This stability analysis is useful to create an alert system in case the motorcycle condition is located in the instability region, however, to elaborate the stability and instability regions for different factors, a state estimator/observer is necessary. In chapter 5 we have synthesized a state observer (higher order sliding mode) for the ideal case where all positions and angles are measured, and then the system had to be decoupled into sub-models and high gain observes were also used, as not all of the position vector is always measured nor is the velocity vector (both containing 13 state variables). Simulation results of comparing real state variables with their estimates was then shown and their performances evaluated and commented.

6.2 Study Recommendations

Many difficulties were encountered during this work, notably the fact that the model presents many non-linearities and is too large, obtaining the inverse of the analytical value of the mass matrix M was not feasible for example, so a smaller but even less slightly efficient model could have easily been tolerated. For stability analysis, it is crucial to further improve the stability testing algorithm as it does not take into account a number of real time factors (it is in fact an algorithm that is based on off-line testing), linearities the system and analysing stability in the traditional could prove to be efficient as well. And as for the observers, as mentioned before having a system where the mass matrix can be inverted and expressions shrank, could have made the synthesis of the observers smoother. The idea behind all of this is to develop an interactive alert system as is depicted in figure 6.1 either for the driver, or a stabilising control system for the motorbike.

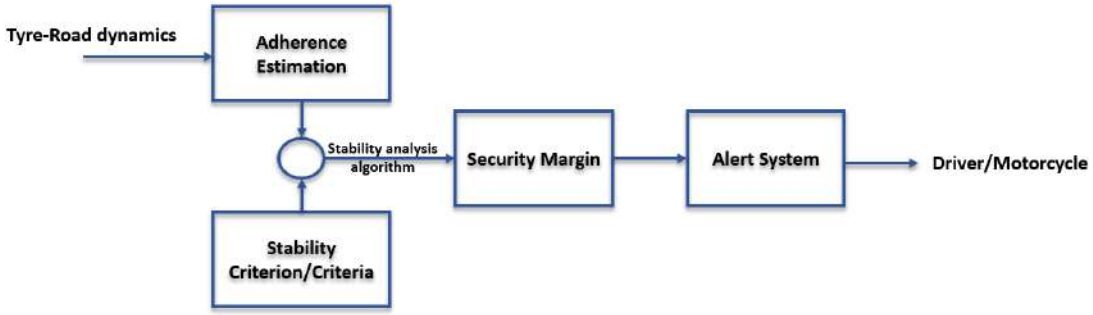

Figure 6.1: Stability - adherence alert system.

Appendix A
Motorcycle Parameters

```
%------------------------------------------------------------------------%
%                                    Parameters
%------------------------------------------------------------------------%
% rear wheel parameters
            % parameters relating to the shape
                a1 = .09 ; % crown radius
                b1 = .3149-.09 ; % centerline radius
            % dynamic parameters
                m1 = 16.85 ; % mass
                i1 = .8380 ; % inertia around rotation axis
                j1 = .4796 ; % inertia around the other two axes
            % parameters relating to the interaction forces
                f1 = 20 ; % friction coefficient
                e1 = 1 ; % rolling resistance coefficient
                k1 = 1e6/2 ; % normal force stiffness
                d1 = 1500 ; % normal force damping
                t1 = 1 ; % tangential stiffness (for numerical stability)
% Rear suspension parameters
            % shape parameters
                l2 = 0.5675 ; % swingarm length
            % dynamic parameters
                m2 = 19.31 ; % mass
                x2 = .2 ; % mass local x position
                i2 = .8 ; % inertia (average inertia to reduce parameter set)
            % parameters relating to the interaction forces
                t2 = 1 ; % top end
                b2 = 1000 ; % bottom end
                p2 = 1 ; % preload damping
                d2 = 1 ; % compression damping
                e2 = 1 ; % rebound damping
                k2 = 20000 ; % spring stiffness
                n2 = 1 ; % spring progressiveness
                f2 = 1 ; % friction coefficient
% Main frame parameters (sprung)
            % shape parameters
                l3 = 0.816630 ; % frame length
            % dynamic parameters
                m3 = 224.2+78.13 ; % mass
                x3 = .31 ; % mass local x position
                z3 = 0.3 ; % mass local z position
                i3 = 30 ; % inertia (average inertia to reduce parameter set)
                k3 = 1e9 ; % frame torsion stiffness (together with fork and swingarm)
                d3 = 1 ; % frame torsion damping (together with fork and swingarm)
% Steering head parameters (sprung)
            % shape parameters
                 l4 = 0.0198 ; % fork offset
            % dynamic parameters
                m4 = 9.09 ; % mass
                x4 = 0.036 ; % mass local x position
                z4 = 0.2235 + 0.09985863931372 ; % mass local z position
                i4 = .5 ; % inertia (average inertia to reduce parameter set)
% Front fork/suspension parameters (unsprung)
            % dynamic parameters
                m5 = 9.02 ; % mass
```

```
            x5 = -0.0114 ; % mass local x position
            z5 = 0.15 ; % mass local z position
            i5 = .3 ; % inertia (average inertia to reduce parameter set)
        % parameters relating to the interaction forces
            t5 = .5 ; % top end
            b5 = .3 ; % bottom end
            p5 = 0.45 ; % preload damping
            d5 = 6500 ; % compression damping
            e5 = 12000 ; % rebound damping
            k5 = 15000 ; % spring stiffness
            n5 = 1 ; % spring progressiveness
            f5 = 1 ; % friction coefficient
% Front wheel parameters
        % parameters relating to the shape
            a6 = .06 ; % crown radius
            b6 = .2999-.06 ; % centerline radius
        % dynamic parameters
            m6 = 13.57 ; % mass
            i6 = .5020 ; % inertia around rotation axis
            j6 = .333 ; % inertia around the other two axes
        % parameters relating to the interaction forces
            f6 = 20 ; % friction coefficient
            e6 = 1 ; % rolling resistance coefficient
            k6 = 1 ; % normal force stiffness
            d6 = 1 ; % normal force damping
            t6 = 2000 ; % tangential stiffness (for numerical stability)
```

Appendix B

Mass Matrix

```
%-------------------------------------------------------------------------%
%                              Mass Matrix
%-------------------------------------------------------------------------%

M(1,1) = m1 + m2 + m3 + m4 + m5 + m6;
M(1,2) = 0;
M(1,3) = 0;
M(1,4) = -sin(q0)*(cos(q2)*((x3 - l3)*m3 - l3*(m1 + m2)) + sin(q2)*z3*m3 +
 cos(q7)*((x2 - l2)*m2 - l2*m1)) + cos(q0)*sin(q1)*(-sin(q2)*((x3 - l3)*m3 - l3*(m1
  + m2)) + cos(q2)*z3*m3- sin(q7)*((x2 - l2)*m2 - l2*m1));
M(1,5) = sin(q0)*cos(q1)*(-sin(q2)*((x3 - l3)*m3 - l3*(m1 + m2)) + cos(q2)*z3*m3
 - sin(q7)*((x2 - l2)*m2 - l2*m1));
M(1,6) = cos(q0)*(-sin(q2)*((x3 - l3)*m3 - l3*(m1 + m2)) + cos(q2)*z3*m3) +
 sin(q0)*sin(q1)*(-cos(q2)*((x3 - l3)*m3 - l3*(m1 + m2)) - sin(q2)*z3*m3);
M(1,7) = -sin(q4)*(cos(q6)*(x4*m4 + (l4 + x5)*m5 + l4*m6) + sin(q6)*(z4*m4 +
 z5*m5 + qf*(-m5 - m6))) + cos(q4)*sin(q5)*(-sin(q6)*(x4*m4 + (l4 + x5)*m5 +
  l4*m6)+ cos(q6)*(z4*m4 + z5*m5 + qf*(-m5 - m6)));
M(1,8) = sin(q4)*cos(q5)*(-sin(q6)*(x4*m4 + (l4 + x5)*m5 + l4*m6) +
 cos(q6)*(z4*m4 + z5*m5 + qf*(-m5 - m6)));
M(1,9) = cos(q4)*(-sin(q6)*(x4*m4 + (l4 + x5)*m5 + l4*m6)+ cos(q6)*(z4*m4 +
 z5*m5 + qf*(-m5 - m6))) + sin(q4)*sin(q5)*( -cos(q6)*(x4*m4 + (l4 + x5)*m5 +
  l4*m6) - sin(q6)*(z4*m4 + z5*m5 + qf*(-m5 - m6)));
M(1,10)= -cos(q0)*sin(q7)*((x2 - l2)*m2 - l2*m1) - sin(q0)*sin(q1)*cos(q7)*((x2 -
 l2)*m2 - l2*m1);
M(1,11)= cos(q4)*sin(q6)*(-m5 - m6) + sin(q4)*sin(q5)*cos(q6)*(-m5 - m6);
M(1,12) = 0;
M(1,13) = 0;

M(2,1) = 0;
M(2,2) = m1 + m2 + m3 + m4 + m5 + m6;
M(2,3) = 0;
M(2,4) = cos(q0)*(cos(q2)*((x3 - l3)*m3 - l3*(m1 + m2)) + sin(q2)*z3*m3 +
 cos(q7)*((x2 - l2)*m2 - l2*m1)) + sin(q0)*sin(q1)*(-sin(q2)*((x3 - l3)*m3 - l3*(m1
  + m2)) + cos(q2)*z3*m3 - sin(q7)*((x2 - l2)*m2 - l2*m1));
M(2,5) = -cos(q0)*cos(q1)*(-sin(q2)*((x3 - l3)*m3 - l3*(m1 + m2)) + cos(q2)*z3*m3
 - sin(q7)*((x2 - l2)*m2 - l2*m1));
M(2,6) = sin(q0)*(-sin(q2)*((x3 - l3)*m3 - l3*(m1 + m2)) + cos(q2)*z3*m3) -
 cos(q0)*sin(q1)*(-cos(q2)*((x3 - l3)*m3 - l3*(m1 + m2)) - sin(q2)*z3*m3);
M(2,7) = cos(q4)*(cos(q6)*(x4*m4 + (l4 + x5)*m5 + l4*m6) + sin(q6)*(z4*m4 +
 z5*m5 + qf*(-m5 - m6))) + sin(q4)*sin(q5)*(-sin(q6)*(x4*m4 + (l4 + x5)*m5 +
  l4*m6)+cos(q6)*(z4*m4 + z5*m5 + qf*(-m5 - m6)));
M(2,8) = -cos(q4)*cos(q5)*(-sin(q6)*(x4*m4 + (l4 + x5)*m5 + l4*m6)+
 cos(q6)*(z4*m4 + z5*m5 + qf*(-m5 - m6)));
M(2,9) = sin(q4)*(-sin(q6)*(x4*m4 + (l4 + x5)*m5 + l4*m6) + cos(q6)*(z4*m4 +
 z5*m5 + qf*(-m5 - m6))) - cos(q4)*sin(q5)*(-cos(q6)*(x4*m4 + (l4 + x5)*m5 +
l4*m6)- sin(q6)*(z4*m4 + z5*m5 + qf*(-m5 - m6)));
M(2,10)= -sin(q0)*sin(q7)*((x2 - l2)*m2 - l2*m1)+ cos(q0)*sin(q1)*cos(q7)*((x2 -
 l2)*m2 - l2*m1);
M(2,11)= sin(q4)*sin(q6)*(-m5 - m6) - cos(q4)*sin(q5)*cos(q6)*(-m5 - m6);
M(2,12) = 0;
M(2,13) = 0;
```

```
M(3,1) = 0;
M(3,2) = 0;
M(3,3) = m1 + m2 + m3 + m4 + m5 + m6;
M(3,4) = 0;
M(3,5) = -sin(q1)*(-sin(q2)*((x3 - l3)*m3 - l3*(m1 + m2)) + cos(q2)*z3*m3-
 sin(q7)*((x2 - l2)*m2 - l2*m1));
M(3,6) = cos(q1)*(-cos(q2)*((x3 - l3)*m3 - l3*(m1 + m2)) - sin(q2)*z3*m3);
M(3,7) = 0;
M(3,8) = -sin(q5)*(-sin(q6)*(x4*m4 + (l4 + x5)*m5 + l4*m6)+ cos(q6)*(z4*m4 +
 z5*m5 + qf*(-m5 - m6)));
M(3,9) = cos(q5)*(-cos(q6)*(x4*m4 + (l4 + x5)*m5 + l4*m6)- sin(q6)*(z4*m4 +
 z5*m5 + qf*(-m5 - m6)));
M(3,10)= -cos(q1)*cos(q7)*((x2 - l2)*m2 - l2*m1);
M(3,11)= cos(q5)*cos(q6)*(-m5 - m6);
M(3,12) = 0;
M(3,13) = 0;


M(4,1) = -sin(q0)*(cos(q2)*((x3 - l3)*m3 - l3*(m1 + m2)) + sin(q2)*z3*m3 +
 cos(q7)*((x2 - l2)*m2 - l2*m1)) + cos(q0)*sin(q1)*(-sin(q2)*((x3 - l3)*m3 - l3*(m1
  + m2)) + cos(q2)*z3*m3- sin(q7)*((x2 - l2)*m2 - l2*m1));
M(4,2) = cos(q0)*(cos(q2)*((x3 - l3)*m3 - l3*(m1 + m2)) + sin(q2)*z3*m3+
 cos(q7)*((x2 - l2)*m2 - l2*m1)) + sin(q0)*sin(q1)*( -sin(q2)*((x3 - l3)*m3 - l3*(m1
 + m2)) + cos(q2)*z3*m3 - sin(q7)*((x2 - l2)*m2 - l2*m1));
M(4,3) = 0;
M(4,4) = m1*(-cos(q2)*l3 - cos(q7)*l2)^2  + m2*(-cos(q2)*l3 + cos(q7)*(x2 -
l2))^2+ m3*(cos(q2)*(x3 - l3) + sin(q2)*z3)^2  + sin(q1)^2*( m1*(sin(q2)*l3 +
sin(q7)*l2)^2  + m2*(sin(q2)*l3 - sin(q7)*(x2 - l2))^2+ m3*(-sin(q2)*(x3 - l3) +
cos(q2)*z3)^2 ) + I3y + I2y + I1y + (I1x- I1y + I2x - I2y + I3x - I3y + (I2z -
I2x)*cos(q7)^2+ (I3z - I3x)*cos(q2)^2 )*cos(q1)^2;
M(4,5) = -((sin(q2)*l3 + sin(q7)*l2)*(-cos(q2)*l3 - cos(q7)*l2)*m1 +(sin(q2)*l3 +
sin(q7)*l2 - x2*sin(q7))(-cos(q2)*l3 - cos(q7)*l2 + x2*cos(q7))*m2 +(sin(q2)*l3 -
x3*sin(q2) + cos(q2)*z3)*(-cos(q2)*l3 + x3*cos(q2) + sin(q2)*z3)*m3)*cos(q1) +
(I2z - I2x)*cos(q7)*sin(q7)*cos(q1)+ (I3z - I3x)*cos(q2)*sin(q2)*cos(q1);
M(4,6) = ((x3^2  + z3^2 )*m3 + (l3*(m1 + m2 + m3) - 2*x3*m3)*l3 + I3y- ((x2 -
l2)*m2 - l2*m1)*l3*cos(q2 - q7))*sin(q1);
M(4,7) = 0;
M(4,8) = 0;
M(4,9) = 0;
M(4,10)= (l2^2*m1 + (x2 - l2)^2*m2 + I2y + (l2*m1 + (l2 - x2)*m2)*l3*cos(q2 -
q7))*sin(q1);
M(4,11)= 0;
M(4,12)= sin(q1)*I1y;
M(4,13)= 0;


M(5,1) = sin(q0)*cos(q1)*(-sin(q2)*((x3 - l3)*m3 - l3*(m1 + m2)) + cos(q2)*z3*m3-
sin(q7)*((x2 - l2)*m2 - l2*m1));
M(5,2) = -cos(q0)*cos(q1)*(-sin(q2)*((x3 - l3)*m3 - l3*(m1 + m2)) + cos(q2)*z3*m3
- sin(q7)*((x2 - l2)*m2 - l2*m1));
M(5,3) = -sin(q1)*(-sin(q2)*((x3 - l3)*m3 - l3*(m1 + m2)) + cos(q2)*z3*m3 -
sin(q7)*((x2 - l2)*m2 - l2*m1));
M(5,4) = -((sin(q2)*l3 + sin(q7)*l2)*(-cos(q2)*l3 - cos(q7)*l2)*m1 +(sin(q2)*l3 +
sin(q7)*l2 - x2*sin(q7))*(-cos(q2)*l3 - cos(q7)*l2 + x2*cos(q7))*m2 +(sin(q2)*l3 -
x3*sin(q2) + cos(q2)*z3)*(-cos(q2)*l3 + x3*cos(q2) + sin(q2)*z3)*m3)*cos(q1)+
(I2z - I2x)*cos(q7)*sin(q7)*cos(q1) + (I3z - I3x)*cos(q2)*sin(q2)*cos(q1);
M(5,5) = m1*(sin(q2)*l3 + sin(q7)*l2)^2  + m2*(sin(q2)*l3 - sin(q7)*(x2 - l2))^2+
m3*(-sin(q2)*(x3 - l3) + cos(q2)*z3)^2  + (I2x - I2z)*cos(q7)^2+ (I3x -
I3z)*cos(q2)^2  + I3z + I2z + I1x;
M(5,6) = 0;
M(5,7) = 0;
M(5,8) = 0;
M(5,9) = 0;
```

```
M(5,10)= 0;
M(5,11)= 0;
M(5,12)= 0;
M(5,13)= 0;


M(6,1) = cos(q0)*(-sin(q2)*((x3 - l3)*m3 - l3*(m1 + m2)) + cos(q2)*z3*m3) +
sin(q0)*sin(q1)*(-cos(q2)*((x3 - l3)*m3 - l3*(m1 + m2)) - sin(q2)*z3*m3);
M(6,2) = sin(q0)*(-sin(q2)*((x3 - l3)*m3 - l3*(m1 + m2)) + cos(q2)*z3*m3) -
cos(q0)*sin(q1)*(-cos(q2)*((x3 - l3)*m3 - l3*(m1 + m2)) - sin(q2)*z3*m3);
M(6,3) = cos(q1)*(-cos(q2)*((x3 - l3)*m3 - l3*(m1 + m2)) - sin(q2)*z3*m3);
M(6,4) = ((x3^2  + z3^2 )*m3 + (l3*(m1 + m2 + m3) - 2*x3*m3)*l3 + I3y- ((x2 -
l2)*m2 - l2*m1)*l3*cos(q2 - q7))*sin(q1);
M(6,5) = 0;
M(6,6) = l3^2 *(m1 + m2) + ((x3 - l3)^2  + z3^2 )*m3 + I3y;
M(6,7) = 0;
M(6,8) = 0;
M(6,9) = 0;
M(6,10)= (l2*m1 + (l2 - x2)*m2)*l3*cos(q2 - q7);
M(6,11)= 0;
M(6,12)= 0;
M(6,13)= 0;


M(7,1) = -sin(q4)*(cos(q6)*(x4*m4 + (l4 + x5)*m5 + l4*m6)+ sin(q6)*(z4*m4 +
z5*m5 + qf*(-m5 - m6))) + cos(q4)*sin(q5)*(-sin(q6)*(x4*m4 + (l4 + x5)*m5 +
l4*m6) + cos(q6)*(z4*m4 + z5*m5 + qf*(-m5 - m6)));
M(7,2) =  cos(q4)*(cos(q6)*(x4*m4 + (l4 + x5)*m5 + l4*m6)+ sin(q6)*(z4*m4 +
z5*m5 + qf*(-m5 - m6))) + sin(q4)*sin(q5)*(-sin(q6)*(x4*m4 + (l4 + x5)*m5 +
l4*m6)+ cos(q6)*(z4*m4 + z5*m5 + qf*(-m5 - m6)));
M(7,3) = 0;
M(7,4) = 0;
M(7,5) = 0;
M(7,6) = 0;
M(7,7) = m4*(cos(q6)*x4 + sin(q6)*z4)^2  + m5*(cos(q6)*(l4 + x5) + sin(q6)*(-qf +
z5))^2+ m6*(cos(q6)*l4 - sin(q6)*qf)^2  + sin(q5)^2*(m4*(-sin(q6)*x4 +
cos(q6)*z4)^2+ m5*(-sin(q6)*(l4 + x5) + cos(q6)*(-qf + z5))^2+ m6*(-sin(q6)*l4 -
cos(q6)*qf)^2 ) + I6y + I5y + I4y +(I6x - I6y + I5x - I5y + I4x - I4y + (I5z - I5x + I4z -
I4x)*cos(q6)^2 )*cos(q5)^2;
M(7,8) = -(((-x4^2  + z4^2 )*m4 + ((-qf + z5)^2  - (l4 + x5)^2 )*m5 + (-l4^2  + qf^2
)*m6)*sin(q6)*cos(q6)+ (z4*x4*m4 + (-qf + z5)*(l4 + x5)*m5 -
qf*l4*m6)*cos(2*q6))*cos(q5)+ (I5z - I5x + I4z - I4x)*cos(q6)*sin(q6)*cos(q5);
M(7,9) = ((x4^2  + z4^2 )*m4 + ((l4 + x5)^2  + z5^2 )*m5 + I4y + I5y + l4^2*m6 -
qf^2*(-m5 - m6) - 2*qf*z5*m5)*sin(q5);
M(7,10)= 0;
M(7,11)= (l4*m6 + (l4 + x5)*m5)*sin(q5);
M(7,12)= 0;
M(7,13)= sin(q5)*I6y;


M(8,1) = sin(q4)*cos(q5)*(-sin(q6)*(x4*m4 + (l4 + x5)*m5 + l4*m6)+
cos(q6)*(z4*m4 + z5*m5 + qf*(-m5 - m6)));
M(8,2) = -cos(q4)*cos(q5)*(-sin(q6)*(x4*m4 + (l4 + x5)*m5 + l4*m6)+
cos(q6)*(z4*m4 + z5*m5 + qf*(-m5 - m6)));
M(8,3) = -sin(q5)*(-sin(q6)*(x4*m4 + (l4 + x5)*m5 + l4*m6) + cos(q6)*(z4*m4 +
z5*m5 + qf*(-m5 - m6)));
M(8,4) = 0;
M(8,5) = 0;
M(8,6) = 0;
M(8,7) = -(((-x4^2  + z4^2 )*m4 + ((-qf + z5)^2  - (l4 + x5)^2 )*m5 + (-l4^2  + qf^2
)*m6)*sin(q6)*cos(q6) + (z4*x4*m4 + (-qf + z5)*(l4 + x5)*m5 -
qf*l4*m6)*cos(2*q6))*cos(q5)+ (I5z - I5x + I4z - I4x)*cos(q6)*sin(q6)*cos(q5);
M(8,8) = m4*(-sin(q6)*x4 + cos(q6)*z4)^2 + m5*(-sin(q6)*(l4 + x5) + cos(q6)*(-qf +
```

```
z5))^2+ m6*(-sin(q6)*l4 - cos(q6)*qf)^2  - (I5z - I5x + I4z - I4x)*cos(q6)^2+ I4z +
I5z + I6x;
M(8,9) = 0;
M(8,10)= 0;
M(8,11)= 0;
M(8,12)= 0;
M(8,13)= 0;


M(9,1) = cos(q4)*(-sin(q6)*(x4*m4 + (l4 + x5)*m5 + l4*m6)+ cos(q6)*(z4*m4 +
z5*m5 + qf*(-m5 - m6))) + sin(q4)*sin(q5)*(-cos(q6)*(x4*m4 + (l4 + x5)*m5 +
l4*m6) - sin(q6)*(z4*m4 + z5*m5 + qf*(-m5 - m6)));
M(9,2) = sin(q4)*(-sin(q6)*(x4*m4 + (l4 + x5)*m5 + l4*m6) + cos(q6)*(z4*m4 +
z5*m5 + qf*(-m5 - m6))) - cos(q4)*sin(q5)*(-cos(q6)*(x4*m4 + (l4 + x5)*m5 +
l4*m6)- sin(q6)*(z4*m4 + z5*m5 + qf*(-m5 - m6)));
M(9,3) = cos(q5)*(-cos(q6)*(x4*m4 + (l4 + x5)*m5 + l4*m6) - sin(q6)*(z4*m4 +
z5*m5 + qf*(-m5 - m6)));
M(9,4) = 0;
M(9,5) = 0;
M(9,6) = 0;
M(9,7) = ((x4^2  + z4^2 )*m4 + ((l4 + x5)^2  + z5^2 )*m5 + I4y + I5y + l4^2*m6 -
qf^2*(-m5 - m6) - 2*qf*z5*m5)*sin(q5);
M(9,8) = 0;
M(9,9) = (x4^2  + z4^2 )*m4 + ((l4 + x5)^2  + z5^2 )*m5 + I4y + I5y + l4^2*m6 -
qf^2*(-m5 - m6)- 2*qf*z5*m5;
M(9,10)= 0;
M(9,11)= l4*m6 + (l4 + x5)*m5;
M(9,12)= 0;
M(9,13)= 0;


M(10,1) = -cos(q0)*sin(q7)*((x2 - l2)*m2 - l2*m1) -sin(q0)*sin(q1)*cos(q7)*((x2 -
l2)*m2 - l2*m1);
M(10,2) = -sin(q0)*sin(q7)*((x2 - l2)*m2 - l2*m1)+ cos(q0)*sin(q1)*cos(q7)*((x2 -
l2)*m2 - l2*m1);
M(10,3) = -cos(q1)*cos(q7)*((x2 - l2)*m2 - l2*m1);
M(10,4) = (l2^2*m1 + (x2 - l2)^2*m2 + I2y + (l2*m1 + (l2 - x2)*m2)*l3*cos(q2 -
q7))*sin(q1);
M(10,5) = 0;
M(10,6) = (l2*m1 + (l2 - x2)*m2)*l3*cos(q2 - q7);
M(10,7) = 0;
M(10,8) = 0;
M(10,9) = 0;
M(10,10)= l2^2*m1 + (x2 - l2)^2*m2 + I2y;
M(10,11)= 0;
M(10,12)= 0;
M(10,13)= 0;


M(11,1) = cos(q4)*sin(q6)*(-m5 - m6) + sin(q4)*sin(q5)*cos(q6)*(-m5 - m6);
M(11,2) = sin(q4)*sin(q6)*(-m5 - m6) - cos(q4)*sin(q5)*cos(q6)*(-m5 - m6);
M(11,3) = cos(q5)*cos(q6)*(-m5 - m6);
M(11,4) = 0;
M(11,5) = 0;
M(11,6) = 0;
M(11,7) = (l4*m6 + (l4 + x5)*m5)*sin(q5);
M(11,8) = 0;
M(11,9) = l4*m6 + (l4 + x5)*m5;
M(11,10)= 0;
M(11,11)= m5 + m6;
M(11,12)= 0;
M(11,13)= 0;
```

```
M(12,1) = 0;
M(12,2) = 0;
M(12,3) = 0;
M(12,4) = sin(q1)*I1y;
M(12,5) = 0;
M(12,6) = 0;
M(12,7) = 0;
M(12,8) = 0;
M(12,9) = 0;
M(12,10)= 0;
M(12,11)= 0;
M(12,12)= I1y;
M(12,13)= 0;


M(13,1) = 0;
M(13,2) = 0;
M(13,3) = 0;
M(13,4) = 0;
M(13,5) = 0;
M(13,6) = 0;
M(13,7) = sin(q5)*I6y;
M(13,8) = 0;
M(13,9) = 0;
M(13,10)= 0;
M(13,11)= 0;
M(13,12)= 0;
M(13,13)= I6y;
```

Appendix C

Full scope simulations

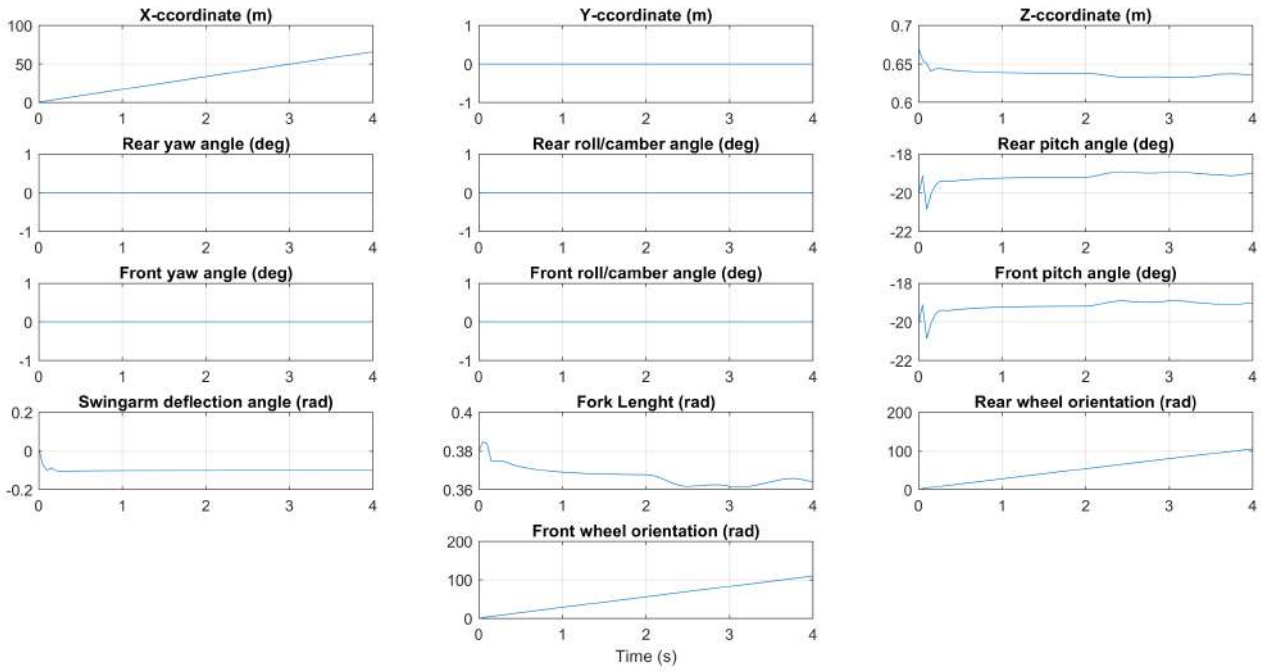

Figure 2: Selected generalized coordinates in case of a straight line (No steer).

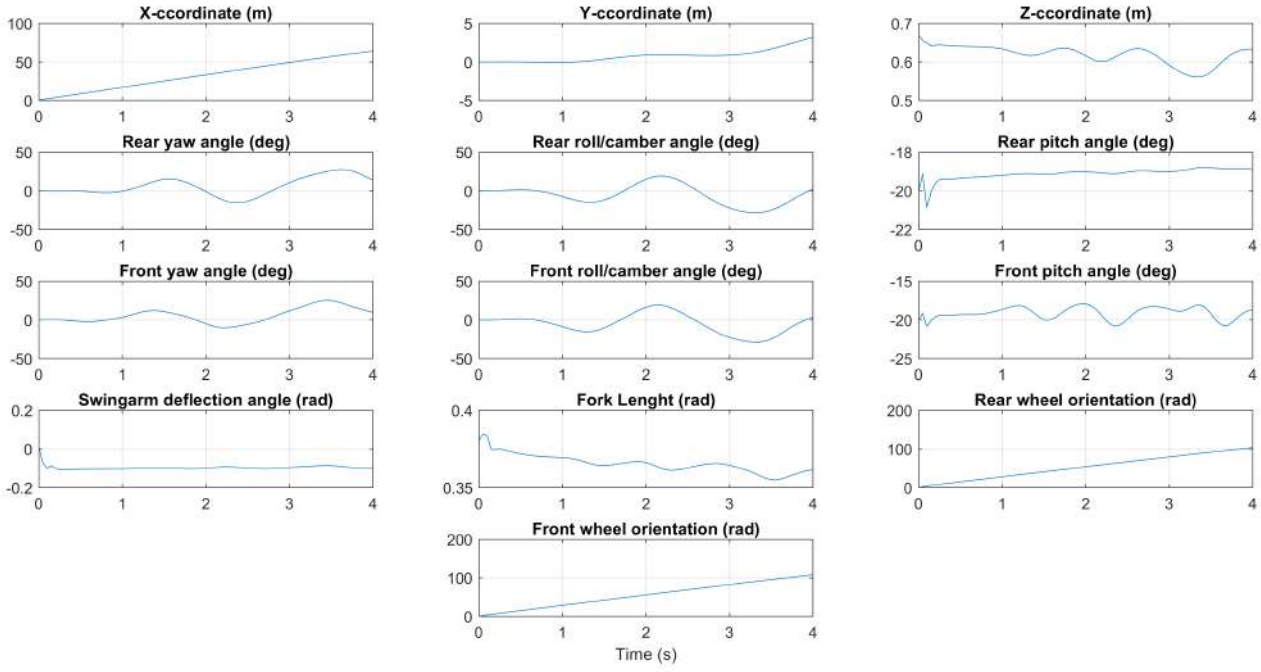

Figure 3: Selected generalized coordinates in case of a curve (No engine torque).

BIBLIOGRAPHY

[1] ONISR. *Les grandes données de l'accidentologie 2009, caractéristiques et causes des accidents de la route,* , 2009.

[2] W. Ooms BSc. *Motorcycle Modeling and Control*, DCT 2011.01.

[3] K. Majka, A. Blatt, M. Flanigan.. *Use of geocoded FARS data to analyse fatal motorcycle crashes. ESV : 20th international technical conference on the Enhanced Safety of Vehicles, June 18-21, Lyon - France.* Paper N07-0287, 2007.

[4] Motorcycling safety. *Position paper of the Royal Society for the Prevention of Accidents*, 2001.

[5] V. Cossalter. *Motorcycle Dynamics. Greendale, second edition edition*, 2006.

[6] F. J. W. Whipple. *The stability of the motion of a bicycle. Quarterly Journal of Pure and Applied Mathematics, 30:312–348.* 1899.

[7] E. Carvallo. *Theorie du mouvement du monocycle et de la bicyclette. Paris: Gauthier-Villars*, 1899.

[8] E. Döhring. *Über die Stabilität und Lenkkräfte von Einspuhrfahrzeugen. PhD thesis, University of Technology, Braunschweig*, 1954.

[9] J.P. Meijaard, J.M. Papadopoulos, A. Ruina, and A.L. Schwab. *Linearized dynamics equations for the balance and steer of a bicycle: a benchmark and review. The Royal Society, (463):1955–1982*, 2007.

[10] N. H. Getz. *Control for an autonomous bicycle. IEEE International Conference on Robotics and Automation, pages 1397–1402*, 1995.

[11] H. B. Pacejka. *Tyre and Vehicle Dynamics. Elsevier Ltd., second edition edition*, 2006.

[12] C. de Wit. *Dynamic tire friction models for vehicle traction control, 38th IEE-CDC*, 1994.

[13] B. L. Walcott, M. J. Corless, and S. H. Zak. *Comparative study of nonlinear state observation techniques. Int. J. of Control, 45(6) :2109–2132*, 1987.

[14] E. A. Misawa and J. K. Hedrick. *Nonlinear observers-a state of the art survey. ASME Journal of Dynamic Systems, Measurement, and Control, 111 :344–352*, 1989.

[15] F. E. Thau. *Observing the state of nonlinear dynamic systems. Int. J. of Control, 17(3) :471–479*, 1973.

[16] J. Lohmiller and J.-J. E.Slotine. *On contraction analysis for nonlinear systems. Automatica, 34(6) :683–696*, 1998.

[17]] J. Lohmiller and J.-J. E.Slotine. *Control system design for mechanical systems using contraction theory. IEEE Trans. Aut. Control, 45(5) :984–989*, 2000.

[18] W. Lohmiller and J.J.E. Slotine. *Contraction analysis of nonlinear distributed systems. International Journal of Control*, 2005.

[19] K. El Rifai and J.J.E. Slotine. *Compositional contraction analysis of hybrid nonlinear systems. IEEE. Trans. Aut. Control*, 2006.

[20] S.V. Emelyanov. *Variable Structure Control Systems. Nauka, Moscow*, 1967.

[21] M.Vidyasagar M. W. Spong, Seth Hutchingson. *Robot Modeling and Control. New York: Wiley*, 2005.

[22] V. Cossalter, A. Doria, R.. *Lot, Steady Turning Of Two Wheel Vehicles, Vehicle System Dynamics, 31, pp. 157-181*, 1999.

[23] I.D. Landau et R. Horowitz. *Synthesis of adaptive controllers for robot manipulators using a passive feedback systems approach. In IEEE International Conference on Robotics and Automation, Philadelphia, USA*, 1988.

[24] Belgacem Jaballah. *Observateurs robustes pour le diagnostic et la dynamique des véhicules*, 2011.

[25] Griffith 1971, Kou 1975, Hermann 1997, Boutat .

[26] A. Levant. *Hight order sliding modes differentiation and output feedback control. International Journal of Control, vol. 76, pages 924–941*, 2003.

[27] Jorge Davila, Leonid Fridman, Arie Levant. *Second Order Sliding Mode Observer for Mechanical Systems with Coulomb Friction*, 2004.

[28] Motorcycle Stability. *motorbikeana.it*.